Electronic Supplementary Material (ESI) for Journal of Materials Chemistry A.
This journal is © The Royal Society of Chemistry 2021

Supplementary Information

Fast identification of stability of atomically dispersed bi-atom catalysts by a structure descriptor-based simple model

Danyang Li, Haoxiang Xu*, Jiqin Zhu and Dapeng Cao*

State Key Laboratory of Organic-Inorganic Composites and Beijing Advanced Innovation Center for Soft Matter Science and Engineering, Beijing University of Chemical Technology, Beijing 100029, People's Republic of China

*Corresponding Author. E-mail: xuhx@mail.buct.edu.cn and caodp@mail.buct.edu.cn

Contents

Supplementary Methods 1

Section 1. Computational methods 1

Section 2. Stability against aggregation calculation 2

Section 3. Structure descriptor of stability against atom aggregation 3

Section 4. Dissolution potential calculation 5

Supplementary Tables 7

Supplementary Figures 61

Supplementary References 87

Supplementary Methods

Section 1. Computational methods

All the structures relaxation were calculated by density functional theory (DFT) , as implemented in Vienna ab initio Simulation Package (VASP) 5.4 code[1, 2]. The exchange correlation energy was modelled by Perdew Burke-Ernzerhof (PBE) functional within the generalized gradient approximation (GGA), and the projector augmented wave (PAW) pseudo-potentials were used to describe ionic cores[3, 4]. The energy cutoff of 500 eV was adopted for the plane-wave basis. A Gaussian smearing of 0.02 eV to the orbital occupation was applied during the geometry optimization and for the total energy computations. The energy and force convergence thresholds for the iteration in self-consistent filed (SCF) were set to 10^{-5} eV and 0.01 eV/Å, respectively. DFT-D3 method with Beche-Jonson damping were used in van der Waals (vdW) corrections[5]. We modeled bimetallic atoms doped graphene where the graphene was modeled with a (4x3√3) supercell, and a vacuum slab of 15Å was inserted in the z direction for surface isolation to prevent interaction between two neighboring surfaces. In structural optimizations, the Brillouin zone was sampled by 2×2×1 k-points using Monkhorst-Pack scheme. We employed the DFT + U method[6] to correct the local 3d electron correlation through on-site Coulomb and exchange interactions. Here we followed the rotation invariant method and used the corresponding U values for different transitions in previous studies[6, 7].

Section 2. Stability against aggregation calculation

A chemical potential-based thermodynamic model developed by JinCheng Liu and his co-workers[8] could be used to explore the stability of SACs against metal atom aggregation. Therefore, according to this method, we obtained the chemical potentials of M_1M_2-NC and metal NP. In this model, the chemical potential of metal NP ($\mu_{NP}(R)$) can be expressed by the Gibbs−Thomson (G-T) relation[9],

$$\mu_{NP}(R) = 2\Omega\gamma_{me}/R \quad (1)$$

where Ω is the molar volume of bulk metal atom. And γ_{me} is the surface energy of the NP, which is taken from the Materials Project[10]. We calculated the chemical potential of M_1 and M_2 atom in M_1M_2-NC, respectively. The chemical potential of metal SA can be approximately defined as the formation energy of metal SA with respect to the bulk metal ($\mu_{bulk} = 0$):

$$\mu_{M_1} \approx E_{M_1M_2\text{-NC}} - E_{M_2\text{-NC}} - E_{M_1} \quad (2)$$

$$\mu_{M_2} \approx E_{M_1M_2\text{-NC}} - E_{M_1\text{-NC}} - E_{M_2} \quad (3)$$

where $E_{M_1M_2\text{-NC}}$ is the total energy of M_1M_2-NC, E_{M_1/M_2} the energy of bulk gold energy per atom, and $E_{M_1\text{-NC}/M_2\text{-NC}}$ the energy of M_1-NC or M_2-NC. The energy change for subtracting a metal SA from a metal NP can be estimated by the difference of the chemical potentials between metal SA and metal NP

$$\Delta E_{SA}^{f}(R) = \mu_{SA} - \mu_{NP}(R) \quad (4)$$

where μ_{SA} is the chemical potential of M_1 (μ_{M_1}) or M_2 (μ_{M_2}). Here, $\Delta E_{SA}^{f}(R) < 0$ eV generally indicates that metal SAs in M_1M_2-NC are difficult to disintegrate from the heteronuclear dimer-atom sites and aggregate into NPs.

Section 3. Structure descriptor of stability against atom aggregation

To predict the stability of BACs against atom aggregation, we associate the ΔE_{SA}^{f} with properties of metal atom, respectively. Generally, the larger atomic radius are, the more difficult they are to embed into the N_6-C cavity, and a smaller the bulk cohesive energy (E^{coh}) indicates that metal single atoms are easier to aggregate into NPs.

$$E^{coh} = E_{bulk} - n \times E_{free-atom} \quad (5)$$

where n is the number of atoms in the bulk, E_{bulk} and $E_{free-atom}$ is the energy of the metal bulk and free atom, respectively.

Therefore, the difference of the chemical potentials between metal SA and metal NP (ΔE_{SA}^{f}) of configurations 4 is not only related to valence-electron numbers and electronegativity, but also related to atomic radius and the bulk cohesive energy (E^{coh}). Since all E^{coh} calculated in this work are negative value, the absolute value of E^{coh} is used in subsequent calculations.

We build descriptors (φ_{agg1} and φ_{agg2}) in this work by considering the effects of agglomerated atoms (M_1 atoms) and non-agglomerated atoms (M_2 atoms) in M_1M_2-NC on the $\Delta E_{M_1}^{f}$. For 3d metals atom aggregation, the descriptors (φ_{agg1} and φ_{agg2}) of the M_1M_2-NC-4 are as follow:

$$\varphi agg1 = \theta_{M_1}\sqrt{E_{M_1}} + \sqrt{\left|E_{M_1}^{coh}\right|} + R_{M_1} \quad (6)$$

$$\varphi agg2 = E_{M_2}R^2{}_{M_2} \quad (7)$$

Where $E_{M1/M2}$ and $R_{M1/M2}$ are the electronegativity and radius, θ_{M1} are the valence-electron number, and $|E^{coh}{}_{M1}|$ are the absolute value of E^{coh} for M_1 atom. We have performed a quadratic fitting of the $\Delta E_{M_1}^{f}$ with φ_{agg1} and φ_{agg2}, the formula is as follows:

$$\Delta E_{SA}^{f} = -21.68 - 1.69\varphi agg1 + 15.62\varphi agg2 + 0.063(\varphi agg1)^2 - 2.05(\varphi agg2)^2 + 0.0005\varphi agg1\varphi agg2 \quad (8)$$

$$\Delta E_{SA}^{f} = 16.23 - 2.05\varphi agg1 - 2.00\varphi agg2 + 0.07(\varphi agg1)^2 + 0.149(\varphi agg2)^2 + 0.0287\varphi agg1\varphi agg2 \quad (9)$$

Eq 8 and eq 9 apply to 3d-3d and 3d-4d/5d M_1M_2-NC respectively. The $\Delta E_{M_1}^{f}$ is as a function of both the φ_{agg1} and φ_{agg2} in **Figure S16**. At this time, the ΔE_{SA}^{f} is mainly related to properties of agglomerate atom. As is shown in **Figure S16**, a smaller value of φ_{agg1} generally indicates that M_1 metal atom are more difficult to aggregate into NPs. Compared with 3d metals, M_2 atoms of 4d and 5d metals have stronger adsorption capacity for M_1 atoms.

For 4d metals atom aggregation, the ΔE_{SA}^{f} is also mainly related to properties of agglomerate atom. However, atomic radius and E^{coh} of agglomerate atom have a greater impact on ΔE_{SA}^{f}. Thus, the φ_{agg1} of the M_1M_2-NC-4 are as follow:

$$\varphi agg1 = \theta_{M_1} + \left|E_{M_1}^{coh}\right| + R^{n}{}_{M_1} \quad (10)$$

The quadratic fitting of the $\Delta E_{M_1}^{f}$ with φ_{agg1} and φ_{agg2} are performed, the formula is as follows:

$$\Delta E_{SA}^{f} = - 14.30 - 1.52\varphi agg1 + 18.28\varphi agg2 + 0.03(\varphi agg1)^2 - 2.12(\varphi agg2)^2 - 0.088\varphi agg1\varphi agg2 \ (4d - \quad (11)$$

$$\Delta E_{SA}^{f} = - 6.28 + 0.89\varphi agg1 - 0.225\varphi agg2 - 0.026(\varphi agg1)^2 + 0.057(\varphi agg2)^2 - 0.009\varphi agg1\varphi agg2(4d - 4 \quad (12)$$

The $\Delta E_{M_1}^{f}$ is as a function of both the φ_{agg1} and φ_{agg2} in **Figure S17**. For 5d metal atom aggregation, the influence of M_2 atom for $\Delta E_{M_1}^{f}$ increases, as they usually have a larger atomic radius, and thus the φ_{agg2} of the M_1M_2-NC-4 are as follow:

$$\varphi agg2 = E_{M_2}R^{5}{}_{M_2} \quad (13)$$

Noteworthy, we found that the φ_{agg1} is different with the difference of M_2 atom in M_1M_2-NC. When M_2 atoms are 7~9 group transition metal atom, the φ_{agg1} is as follow:

$$\varphi agg1 = \sqrt{E_{M_1}}\theta_{M_1} + \left|E^{coh}_{M_1}\right| + R^{n}_{M_1} \quad (14)$$

In the contrast, when M_2 atoms are 10~12 group transition metal atom, the φ_{agg1} is as follow:

$$\varphi agg1 = \theta_{M_1} + \left|E^{coh}_{M_1}\right| + R_{M_1} \quad (15)$$

The quadratic fitting of the $\Delta E^{f}_{M_1}$ with φ_{agg1} and φ_{agg2} will be performed as follows:

$$\Delta E^{f}_{SA} = Z_0 + a\varphi agg1 - b\varphi agg2 - c(\varphi agg1)^2 + d(\varphi agg2)^2 - f\varphi agg1\varphi agg2 \quad (16)$$

The data of Z_0, a, b, c, d and f are listed in **Table S29**, and the dissolution potential of M_1 in **Figure S18** are as a function of both the φ_{agg1} and φ_{agg2}. According to our forecasting model, the M_1M_2-NC obtained from experiments are predicted to be stable against metal atom aggregation ($\Delta E^{f}_{SA}<0$), as is shown in **Figure S16-S18**. This result validates our prediction.

Section 4. Dissolution potential calculation

A simple scheme formulated by Jincheng Liu and his colleagues[11] was used to calculate dissolution potential of BACs, in which the leaching process is investigated with differential leaching steps.

$$M_1M_2 - NC \rightarrow M_2 - NC + M^{n+}_1(aq) + ne^- \quad (17)$$

Most transition metal atoms (except Ag, Re and Ir) which was calculated in this work will lose two electrons to form divalent metal ions. Thus the corresponding reaction free energies at a certain applied potential U can be written as,

$$\Delta G_{(M_1M_2 - NC \text{ to } M_2 - NC)} = G_{(M_2 - NC)} + G_{(M^{n+}(aq))} - G_{(M_1M_2 - NC)} + neU \quad (18)$$

Where e is -1 and the free energies of solvated cations $G_{(M^{n+}(aq))}$ is calculated from the experimental standard reduction potentials U_0 (vs SHE) and the free energies of

bulk metals $E_{(M(s))}$ as follows:

$$G_{(M^{n+}(aq))} = G_{(M(S))} - neU_0 \tag{19}$$

The free energies $G_{(M_1M_2\text{ - NC})}$ and $G_{(M_2\text{ - NC})}$ are linearly dependent on U as follow,

$$G_{(M_1M_2\text{ - NC})} = k_1U + G^0_{(M_1M_2\text{ - NC})} \tag{20}$$

$$G_{(M_2\text{ - NC})} = k_2U + G^0_{(M_2\text{ - NC})} \tag{21}$$

where k is the linear coefficient for U dependence, and G^0 is the free energy at U = 0 V.

$$\Delta G_{M_1} = G^0_{(M_2\text{ - NC})} + G_{(M^{n+}_1(aq))} - G^0_{(M_1M_2\text{ - NC})} + (k_2 - k_1 + n)eU \tag{22}$$

It requires $\Delta G_{M_1} < 0$ for the leaching step to take place spontaneously, and thus the dissolution potential U for BACs is

$$U = \frac{G^0_{(M_2\text{ - NC})} + G_{(M^{n+}_1(aq))} - G^0_{(M_1M_2\text{ - NC})}}{k2 - k1 + n} \tag{23}$$

We further assume k_1=k_2, and consequently we write eq 11 in the form

$$U = \frac{G^0_{(M_2\text{ - NC})} + G_{(M^{n+}_1(aq))} - G^0_{(M_1M_2\text{ - NC})}}{n} \tag{24}$$

In alkaline conditions, the leached metal ions may be converted into hydroxides or oxide in the solution. Taking the hydroxides as an example, the reaction equation for dissolution is

$$M_1M_2\text{ - NC} \rightarrow M_2\text{ - NC} + M_1(OH)_n + ne^- \tag{25}$$

According to the calculation result of DFT studies by Pourbaix et al[12], the dissolved product and the energy of metal bulk converted into hydroxide is determined.

$$M_1 + nH_2O \rightarrow M_1(OH)_n + ne^- + nH^+ \qquad \Delta G^0 \tag{26}$$

The corresponding reaction free energies at a certain applied potential U can be written as,

$$\Delta G_{M_1} = G^0_{(M_2\text{ - NC})} + G_{(M_1(S))} - G^0_{(M_1M_2\text{ - NC})} + neU + \Delta G^0 \tag{27}$$

It requires $^{\Delta G_{M_1}} < 0$ for the leaching step to take place spontaneously, and thus the dissolution potential U (vs SHE) for BACs is

$$U_{SHE} = \frac{G^0_{(M_2 - NC)} + G_{(M_1(S))} - G^0_{(M_1M_2 - NC)} + \Delta G^0}{n} \quad (28)$$

The dissolution potential U (vs RHE) for BACs is

$$U_{RHE} = U_{SHE} + 0.0591 \times pH \quad (29)$$

Supplementary Tables

Table S1 The adsorption energies (E_{ad}) in eV for 3d-3d heteronuclear BACs.

M_1,M_2	M_1M_2-NC-1	M_1M_2-NC-2	M_1M_2-NC-3	M_1M_2-NC-4	M_1M_2-NC-5
NiCo	-1.75	-5.41	-0.87	-6.05	-2.64
CuNi	-2.36	-5.21	-1.30	-5.58	-3.04
CuCo	-2.36	-5.27	-1.05	-5.50	-2.73
NiFe	-1.29	-5.01	-0.22	-5.89	-2.85
FeCo	-1.15	-5.05	0.22	-5.87	-2.46
FeCu	-2.03	-4.88	-0.36	-5.31	-3.06
NiZn	-0.83	-4.04	0.85	-4.14	-2.39
ZnCo	-0.62	-4.16	1.38	-4.00	-1.68
CuZn	-1.61	-4.01	0.20	-3.90	-2.31
NiMn	-0.43	-3.97	0.96	-4.80	-1.73
MnCo	0.33	-3.99	1.46	-4.82	-1.15
CuMn	-0.88	-3.94	0.64	-4.31	-2.01
ZnFe	-0.11	-3.78	1.62	-3.93	-1.74
MnFe	0.58	-3.56	2.18	-4.30	-0.48
ZnMn	1.03	-2.85	2.52	-2.83	1.17

Table S2 The adsorption energies (E_{ad}) in eV for 3d-3d homonuclear BACs and SACs. The adsorption energy of $2M_1/2M_2$-NC is the average of the adsorption energy of $2M_1$-NC and $2M_2$-NC.

M_1,M_2	$2M_1/2M_2$-NC-1	$2M_1/2M_2$-NC-2	$2M_1/2M_2$-NC-3	$2M_1/2M_2$-NC-4	$2M_1/2M_2$-NC-5	M_1M_2-SAC
Mn	1.79	-2.21	3.60	-2.79	0.72	-1.57
Fe	-0.53	-4.61	0.97	-5.50	-2.14	-4.70
Co	-1.53	-5.44	-0.35	-6.07	-2.69	-5.56
Ni	-1.81	-5.43	-1.12	-6.20	-2.78	-5.58
Cu	-2.90	-5.08	-1.54	-5.32	-2.53	-5.01
Zn	0.32	-2.91	2.06	-2.14	-1.43	-2.67
NiCo	-1.67	-5.44	-0.74	-6.14	-2.74	-5.58
CuNi	-2.35	-5.26	-1.33	-5.76	-2.66	-5.30
CuCo	-2.21	-5.26	-0.95	-5.69	-2.61	-5.29
NiFe	-1.17	-5.02	-0.07	-5.85	-2.46	-5.15
FeCo	-1.03	-5.03	0.31	-5.79	-2.41	-5.14
FeCu	-1.71	-4.85	-0.28	-5.41	-2.34	-4.83
NiZn	-0.74	-4.17	0.47	-4.17	-2.10	-4.13
ZnCo	-0.60	-4.17	0.85	-4.11	-2.06	-4.13
CuZn	-1.29	-3.99	0.26	-3.73	-1.98	-3.85
NiMn	-0.01	-3.82	1.24	-4.49	-1.03	-3.58
MnCo	0.13	-3.82	1.62	-4.43	-0.99	-3.56
CuMn	-0.55	-3.64	1.03	-4.05	-0.91	-3.32
ZnFe	-0.10	-3.76	1.52	-3.82	-1.78	-3.29
MnFe	0.63	-3.41	2.29	-4.15	-0.71	-3.05
ZnMn	1.06	-2.56	2.83	-2.46	-0.35	-2.16

Table S3 The adsorption energies (E_{ad}) in eV for 3d-4d heteronuclear BACs, homonuclear BACs and SACs. The adsorption energy of $2M_1/2M_2$-NC is the average of the adsorption energy of $2M_1$-NC and $2M_2$-NC.

M_1,M_2	M_1M_2-NC-2	M_1M_2-NC-4	$2M_1/2M_2$-NC-2	$2M_1/2M_2$-NC-4	M_1M_2-SAC
PdCo	-6.75	-6.78	-6.68	-6.80	-6.72
PdNi	-6.73	-6.83	-6.67	-6.86	-6.70
PdCu	-6.53	-6.43	-6.50	-6.42	-6.44
PdFe	-6.34	-6.80	-6.26	-6.51	-6.29
RhCo	-5.74	-6.76	-5.78	-6.90	-5.66
RhNi	-5.85	-6.33	-5.77	-6.96	-5.43
RhCu	-5.58	-5.86	-5.60	-6.52	-5.38
PdZn	-5.40	-5.04	-5.41	-4.83	-5.29
PdMn	-5.29	-5.69	-5.06	-5.16	-4.73
RhFe	-5.36	-6.49	-5.36	-6.61	-4.64
RuCo	-4.33	-6.39	-4.66	-6.47	-4.23
RhZn	-4.45	-4.38	-4.51	-4.93	-4.22
RuNi	-4.41	-6.04	-4.65	-6.53	-4.20
RuCu	-4.33	-5.56	-4.48	-6.09	-3.96
RuFe	-3.97	-6.15	-4.24	-6.18	-3.80
TcNi	-4.26	-6.26	-4.11	-6.64	-3.74
TcCo	-4.28	-6.54	-4.12	-6.58	-3.71
RhMn	-4.24	-5.59	-4.16	-5.26	-3.65
TcCu	-4.38	-5.82	-3.94	-6.20	-3.49
TcFe	-3.76	-6.15	-3.71	-6.29	-3.38
AgNi	-3.78	-4.04	-3.83	-4.24	-3.18
AgCo	-3.84	-3.96	-3.84	-4.18	-3.13
AgCu	-3.68	-3.74	-3.66	-3.80	-2.96

AgFe	-3.51	-3.73	-3.42	-3.89	-2.69
RuZn	-3.13	-4.17	-3.39	-4.50	-2.68
CdNi	-2.83	-2.48	-3.14	-3.25	-2.65
CdCo	-2.90	-2.43	-3.15	-3.18	-2.64
CdCu	-2.43	-2.31	-2.97	-2.81	-2.36
TcZn	-3.17	-4.50	-2.85	-4.61	-2.35
RuMn	-2.84	-4.95	-3.04	-4.83	-2.22
CdFe	-2.61	-2.44	-2.73	-2.90	-2.17
TcMn	-2.63	-5.11	-2.50	-4.93	-1.79
AgZn	-2.60	-2.39	-2.57	-2.21	-1.76
AgMn	-2.45	-2.71	-2.22	-2.54	-1.17
CdZn	-1.86	-0.83	-1.88	-1.22	-1.17
CdMn	-1.71	-1.46	-1.53	-1.54	-0.60

Table S4 The adsorption energies (E_{ad}) in eV for 3d-5d heteronuclear BACs, homonuclear BACs and SACs. The adsorption energy of $2M_1/2M_2$-NC is the average of the adsorption energy of $2M_1$-NC and $2M_2$-NC.

M_1,M_2	M_1M_2-NC-2	M_1M_2-NC-4	$2M_1/2M_2$-NC-2	$2M_1/2M_2$-NC-4	M_1M_2-SAC
IrCo	-7.68	-8.65	-7.59	-8.72	-7.48
IrNi	-7.69	-8.12	-7.59	-8.78	-7.46
PtCo	-7.44	-7.46	-7.35	-7.36	-7.41
PtNi	-7.46	-7.49	-7.34	-7.42	-7.39
IrCu	-7.48	-7.63	-7.41	-8.34	-7.21
PtCu	-7.24	-7.05	-7.17	-6.98	-7.15
IrFe	-7.35	-8.53	-7.18	-8.43	-7.05
PtFe	-6.79	-7.42	-6.93	-7.07	-7.00
IrZn	-6.31	-6.28	-6.32	-6.75	-6.06
PtZn	-6.12	-5.69	-6.08	-5.39	-6.00
IrMn	-5.99	-7.47	-5.97	-7.08	-5.48

PtMn	-5.96	-6.33	-5.73	-5.72	-5.45
OsCo	-4.55	-6.70	-4.68	-6.74	-4.24
OsNi	-4.62	-6.27	-4.67	-6.80	-4.03
OsCu	-4.47	-5.81	-4.50	-6.36	-3.98
OsFe	-4.02	-6.44	-4.27	-6.45	-3.81
ReCo	-3.40	-6.15	-3.47	-6.08	-2.79
ReNi	-3.38	-5.77	-3.46	-6.14	-2.75
OsZn	-3.16	-4.53	-3.41	-4.77	-2.63
ReCu	-3.50	-5.35	-3.29	-5.70	-2.51
ReFe	-2.98	-5.75	-3.05	-5.79	-2.39
OsMn	-2.58	-5.31	-3.06	-5.10	-2.23
ReZn	-2.31	-4.12	-2.20	-4.11	-1.38
ReMn	-1.72	-4.71	-1.85	-4.43	-0.79

Table S5 The adsorption energies (E_{ad}) in eV for 4d-4d heteronuclear BACs, homonuclear BACs and SACs. The adsorption energy of $2M_1/2M_2$-NC is the average of the adsorption energy of $2M_1$-NC and $2M_2$-NC.

M_1,M_2	M_1M_2-NC-2	M_1M_2-NC-4	$2M_1/2M_2$-NC-2	$2M_1/2M_2$-NC-4	M_1M_2-SAC
Tc			-2.80	-7.08	-2.06
Ru			-3.87	-6.87	-2.89
Rh			-6.11	-7.72	-5.84
Pd			-7.92	-7.53	-7.89
Ag			-2.24	-2.28	-0.90
Cd			-0.85	-0.30	0.69
RhPd	-7.13	-7.19	-7.02	-7.62	-6.83
TcPd	-5.52	-7.28	-5.36	-7.30	-5.95
PdRu	-5.78	-7.08	-5.90	-7.20	-5.42
AgPd	-5.11	-4.78	-5.08	-4.91	-4.39
RhRu	-4.96	-7.30	-4.99	-7.30	-4.37

TcRh	-4.79	-7.47	-4.46	-7.40	-3.79
CdPd	-4.06	-3.46	-4.38	-3.91	-3.79
AgRh	-4.20	-3.93	-4.18	-5.00	-3.48
CdRh	-3.26	-3.35	-3.48	-4.01	-2.73
TcAg	-3.02	-4.75	-2.52	-4.68	-2.51
TcRu	-3.81	-7.07	-3.34	-6.97	-2.41
AgRu	-3.09	-4.40	-3.06	-4.58	-2.07
CdRu	-2.10	-3.56	-2.36	-3.58	-1.26
TcCd	-2.03	-3.96	-1.82	-3.69	-0.85
CdAg	-1.71	-0.90	-1.54	-1.29	-0.27

Table S6 The adsorption energies (E_{ad}) in eV for 4d-5d heteronuclear BACs, homonuclear BACs and SACs. The adsorption energy of $2M_1/2M_2$-NC is the average of the adsorption energy of $2M_1$-NC and $2M_2$-NC.

M_1,M_2	M_1M_2-NC-2	M_1M_2-NC-4	$2M_1/2M_2$-NC-2	$2M_1/2M_2$-NC-4	M_1M_2-SAC
PdPt	-8.57	-8.11	-8.59	-8.09	-8.60
RhIr	-7.98	-9.56	-7.93	-9.54	-7.66
TcPt	-6.18	-7.89	-6.03	-7.86	-5.65
TcIr	-6.50	-9.33	-6.27	-9.22	-5.64
OsRh	-4.90	-7.56	-5.02	-7.56	-4.25
RhPt	-7.74	-7.78	-7.68	-8.18	-7.54
RuIr	-6.67	-9.17	-6.81	-9.12	-6.11
RuPt	-6.42	-7.68	-6.56	-7.76	-6.13
TcOs	-3.86	-7.30	-3.36	-7.24	-2.41
OsPd	-5.80	-7.25	-5.92	-7.47	-5.23
PdIr	-8.94	-8.91	-8.83	-9.44	-8.66
OsRu	-3.88	-7.15	-3.90	-7.14	-2.89
ReRh	-3.92	-7.09	-3.80	-6.90	-2.82
RePd	-4.62	-6.76	-4.70	-6.80	-3.96

ReRu	-3.01	-6.53	-2.68	-6.47	-1.46
ReTc	-2.73	-6.58	-2.14	-6.58	-0.41
ReAg	-2.26	-4.52	-1.86	-4.18	-0.53
OsAg	-3.28	-4.90	-3.08	-4.85	-2.03
AgIr	-6.03	-6.55	-5.99	-6.82	-5.28
AgPt	-5.80	-5.31	-5.75	-5.46	-5.11
ReCd	-1.35	-3.61	-1.17	-3.19	0.09
CdOs	-2.12	-3.96	-2.38	-3.85	-1.26
CdIr	-5.04	-5.35	-5.29	-5.83	-4.57
CdPt	-4.81	-4.14	-5.05	-4.47	-4.06

Table S7 The adsorption energies (E_{ad}) in eV for 5d-5d heteronuclear BACs, homonuclear BACs and SACs. The adsorption energy of $2M_1/2M_2$-NC is the average of the adsorption energy of $2M_1$-NC and $2M_2$-NC.

M_1,M_2	M_1M_2-NC-2	M_1M_2-NC-4	$2M_1/2M_2$-NC-2	$2M_1/2M_2$-NC-4	M_1M_2-SAC
Re			-1.49	-6.08	-0.08
Os			-3.92	-7.41	-2.75
Ir			-9.74	-11.36	-9.48
Pt			-9.25	-8.64	-9.32
PtIr	-9.60	-9.49	-9.50	-10.00	-9.37
OsPt	-6.44	-7.81	-6.59	-8.03	-6.13
OsIr	-6.58	-9.38	-6.83	-9.38	-6.10
RePt	-5.19	-7.34	-5.37	-7.36	-4.68
ReIr	-5.78	-8.95	-5.61	-8.72	-4.66
ReOs	-3.02	-6.71	-2.70	-6.74	-1.38

Table S8 The difference of adsorption energies of the metal atom between M_1M_2-NC and M_1M_2-SAC ($\Delta E_{ad(SAC)}$) in eV for 3d-3d M_1M_2-NC. The BACs possess instability against forming single-atom sites are marked in red.

	configurations 2	configurations 4
2Mn-NC	-0.63	-1.22
2Fe-NC	0.09	-0.80
2Co-NC	0.12	-0.51
2Ni-NC	0.16	-0.61
2Cu-NC	-0.07	-0.30
2Zn-NC	-0.24	0.53
NiFe-NC	0.14	-0.74
NiCo-NC	0.17	-0.47
FeCo-NC	0.08	-0.74
CuNi-NC	0.10	-0.28
FeCu-NC	-0.05	-0.48
MnFe-NC	-0.51	-1.25
CuCo-NC	0.02	-0.21
NiMn-NC	-0.39	-1.22
ZnFe-NC	-0.50	-0.64
MnCo-NC	-0.43	-1.26
CuMn-NC	-0.62	-0.99
NiZn-NC	0.09	-0.01
CuZn-NC	-0.16	-0.05
ZnMn-NC	-0.69	-0.67
ZnCo-NC	-0.03	0.13

Table S9 The difference of adsorption energies of the metal atom between M_1M_2-NC and M_1M_2-SAC ($\Delta E_{ad(SAC)}$) in eV for 3d-4d M_1M_2-NC. The BACs possess instability against forming single-atom sites are marked in red.

	configurations 2	**configurations 4**
PdNi-NC	-0.03	-0.13
PdFe-NC	-0.04	-0.50
PdCo-NC	-0.03	-0.06
RhCo-NC	-0.08	-1.10
PdCu-NC	-0.08	0.02
AgFe-NC	-0.82	-1.03
RhFe-NC	-0.72	-1.86
RuCo-NC	-0.10	-2.16
TcCo-NC	-0.56	-2.82
RhNi-NC	-0.43	-0.91
AgNi-NC	-0.60	-0.86
RuFe-NC	-0.17	-2.35
RuNi-NC	-0.21	-1.84
TcNi-NC	-0.52	-2.52
TcFe-NC	-0.38	-2.77
AgCu-NC	-0.71	-0.78
RhCu-NC	-0.20	-0.48
PdMn-NC	-0.55	-0.96
AgCo-NC	-0.71	-0.83
TcCu-NC	-0.89	-2.33
RuCu-NC	-0.36	-1.59
RhMn-NC	-0.59	-1.94
AgMn-NC	-1.28	-1.54
AgZn-NC	-0.84	-0.63

PdZn-NC	-0.12	0.25
RuMn-NC	-0.62	-2.73
TcMn-NC	-0.84	-3.32
CdFe-NC	-0.44	-0.26
RhZn-NC	-0.22	-0.16
TcZn-NC	-0.82	-2.15
CdZn-NC	-0.68	0.34
RuZn-NC	-0.45	-1.50
CdNi-NC	-0.18	0.17
CdCu-NC	-0.07	0.05
CdMn-NC	-1.12	-0.87
CdCo-NC	-0.26	0.20

Table S10 The difference of adsorption energies of the metal atom between M_1M_2-NC and M_1M_2-SAC ($\Delta E_{ad(SAC)}$) in eV for 3d-5d M_1M_2-NC. The BACs possess instability against forming single-atom sites are marked in red.

	configurations 2	**configurations 4**
IrCo-NC	-0.20	-1.17
IrNi-NC	-0.23	-0.66
PtCo-NC	-0.03	-0.05
PtNi-NC	-0.06	-0.09
IrCu-NC	-0.27	-0.42
PtCu-NC	-0.09	0.10
IrFe-NC	-0.29	-1.48
PtFe-NC	0.21	-0.41
IrZn-NC	-0.24	-0.18
PtZn-NC	-0.12	0.31
IrMn-NC	-0.51	-1.99
PtMn-NC	-0.51	-0.88

OsCo-NC	-0.31	-2.47
OsNi-NC	-0.59	-2.24
OsCu-NC	-0.49	-1.83
OsFe-NC	-0.21	-2.63
ReCo-NC	-0.61	-3.36
ReNi-NC	-0.63	-3.02
OsZn-NC	-0.52	-1.90
ReCu-NC	-0.99	-2.84
ReFe-NC	-0.59	-3.36
OsMn-NC	-0.35	-3.08
ReZn-NC	-0.93	-2.74
ReMn-NC	-0.93	-3.91

Table S11 The difference of adsorption energies of the metal atom between M_1M_2-NC and M_1M_2-SAC ($\Delta E_{ad(SAC)}$) in eV for 4d-4d M_1M_2-NC. The BACs possess instability against forming single-atom sites are marked in red.

	configurations 2	**configurations 4**
2Tc-NC	-0.74	-5.02
2Ru-NC	-0.99	-3.98
2Rh-NC	-0.28	-1.89
2Pd-NC	-0.03	0.36
2Ag-NC	-1.34	-1.39
2Cd-NC	-1.53	-0.98
RhPd-NC	-0.31	-0.37
TcPd-NC	-0.58	-2.35
PdRu-NC	-0.36	-1.66
AgPd-NC	-0.73	-0.40
RhRu-NC	-0.59	-2.93
TcRh-NC	-0.99	-3.68

CdPd-NC	-0.27	0.33
AgRh-NC	-0.73	-0.45
CdRh-NC	-0.54	-0.62
TcAg-NC	-1.51	-3.24
TcRu-NC	-1.40	-4.66
AgRu-NC	-1.02	-2.33
CdRu-NC	-0.83	-2.30
TcCd-NC	-1.19	-3.11
CdAg-NC	-1.44	-0.62

Table S12 The difference of adsorption energies of the metal atom between M_1M_2-NC and M_1M_2-SAC ($\Delta E_{ad(SAC)}$) in eV for 4d-5d M_1M_2-NC. The BACs possess instability against forming single-atom sites are marked in red.

	configurations 2	**configurations 4**
PdPt-NC	0.03	0.49
RhIr-NC	-0.32	-1.90
TcPt-NC	-0.52	-2.24
TcIr-NC	-0.86	-3.68
OsRh-NC	-0.65	-3.30
RhPt-NC	-0.20	-0.24
RuIr-NC	-0.56	-3.06
RuPt-NC	-0.29	-1.55
TcOs-NC	-1.45	-4.88
OsPd-NC	-0.57	-2.02
PdIr-NC	-0.28	-0.25
OsRu-NC	-0.98	-4.26
ReRh-NC	-1.10	-4.27
RePd-NC	-0.66	-2.80
ReRu-NC	-1.55	-5.07

ReTc-NC	-2.32	-6.17
ReAg-NC	-1.73	-3.99
OsAg-NC	-1.25	-2.87
AgIr-NC	-0.75	-1.26
AgPt-NC	-0.69	-0.20
ReCd-NC	-1.44	-3.70
CdOs-NC	-0.86	-2.71
CdIr-NC	-0.47	-0.78
CdPt-NC	-0.75	-0.08

Table S13 The difference of adsorption energies of the metal atom between M_1M_2-NC and M_1M_2-SAC ($\Delta E_{ad(SAC)}$) in eV for 5d-5d dimer-atom sites. The BACs possess instability against forming single-atom sites are marked in red.

	configurations 2	**configurations 4**
2Re-NC	-1.41	-6.00
2Os-NC	-1.17	-4.65
2Ir-NC	-0.26	-1.88
2Pt-NC	0.06	0.67
PtIr-NC	-0.22	-0.11
OsPt-NC	-0.30	-1.68
OsIr-NC	-0.48	-3.28
RePt-NC	-0.51	-2.66
ReIr-NC	-1.11	-4.29
ReOs-NC	-1.65	-5.33

Table S14 The data of θ_M, E_M and φ_{BAC} for 3d-3d M_1M_2-NC.

	θ_M		E_M		φ_{BAC}
	M_1	M_2	M_1	M_2	
2Co-NC	9	9	1.88	1.88	24.68
2Ni-NC	10	10	1.91	1.91	27.64
NiCo-NC	10	9	1.91	1.88	26.16
CuCo-NC	11	9	1.90	1.88	27.50
FeCo-NC	8	9	1.83	1.88	23.16
2Cu-NC	11	11	1.90	1.90	30.32
CuNi-NC	11	10	1.90	1.91	28.98
NiFe-NC	10	8	1.91	1.83	24.64
FeCu-NC	8	11	1.83	1.90	25.98
2Fe-NC	8	8	1.83	1.83	21.64
2Zn-NC	12	12	1.65	1.65	30.83
ZnCo-NC	12	9	1.65	1.88	27.75
MnCo-NC	7	9	1.55	1.88	21.06
ZnMn-NC	12	7	1.65	1.55	24.13
CuZn-NC	11	12	1.90	1.65	30.58
ZnFe-NC	12	8	1.65	1.83	26.24
CuMn-NC	11	7	1.90	1.55	23.88
NiZn-NC	10	12	1.91	1.65	29.23
NiMn-NC	10	7	1.91	1.55	22.54
MnFe-NC	7	8	1.55	1.83	19.54
2Mn-NC	7	7	1.55	1.55	17.43

Table S15 The data of θ_M, E_M and φ_{BAC} for 3d-4d M_1M_2-NC.

	θ_M		E_M		φ_{BAC}
	M_1	M_2	M_1	M_2	
PdNi-NC	10	10	2.20	1.91	19.44
PdFe-NC	10	8	2.20	1.83	18.44
PdCo-NC	10	9	2.20	1.88	18.95
RhCo-NC	9	9	2.28	1.88	17.70
PdCu-NC	10	11	2.20	1.90	19.89
AgFe-NC	11	8	1.93	1.83	18.89
RhFe-NC	9	8	2.28	1.83	17.20
RuCo-NC	8	9	2.20	1.88	15.98
TcCo-NC	7	9	1.90	1.88	13.76
RhNi-NC	9	10	2.28	1.91	18.20
AgNi-NC	11	10	1.93	1.91	19.89
RuFe-NC	8	8	2.20	1.83	15.47
RuNi-NC	8	10	2.20	1.91	16.47
TcNi-NC	7	10	1.90	1.91	14.26
TcFe-NC	7	8	1.90	1.83	13.26
AgCu-NC	11	11	1.93	1.90	20.34
RhCu-NC	9	11	2.28	1.90	18.64
PdMn-NC	10	7	2.20	1.55	17.74
AgCo-NC	11	9	1.93	1.88	19.40
TcCu-NC	7	11	1.90	1.90	14.70
RuCu-NC	8	11	2.20	1.90	16.92
RhMn-NC	9	7	2.28	1.55	16.49
AgMn-NC	11	7	1.93	1.55	18.19
AgZn-NC	11	12	1.93	1.65	20.42
PdZn-NC	10	12	2.20	1.65	19.97

RuMn-NC	8	7	2.20	1.55	14.77
TcMn-NC	7	7	1.90	1.55	12.55
CdFe-NC	12	8	1.69	1.83	19.21
RhZn-NC	9	12	2.28	1.65	18.73
TcZn-NC	7	12	1.90	1.65	14.79
CdZn-NC	12	12	1.69	1.65	20.74
RuZn-NC	8	12	2.20	1.65	17.00
CdNi-NC	12	10	1.69	1.91	20.21
CdCu-NC	12	11	1.69	1.90	20.65
CdMn-NC	12	7	1.69	1.55	18.50
CdCo-NC	12	9	1.69	1.88	19.71

Table S16 The data of θ_M, E_M and φ_{BAC} for 3d-5d M_1M_2-NC.

	θ_M		**E_M**		**φ_{BAC}**
	M_1	M_2	M_1	M_2	
PtCo-NC	10	9	2.28	1.88	19.21
PtNi-NC	10	10	2.28	1.91	19.71
PtFe-NC	10	8	2.28	1.83	18.71
ReCo-NC	7	9	1.90	1.88	13.76
IrCo-NC	9	9	2.20	1.88	17.46
PtCu-NC	10	11	2.28	1.90	20.15
IrFe-NC	9	8	2.20	1.83	16.96
OsCo-NC	8	9	2.20	1.88	15.98
ReFe-NC	7	8	1.90	1.83	13.26
ReNi-NC	7	10	1.90	1.91	14.26
OsFe-NC	8	8	2.20	1.83	15.47
IrNi-NC	9	10	2.20	1.91	17.96
OsNi-NC	8	10	2.20	1.91	16.47

ReCu-NC	7	11	1.90	1.90	14.70
PtMn-NC	10	7	2.28	1.55	18.00
IrCu-NC	9	11	2.20	1.90	18.40
OsCu-NC	8	11	2.20	1.90	16.92
IrMn-NC	9	7	2.20	1.55	16.25
ReMn-NC	7	7	1.90	1.55	12.55
OsMn-NC	8	7	2.20	1.55	14.77
ReZn-NC	7	12	1.90	1.65	14.79
OsZn-NC	8	12	2.20	1.65	17.00
IrZn-NC	9	12	2.20	1.65	18.49
PtZn-NC	10	12	2.28	1.65	20.24

Table S17 The data of θ_M, E_M and φ_{BAC} for 4d-4d M_1M_2-NC.

	θ_M		**E_M**		**φ_{BAC}**
	M_1	M_2	M_1	M_2	
TcRh-NC	7	9	1.9	2.28	23.24
RhRu-NC	9	8	2.28	2.20	25.46
RhPd-NC	10	9	2.28	2.20	28.45
PdRu-NC	10	8	2.20	2.20	26.70
TcPd-NC	7	10	1.90	2.20	24.48
TcRu-NC	7	8	1.90	2.20	21.51
AgRh-NC	11	9	1.93	2.28	28.87
TcAg-NC	7	11	1.90	1.93	24.93
AgRu-NC	11	8	1.93	2.20	27.15
AgPd-NC	11	10	1.93	2.20	30.11
TcCd-NC	7	12	1.90	1.63	24.97
CdAg-NC	12	11	1.63	1.93	30.60
CdRu-NC	12	8	1.63	2.20	27.19

CdPd-NC	12	10	1.63	2.20	30.15
CdRh-NC	12	9	1.63	2.28	28.91
2Tc-NC	7	7	1.90	1.90	19.30
2Ru-NC	8	8	2.20	2.20	23.73
2Rh-NC	9	9	2.28	2.28	27.18
2Pd-NC	10	10	2.20	2.20	29.66
2Ag-NC	11	11	1.93	1.93	30.56
2Cd-NC	12	12	1.63	1.63	30.64

Table S18 The data of θ_M, E_M and φ_{BAC} for 4d-5d M_1M_2-NC.

	θ_M		**E_M**		**φ_{BAC}**
	M_1	M_2	M_1	M_2	
PdPt-NC	10	10	2.20	2.28	29.93
RhIr-NC	9	9	2.28	2.20	26.94
TcPt-NC	7	10	1.90	2.28	24.75
TcIr-NC	7	9	1.90	2.20	23.00
OsRh-NC	8	9	2.20	2.28	25.46
RhPt-NC	9	10	2.28	2.28	28.69
RuIr-NC	8	9	2.20	2.20	25.22
RuPt-NC	8	10	2.28	2.20	26.91
TcOs-NC	7	8	1.90	2.20	21.51
OsPd-NC	8	10	2.20	2.20	26.70
PdIr-NC	10	9	2.20	2.20	28.18
OsRu-NC	8	8	2.20	2.20	23.73
ReRh-NC	7	9	1.90	2.28	23.24
RePd-NC	7	10	1.90	2.20	24.48
ReRu-NC	7	8	1.90	2.20	21.51
ReTc-NC	7	7	1.90	1.90	19.30

ReAg-NC	7	11	1.90	1.93	24.93
OsAg-NC	8	11	1.93	2.20	27.43
AgIr-NC	11	9	1.93	2.20	28.63
AgPt-NC	11	10	1.93	2.28	30.38
ReCd-NC	7	12	1.90	1.63	24.97
CdOs-NC	12	8	1.63	2.20	27.19
CdIr-NC	12	9	1.63	2.20	28.67
CdPt-NC	12	10	1.63	2.28	30.42

Table S19 The data of θ_M, E_M and φ_{BAC} for 5d-5d M_1M_2-NC.

	θ_M		**E_M**		**φ_{BAC}**
	M_1	M_2	M_1	M_2	
PtIr-NC	10	9	2.28	2.20	28.45
OsIr-NC	8	9	2.20	2.20	25.22
OsPt-NC	8	10	2.20	2.28	26.97
ReIr-NC	7	9	1.90	2.20	23.00
RePt-NC	7	10	1.90	2.28	24.75
ReOs-NC	7	8	1.90	2.20	21.51
2Re-NC	7	7	1.90	1.90	19.30
2Os-NC	8	8	2.20	2.20	23.73
2Ir-NC	9	9	2.20	2.20	26.70
2Pt-NC	10	10	2.28	2.28	30.20

Table S20 The difference of adsorption energies of the metal atom between heteronuclear BACs and homonuclear BACs (ΔE_{ad}) of configurations 2 in eV.

	ΔE_{ad}		ΔE_{ad}		ΔE_{ad}		ΔE_{ad}
3d-3d		RhCu-NC	0.02	IrMn-NC	-0.02	ReAg-NC	-0.39
MnFe-NC	-0.15	RhZn-NC	0.06	IrFe-NC	-0.17	ReCd-NC	-0.18
MnCo-NC	-0.16	PdMn-NC	-0.22	IrCo-NC	-0.09	TcOs-NC	-0.50
NiMn-NC	-0.16	PdFe-NC	-0.07	IrNi-NC	-0.11	OsRu-NC	0.02
CuMn-NC	-0.29	PdCo-NC	-0.07	IrCu-NC	-0.07	OsRh-NC	0.11
ZnMn-NC	-0.30	PdNi-NC	-0.05	IrZn-NC	0.02	OsPd-NC	0.12
FeCo-NC	-0.02	PdCu-NC	-0.03	PtMn-NC	-0.23	OsAg-NC	-0.20
NiFe-NC	0.01	PdZn-NC	0.01	PtFe-NC	0.14	CdOs-NC	0.27
FeCu-NC	-0.03	AgMn-NC	-0.23	PtCo-NC	-0.10	TcIr-NC	-0.23
ZnFe-NC	-0.03	AgFe-NC	-0.09	PtNi-NC	-0.12	RuIr-NC	0.14
NiCo-NC	0.02	AgCo-NC	0.00	PtCu-NC	-0.07	RhIr-NC	-0.06
CuCo-NC	-0.01	AgNi-NC	0.06	PtZn-NC	-0.04	PdIr-NC	-0.11
ZnCo-NC	0.01	AgCu-NC	-0.01	4d-4d		AgIr-NC	-0.04
CuNi-NC	0.05	AgZn-NC	-0.03	TcRu-NC	-0.48	CdIr-NC	0.26
CuZn-NC	-0.01	CdMn-NC	-0.19	TcRh-NC	-0.33	TcPt-NC	-0.15
NiZn-NC	0.13	CdFe-NC	0.12	TcPd-NC	-0.16	RuPt-NC	0.14
3d-4d		CdCo-NC	0.25	TcAg-NC	-0.50	RhPt-NC	-0.05
TcMn-NC	-0.12	CdNi-NC	0.31	TcCd-NC	-0.21	PdPt-NC	0.02
TcFe-NC	-0.05	CdCu-NC	0.54	RhRu-NC	0.03	AgPt-NC	-0.05
TcCo-NC	-0.16	CdZn-NC	0.02	PdRu-NC	0.12	CdPt-NC	0.24
TcNi-NC	-0.15	3d-5d		AgRu-NC	-0.04	5d-5d	
TcCu-NC	-0.43	ReMn-NC	0.12	CdRu-NC	0.26	ReOs-NC	-0.32
TcZn-NC	-0.32	ReFe-NC	0.07	RhPd-NC	-0.12	ReIr-NC	-0.16
RuMn-NC	0.20	ReCo-NC	0.06	AgRh-NC	-0.03	RePt-NC	0.18
RuFe-NC	0.28	ReNi-NC	0.07	CdRh-NC	0.22	OsIr-NC	0.25

RuCo-NC	0.33	ReCu-NC	-0.22	AgPd-NC	-0.04	OsPt-NC	0.15
RuNi-NC	0.24	ReZn-NC	-0.12	CdPd-NC	0.32	PtIr-NC	-0.10
RuCu-NC	0.15	OsMn-NC	0.48	CdAg-NC	-0.17		
RuZn-NC	0.25	OsFe-NC	0.24	4d-5d			
RhMn-NC	-0.08	OsCo-NC	0.13	ReTc-NC	-0.59		
RhFe-NC	0.01	OsNi-NC	0.06	ReRu-NC	-0.33		
RhCo-NC	0.04	OsCu-NC	0.03	ReRh-NC	-0.12		
RhNi-NC	-0.08	OsZn-NC	0.26	RePd-NC	0.08		

Table S21 The difference of adsorption energies of the metal atom between heteronuclear BACs and homonuclear BACs (ΔE_{ad}) of configurations 4 in eV.

	ΔE_{ad}		ΔE_{ad}		ΔE_{ad}		ΔE_{ad}
3d-3d		RhCu-NC	0.66	IrMn-NC	-0.39	ReAg-NC	-0.33
MnFe-NC	-0.15	RhZn-NC	0.55	IrFe-NC	-0.10	ReCd-NC	-0.42
MnCo-NC	-0.38	PdMn-NC	-0.53	IrCo-NC	0.07	TcOs-NC	-0.05
NiMn-NC	-0.30	PdFe-NC	-0.28	IrNi-NC	0.66	OsRu-NC	-0.02
CuMn-NC	-0.25	PdCo-NC	0.02	IrCu-NC	0.71	OsRh-NC	0.01
ZnMn-NC	-0.36	PdNi-NC	0.03	IrZn-NC	0.51	OsPd-NC	0.22
FeCo-NC	-0.08	PdCu-NC	0.00	PtMn-NC	-0.61	OsAg-NC	-0.05
NiFe-NC	-0.04	PdZn-NC	-0.21	PtFe-NC	-0.34	CdOs-NC	-0.11
FeCu-NC	0.10	AgMn-NC	-0.17	PtCo-NC	-0.10	TcIr-NC	-0.11
ZnFe-NC	-0.11	AgFe-NC	0.16	PtNi-NC	-0.07	RuIr-NC	-0.05
NiCo-NC	0.09	AgCo-NC	0.22	PtCu-NC	-0.07	RhIr-NC	-0.02
CuCo-NC	0.19	AgNi-NC	0.21	PtZn-NC	-0.30	PdIr-NC	0.53
ZnCo-NC	0.11	AgCu-NC	0.06	4d-4d		AgIr-NC	0.28
CuNi-NC	0.17	AgZn-NC	-0.18	TcRu-NC	-0.09	CdIr-NC	0.48
CuZn-NC	-0.17	CdMn-NC	0.08	TcRh-NC	-0.07	TcPt-NC	-0.03
NiZn-NC	0.03	CdFe-NC	0.46	TcPd-NC	0.02	RuPt-NC	0.07

3d-4d		CdCo-NC	0.75	TcAg-NC	-0.07	RhPt-NC	0.40
TcMn-NC	-0.17	CdNi-NC	0.77	TcCd-NC	-0.27	PdPt-NC	-0.02
TcFe-NC	0.14	CdCu-NC	0.50	RhRu-NC	0.00	AgPt-NC	0.16
TcCo-NC	0.04	CdZn-NC	0.39	PdRu-NC	0.12	CdPt-NC	0.33
TcNi-NC	0.38	3d-5d		AgRu-NC	0.17	5d-5d	
TcCu-NC	0.38	ReMn-NC	-0.27	CdRu-NC	0.02	ReOs-NC	0.03
TcZn-NC	0.11	ReFe-NC	0.04	RhPd-NC	0.43	ReIr-NC	-0.23
RuMn-NC	-0.13	ReCo-NC	-0.08	AgRh-NC	1.08	RePt-NC	0.02
RuFe-NC	0.04	ReNi-NC	0.37	CdRh-NC	0.66	OsIr-NC	0.00
RuCo-NC	0.08	ReCu-NC	0.35	AgPd-NC	0.12	OsPt-NC	0.22
RuNi-NC	0.49	ReZn-NC	-0.01	CdPd-NC	0.45	PtIr-NC	0.51
RuCu-NC	0.53	OsMn-NC	-0.21	CdAg-NC	0.39		
RuZn-NC	0.33	OsFe-NC	0.01	4d-5d			
RhMn-NC	-0.33	OsCo-NC	0.04	ReTc-NC	0.00		
RhFe-NC	0.12	OsNi-NC	0.53	ReRu-NC	-0.06		
RhCo-NC	0.14	OsCu-NC	0.55	ReRh-NC	-0.19		
RhNi-NC	0.63	OsZn-NC	0.24	RePd-NC	0.04		

Table S22 The difference of the chemical potentials between metal SA and metal NP ($\Delta E_{SA}^{f}(R)$) in eV for 3d-3d M_1M_2-NC.

	M_1M_2-NC-2		**M_1M_2-NC-4**	
	$\Delta E_{M_1}^{f}(R)$	$\Delta E_{M_2}^{f}(R)$	$\Delta E_{M_1}^{f}(R)$	$\Delta E_{M_2}^{f}(R)$
MnFe-NC	-3.43	-2.72	-4.04	-2.72
MnCo-NC	-3.69	-2.82	-3.59	-2.90
MnNi-NC	-3.43	-2.90	-3.80	-2.83
CuMn-NC	-1.52	-3.66	-1.14	-3.43
MnZn-NC	-3.55	-2.78	-3.77	-1.87
FeCo-NC	-3.28	-3.18	-3.17	-3.79

NiFe-NC	-3.03	-2.99	-3.77	-3.42
FeCu-NC	-3.13	-1.77	-2.95	-1.99
ZnFe-NC	-2.81	-3.01	-2.82	-3.40
CoNi-NC	-3.06	-3.26	-3.25	-2.97
CuCo-NC	-1.92	-3.02	-1.23	-2.82
ZnCo-NC	-3.02	-3.05	-1.93	-3.13
CuNi-NC	-1.61	-3.08	-1.53	-2.84
CuZn-NC	-1.65	-2.89	-1.79	-2.17
NiZn-NC	-3.66	-2.65	-3.23	-2.30
2Mn-NC	-2.85	-2.98	-2.68	-2.68
2Fe-NC	-3.08	-3.01	-3.76	-3.76
2Co-NC	-3.34	-3.09	-3.04	-3.04
2Ni-NC	-3.03	-3.28	-3.35	-3.35
2Cu-NC	-1.59	-1.76	-1.38	-1.38
2Zn-NC	-2.76	-3.53	-2.24	-2.24

Table S23 The difference of the chemical potentials between metal SA and metal NP ($\Delta E_{SA}^{f}(R)$) in eV for 3d-4d M_1M_2-NC. The BACs possess instability against atom aggregation are marked in red.

	M_1M_2-NC-2		**M_1M_2-NC-4**	
	$\Delta E_{M_1}^{f}(R)$	$\Delta E_{M_2}^{f}(R)$	$\Delta E_{M_1}^{f}(R)$	$\Delta E_{M_2}^{f}(R)$
TcMn-NC	-0.10	-2.46	-1.83	-2.38
TcFe-NC	-0.53	-2.12	-2.72	-1.95
TcCo-NC	-0.56	-2.30	-2.14	-2.00
TcNi-NC	-0.55	-2.24	-2.10	-1.68
TcZn-NC	-0.70	-2.16	-2.27	-0.93
TcCu-NC	-0.77	-1.16	-1.77	-0.04
RuMn-NC	-0.20	-3.11	-1.65	-2.47
RuFe-NC	-0.63	-2.77	-2.60	-2.18

RuCo-NC	-0.51	-2.80	-1.88	-2.09
RuNi-NC	-0.59	-2.83	-1.77	-1.70
RuZn-NC	-0.55	-2.56	-1.84	-0.84
RuCu-NC	-0.61	-1.55	-1.40	-0.02
RhMn-NC	-1.32	-3.75	-1.91	-3.02
RhFe-NC	-1.73	-3.38	-2.66	-2.45
RhCo-NC	-1.62	-3.43	-1.96	-2.38
RhNi-NC	-1.74	-3.06	-1.77	-1.91
RhZn-NC	-1.58	-3.10	-1.75	-0.97
RhCu-NC	-1.56	-2.02	-1.41	-0.23
PdMn-NC	-1.86	-3.43	-1.38	-3.27
PdFe-NC	-2.01	-3.01	-2.33	-2.90
PdCo-NC	-2.25	-3.09	-1.36	-2.55
PdNi-NC	-2.23	-3.02	-1.64	-2.55
PdZn-NC	-2.68	-2.71	-1.78	-1.77
PdCu-NC	-2.06	-1.62	-1.35	-0.95
AgMn-NC	-0.06	-3.42	0.57	-2.98
AgFe-NC	-0.22	-3.00	-0.29	-2.53
AgCo-NC	-0.37	-3.00	0.43	-2.43
AgNi-NC	-0.31	-2.89	0.13	-2.46
AgZn-NC	-0.91	-2.72	-0.17	-1.82
AgCu-NC	-0.24	-1.59	0.31	-0.96
CdMn-NC	-0.93	-3.52	0.21	-2.92
CdFe-NC	-0.92	-2.94	-0.61	-2.49
CdCo-NC	-1.04	-2.90	0.35	-2.09
CdNi-NC	-0.97	-2.78	0.08	-2.09
CdZn-NC	-1.76	-2.81	-0.21	-1.44
CdCu-NC	-0.59	-1.18	0.14	-0.72

Table S24 The difference of the chemical potentials between metal SA and metal NP ($\Delta E_{SA}^{f}(R)$) in eV for 3d-5d M_1M_2-NC. The BACs possess instability against atom aggregation are marked in red.

	M_1M_2-NC-2		**M_1M_2-NC-4**	
	$\Delta E_{M_1}^{f}(R)$	$\Delta E_{M_2}^{f}(R)$	$\Delta E_{M_1}^{f}(R)$	$\Delta E_{M_2}^{f}(R)$
ReMn-NC	0.77	-2.03	-1.33	-2.41
ReFe-NC	0.42	-1.81	-2.24	-2.00
ReCo-NC	0.17	-1.90	-1.66	-2.05
ReNi-NC	0.18	-1.84	-1.50	-1.62
ReZn-NC	-0.52	-1.77	-1.79	-0.98
ReCu-NC	0.04	-0.76	-1.20	0.00
OsMn-NC	0.85	-2.33	-1.13	-2.16
OsFe-NC	0.10	-2.30	-2.11	-1.81
OsCo-NC	0.06	-2.49	-1.41	-1.74
OsNi-NC	0.00	-2.51	-1.21	-1.26
OsZn-NC	0.21	-2.06	-1.41	-0.53
OsCu-NC	0.04	-1.17	-0.86	0.40
IrMn-NC	-0.93	-3.17	-1.52	-2.60
IrFe-NC	-1.38	-3.05	-2.42	-2.18
IrCo-NC	-1.54	-3.05	-1.59	-1.97
IrNi-NC	-1.56	-3.02	-1.28	-1.39
IrZn-NC	-1.94	-2.64	-1.39	-0.52
IrCu-NC	-1.37	-1.61	-0.91	0.30
PtMn-NC	-2.01	-3.54	-1.57	-2.92
PtFe-NC	-1.94	-2.90	-2.42	-2.53
PtCo-NC	-2.42	-3.22	-1.51	-2.24

PtNi-NC	-2.44	-3.19	-1.76	-2.22
PtZn-NC	-2.86	-2.86	-1.90	-1.44
PtCu-NC	-2.24	-1.77	-1.44	-0.59

Table S25 The difference of the chemical potentials between metal SA and metal NP ($\Delta E_{SA}^{f}(R)$) in eV for 4d-4d M_1M_2-NC. The BACs possess instability against atom aggregation are marked in red.

	M_1M_2-NC-2		**M_1M_2-NC-4**	
	$\Delta E_{M_1}^{f}(R)$	$\Delta E_{M_2}^{f}(R)$	$\Delta E_{M_1}^{f}(R)$	$\Delta E_{M_2}^{f}(R)$
TcRu-NC	-0.54	-0.37	-1.41	-1.06
TcRh-NC	-0.68	-1.05	-1.73	-1.17
TcPd-NC	-0.50	-1.16	-1.69	-0.35
TcCd-NC	-0.31	-0.30	-2.25	0.33
TcAg-NC	-0.62	0.31	-1.85	1.15
RhRu-NC	-1.66	-0.74	-1.24	-1.45
PdRu-NC	-0.87	-0.65	-0.39	-1.38
CdRu-NC	-0.76	-0.26	0.49	-1.74
AgRu-NC	-0.15	-0.58	1.25	-1.40
RhPd-NC	-1.71	-2.44	-1.20	-0.42
RhAg-NC	-1.40	-0.54	-0.63	1.81
RhCd-NC	-1.14	-1.20	-1.24	0.78
AgPd-NC	-0.52	-1.68	0.81	-0.86
CdPd-NC	-1.07	-1.30	0.52	-0.73
CdAg-NC	-0.91	0.02	0.39	0.81
2Tc-NC	0.53	0.73	-1.18	-1.18
2Ru-NC	-0.87	-0.49	-1.10	-1.10
2Rh-NC	-2.05	-1.61	-1.58	-1.58
2Pd-NC	-2.29	-1.87	-0.91	-0.91
2Ag-NC	-0.03	0.17	0.61	0.61

2Cd-NC	-1.09	-0.73	-0.20	-0.20

Table S26 The difference of the chemical potentials between metal SA and metal NP ($\Delta E_{SA}^{f}(R)$) in eV for 4d-5d M_1M_2-NC. The BACs possess instability against atom aggregation are marked in red.

	M_1M_2-NC-2		**M_1M_2-NC-4**	
	$\Delta E_{M_1}^{f}(R)$	$\Delta E_{M_2}^{f}(R)$	$\Delta E_{M_1}^{f}(R)$	$\Delta E_{M_2}^{f}(R)$
TcIr-NC	-0.51	-0.50	-1.29	-0.76
RhIr-NC	-2.09	-1.21	-1.12	-1.15
RuIr-NC	-1.06	-0.73	-1.02	-0.86
PdIr-NC	-2.42	-1.25	0.16	-0.65
CdIr-NC	-1.15	-1.00	1.09	-0.97
AgIr-NC	-0.54	-0.96	1.49	-0.98
RhPt-NC	-2.26	-2.07	-0.80	-0.48
TcPt-NC	-0.59	-1.28	-1.31	-0.43
RuPt-NC	-1.23	-1.59	-1.00	-0.49
PdPt-NC	-2.46	-1.99	-0.50	-0.96
AgPt-NC	-0.72	-1.83	1.27	-0.85
CdPt-NC	-1.34	-1.89	0.83	-0.87
TcOs-NC	-0.44	0.37	-0.97	-0.50
RhOs-NC	-1.44	0.10	-0.83	-0.92
RuOs-NC	-0.70	0.29	-0.72	-0.62
PdOs-NC	-1.70	0.12	0.11	-0.75
CdOs-NC	-0.65	0.15	0.76	-1.35
AgOs-NC	-0.21	0.03	1.43	-1.10
RhRe-NC	-0.66	-0.15	-1.23	-1.25

TcRe-NC	0.13	0.70	-1.12	-0.58
RuRe-NC	-0.04	-0.02	-0.96	-0.78
PdRe-NC	-0.73	0.08	-0.27	-1.07
CdRe-NC	-0.09	0.11	0.25	-1.80
AgRe-NC	0.61	0.05	0.95	-1.52

Table S27 The difference of the chemical potentials between metal SA and metal NP ($\Delta E_{SA}^{f}(R)$) in eV for 5d-5d M_1M_2-NC. The BACs possess instability against atom aggregation are marked in red.

	M_1M_2-NC-2		**M_1M_2-NC-4**	
	$\Delta E_{M_1}^{f}(R)$	$\Delta E_{M_2}^{f}(R)$	$\Delta E_{M_1}^{f}(R)$	$\Delta E_{M_2}^{f}(R)$
ReIr-NC	-0.18	-0.25	-0.81	-0.82
ReOs-NC	0.14	0.74	-0.28	-0.35
RePt-NC	-0.01	-0.76	-0.66	-0.32
OsIr-NC	0.10	-0.49	-0.44	-0.39
OsPt-NC	-0.46	-1.46	-0.33	0.08
PtIr-NC	-2.54	-1.34	0.12	-0.23
2Re-NC	1.24	1.48	-0.51	-0.51
2Os-NC	0.05	0.40	-0.18	-0.18
2Ir-NC	-1.58	-1.08	-0.65	-0.65
2Pt-NC	-2.62	-2.11	-0.51	-0.51

Table S28 The BACs prepared in experiments[13-27].

	Catalytic reaction	References
2Fe-NC	ORR	Chem. 2019, 5, 1-14
2Co-NC	ORR	Nano Energy. 2018, 46, 396-403
2Cu-NC	CO_2RR	ACS Energy Lett. 2020, 5, 1044-1053
2Ni-NC	CO_2RR	J. Am. Chem. Soc. 2021, 143, 11317-11324
FeCu-NC	ORR	J. Mater. Chem. A, 2020, 8, 16994-17001
FeNi-NC	ORR	J. Phys. Chem. Lett., 2020, 11, 1404-1410
	CO_2RR	Angew. Chem. Int. Ed., 2019, 58, 6972-6976
FeCo-NC	ORR	J. Am. Chem. Soc., 2017, 139, 17281-17284
	ORR	Energy Environ. Sci., 2018, 11, 3375-3379
FeMn-NC	ORR	Appl Catal. B, 2021, 288, 120021
NiCo-NC	ORR	Adv. Mater., 2019, 1905622
ZnCo-NC	ORR	Angew. Chem. Int. Ed., 2019, 58, 2622-2626
PdCu-NC	NRR	Angew. Chem. Int. Ed., 2021, 60, 345-350
PtCo-NC	ORR	J. Am. Chem. Soc., 2018, 140, 10757-10763
PtRu-NC	HER	Nat. Commun., 2019, 10, 4936

Table S29 The data of Z_0, A, B, C, D and F for 5d metal atom aggregation of 5d-3d and 5d-4d/5d BACs.

M_2		Z_0	a	b	c	d	f
7~9 group	5d-3d	-889.41	-4.30	121.90	0.0435	-3.87	0.0516

metal atom	5d-4d/5d	194.51	-9.62	0.028	0.115	-0.0019	0.0044
10~12 group	5d-3d	154.07	-18.94	2.39	0.535	-0.083	-0.022
metal atom	5d-4d/5d	-112.57	11.87	0.062	-0.316	0.001	-0.0037

Table S30 The dissolution potential of M_1 and M_2 atoms in eV for 3d-3d M_1M_2-NC in pH = 0.

	M_1M_2-NC-2		**M_1M_2-NC-4**	
	$U_{dis(M1)}$	$U_{dis(M2)}$	$U_{dis(M1)}$	$U_{dis(M2)}$
MnFe-NC	0.53	0.91	0.83	0.91
MnCo-NC	0.66	1.13	0.61	1.17
NiMn-NC	1.19	0.53	1.16	0.72
CuMn-NC	1.10	0.65	0.91	0.53
ZnMn-NC	0.63	0.59	0.18	0.70
FeCo-NC	1.19	1.21	1.14	1.62
NiFe-NC	1.26	1.05	1.63	1.26
FeCu-NC	1.12	1.11	1.03	1.34
ZnFe-NC	0.64	1.06	0.65	1.25
NiCo-NC	1.37	1.25	1.23	1.34
CuCo-NC	1.30	1.23	0.96	1.13
ZnCo-NC	0.75	1.25	0.20	1.29
CuNi-NC	1.15	1.28	1.11	1.17
CuZn-NC	1.17	0.68	1.24	0.33
NiZn-NC	1.57	0.56	1.36	0.39
2Mn-NC	0.24	0.36	0.16	0.16
2Fe-NC	1.09	1.06	1.43	1.43
2Co-NC	1.26	1.39	1.24	1.24
2Ni-NC	1.26	1.38	1.42	1.42
2Cu-NC	1.14	1.22	1.03	1.03

2Zn-NC	0.62	1.00	0.35	0.35

Table S31 The dissolution potential of M_1 and M_2 atoms in eV for 3d-4d M_1M_2-NC in pH = 0.

	M_1M_2-NC-2		**M_1M_2-NC-4**	
	$U_{dis(M1)}$	$U_{dis(M2)}$	$U_{dis(M1)}$	$U_{dis(M2)}$
TcMn-NC	0.45	0.05	1.32	0.01
TcFe-NC	0.67	0.61	1.76	0.53
TcCo-NC	0.68	0.87	1.47	0.72
TcNi-NC	0.67	0.86	1.45	0.58
TcZn-NC	0.75	0.32	1.54	-0.30
TcCu-NC	0.78	0.92	1.28	0.36
RuMn-NC	0.55	0.37	1.28	0.05
RuFe-NC	0.77	0.94	1.76	0.64
RuCo-NC	0.71	1.12	1.40	0.77
RuNi-NC	0.75	1.16	1.34	0.59
RuZn-NC	0.73	0.52	1.37	-0.34
RuCu-NC	0.76	1.12	1.15	0.35
RhMn-NC	1.26	0.69	1.56	0.33
RhFe-NC	1.46	1.24	1.93	0.78
RhCo-NC	1.41	1.43	1.58	0.91
RhNi-NC	1.47	1.27	1.49	0.70
RhZn-NC	1.39	0.79	1.48	-0.28
RhCu-NC	1.38	1.35	1.30	0.46
PdMn-NC	1.85	0.53	1.61	0.45
PdFe-NC	1.92	1.06	2.08	1.00

PdCo-NC	2.04	1.26	1.59	1.00
PdNi-NC	2.03	1.25	1.73	1.02
PdZn-NC	2.25	0.59	1.81	0.12
PdCu-NC	1.94	1.15	1.59	0.82
AgMn-NC	0.86	0.52	0.23	0.31
AgFe-NC	1.02	1.05	1.09	0.82
AgCo-NC	1.17	1.22	0.37	0.93
AgNi-NC	1.11	1.19	0.67	0.97
AgZn-NC	1.71	0.60	0.97	0.15
AgCu-NC	1.04	1.14	0.49	0.82
CdMn-NC	0.06	0.57	-0.51	0.28
CdFe-NC	0.06	1.02	-0.07	0.80
CdCo-NC	0.12	1.17	-0.58	0.76
CdNi-NC	0.08	1.13	-0.44	0.79
CdZn-NC	0.48	0.65	-0.30	-0.04
CdCu-NC	-0.11	0.93	-0.47	0.70

Table S32 The dissolution potential of M_1 and M_2 atoms in eV for 3d-5d M_1M_2-NC in pH = 0.

	M_1M_2-NC-2		**M_1M_2-NC-4**	
	$U_{dis(M1)}$	$U_{dis(M2)}$	$U_{dis(M1)}$	$U_{dis(M2)}$
ReMn-NC	0.04	-0.17	0.74	0.02
ReFe-NC	0.16	0.46	1.05	0.55
ReCo-NC	0.24	0.67	0.85	0.74
ReNi-NC	0.24	0.66	0.80	0.55
ReZn-NC	0.47	0.12	0.90	-0.27
ReCu-NC	0.29	0.72	0.70	0.34
OsMn-NC	0.49	-0.02	1.42	-0.11
OsFe-NC	0.80	0.70	1.90	0.46

OsCo-NC	0.82	0.96	1.55	0.59
OsNi-NC	0.85	1.00	1.46	0.37
OsZn-NC	0.74	0.27	1.55	-0.50
OsCu-NC	0.83	0.93	1.28	0.14
IrMn-NC	1.47	0.40	1.66	0.12
IrFe-NC	1.62	1.08	1.96	0.64
IrCo-NC	1.67	1.24	1.69	0.71
IrNi-NC	1.68	1.25	1.58	0.44
IrZn-NC	1.80	0.56	1.60	-0.50
IrCu-NC	1.61	1.14	1.46	0.19
PtMn-NC	2.18	0.59	1.97	0.27
PtFe-NC	2.15	1.00	2.39	0.82
PtCo-NC	2.39	1.33	1.93	0.84
PtNi-NC	2.40	1.34	2.06	0.86
PtZn-NC	2.61	0.67	2.13	-0.04
PtCu-NC	2.30	1.22	1.90	0.64

Table S33 The dissolution potential of M_1 and M_2 atoms in eV for 4d-4d M_1M_2-NC in pH = 0.

	M_1M_2-NC-2		**M_1M_2-NC-4**	
	$U_{dis(M1)}$	$U_{dis(M2)}$	$U_{dis(M1)}$	$U_{dis(M2)}$
TcRu-NC	0.67	0.64	1.10	0.98
TcRh-NC	0.74	1.13	1.27	1.19
TcPd-NC	0.65	1.49	1.24	1.09
TcCd-NC	0.55	-0.25	1.53	-0.57
TcAg-NC	0.71	0.49	1.33	-0.35
RhRu-NC	1.43	0.83	1.22	1.18
PdRu-NC	1.61	0.78	1.11	1.14
CdRu-NC	-0.02	0.59	-0.65	1.33

AgRu-NC	0.95	0.74	-0.45	1.15
RhPd-NC	1.46	2.13	1.20	1.13
RhAg-NC	1.30	1.34	0.92	-1.01
RhCd-NC	1.17	0.20	1.22	-0.79
AgPd-NC	1.32	1.75	-0.01	1.34
CdPd-NC	0.13	1.57	-0.66	1.28
CdAg-NC	0.05	0.78	-0.60	-0.01
2Tc-NC	0.13	0.04	0.99	0.99
2Ru-NC	0.89	0.70	1.01	1.01
2Rh-NC	1.62	1.40	1.39	1.39
2Pd-NC	2.06	1.85	1.37	1.37
2Ag-NC	0.83	0.63	0.19	0.19
2Cd-NC	0.14	-0.04	-0.31	-0.31

Table S34 The dissolution potential of M_1 and M_2 atoms in eV for 4d-5d M_1M_2-NC in pH = 0.

	M_1M_2-NC-2		**M_1M_2-NC-4**	
	$U_{dis(M1)}$	$U_{dis(M2)}$	$U_{dis(M1)}$	$U_{dis(M2)}$
TcIr-NC	0.66	1.32	1.04	1.41
RhIr-NC	1.64	1.56	1.16	1.54
RuIr-NC	0.99	1.40	0.96	1.44
PdIr-NC	2.12	1.57	0.83	1.37
CdIr-NC	0.17	1.49	-0.95	1.48
AgIr-NC	1.34	1.48	-0.69	1.48
RhPt-NC	1.73	2.21	1.00	1.42
TcPt-NC	0.70	1.82	1.06	1.40
RuPt-NC	1.07	1.98	0.95	1.42
PdPt-NC	2.15	2.17	1.17	1.66
AgPt-NC	1.52	2.10	-0.47	1.61
CdPt-NC	0.27	2.12	-0.82	1.62

TcOs-NC	0.62	0.66	0.88	1.10
RhOs-NC	1.32	0.80	1.01	1.31
RuOs-NC	0.80	0.70	0.81	1.16
PdOs-NC	1.77	0.79	0.86	1.23
CdOs-NC	-0.08	0.78	-0.78	1.53
AgOs-NC	1.01	0.83	-0.63	1.40
RhRe-NC	0.93	0.35	1.21	0.72
TcRe-NC	0.34	0.07	0.96	0.49
RuRe-NC	0.31	0.48	0.96	0.56
PdRe-NC	1.28	0.27	1.05	0.66
CdRe-NC	-0.36	0.26	-0.53	0.90
AgRe-NC	0.19	0.28	-0.15	0.81

Table S35 The dissolution potential of M_1 and M_2 atoms in eV for 5d-5d M_1M_2-NC in pH = 0.

	M_1M_2-NC-2		**M_1M_2-NC-4**	
	$U_{dis(M1)}$	$U_{dis(M2)}$	$U_{dis(M1)}$	$U_{dis(M2)}$
ReIr-NC	0.36	1.24	0.57	1.43
ReOs-NC	0.25	0.48	0.39	1.02
RePt-NC	0.30	1.56	0.52	1.34
OsIr-NC	0.80	1.32	1.07	1.29
OsPt-NC	1.08	1.91	1.02	1.14
PtIr-NC	2.45	1.60	1.12	1.23
2Re-NC	-0.11	-0.19	0.47	0.47
2Os-NC	0.83	0.65	0.94	0.94
2Ir-NC	1.68	1.52	1.37	1.37
2Pt-NC	2.49	2.23	1.43	1.43

Table S36 The dissolution potential (vs RHE) of M_1 and M_2 atoms in eV for 3d-3d M_1M_2-NC in pH = 14.

	M_1M_2-NC-2		**M_1M_2-NC-4**	
	$U_{dis(M1)}$	$U_{dis(M2)}$	$U_{dis(M1)}$	$U_{dis(M2)}$
MnFe-NC	0.98	1.31	1.29	1.31
MnCo-NC	1.11	1.51	1.06	1.55
NiMn-NC	1.56	0.98	1.52	1.17
CuMn-NC	1.37	1.10	1.18	0.98
ZnMn-NC	0.97	1.04	0.52	1.15
FeCo-NC	1.59	1.69	1.54	2.00
NiFe-NC	1.62	1.45	1.99	1.66
FeCu-NC	1.52	1.49	1.43	1.60
ZnFe-NC	0.98	1.45	0.99	1.65
NiCo-NC	1.74	1.63	1.59	1.72
CuCo-NC	1.57	1.61	1.22	1.51
ZnCo-NC	1.09	1.62	0.54	1.66
CuNi-NC	1.41	1.65	1.37	1.53
CuZn-NC	1.43	1.02	1.50	0.67
NiZn-NC	1.94	0.90	1.72	0.73
2Mn-NC	0.69	0.76	0.61	0.61
2Fe-NC	1.46	1.49	1.83	1.83
2Co-NC	1.64	1.77	1.62	1.62
2Ni-NC	1.62	1.75	1.78	1.78

2Cu-NC	1.40	1.49	1.30	1.30
2Zn-NC	0.96	1.34	0.70	0.70

Table S37 The dissolution potential of M_1 and M_2 atoms in eV for 3d-4d M_1M_2-NC in pH = 14.

	M_1M_2-NC-2		**M_1M_2-NC-4**	
	$U_{dis(M1)}$	$U_{dis(M2)}$	$U_{dis(M1)}$	$U_{dis(M2)}$
TcMn-NC	0.30	0.50	0.73	0.46
TcFe-NC	0.41	1.01	0.95	0.92
TcCo-NC	0.41	1.25	0.81	1.10
TcNi-NC	0.41	1.23	0.80	0.94
TcZn-NC	0.45	0.66	0.84	0.04
TcCu-NC	0.46	1.19	0.71	0.62
RuMn-NC	0.80	0.82	1.29	0.50
RuFe-NC	0.95	1.33	1.61	1.04
RuCo-NC	0.91	1.50	1.37	1.14
RuNi-NC	0.93	1.52	1.33	0.96
RuZn-NC	0.92	0.86	1.35	0.00
RuCu-NC	0.94	1.38	1.20	0.61
RhMn-NC	1.50	1.14	1.79	0.78
RhFe-NC	1.70	1.64	2.17	1.17
RhCo-NC	1.65	1.81	1.82	1.29
RhNi-NC	1.71	1.64	1.72	1.06
RhZn-NC	1.63	1.13	1.72	0.06
RhCu-NC	1.62	1.62	1.54	0.72
PdMn-NC	1.83	0.98	1.59	0.90

PdFe-NC	1.90	1.46	2.06	1.40
PdCo-NC	2.02	1.64	1.58	1.37
PdNi-NC	2.01	1.62	1.72	1.38
PdZn-NC	2.24	0.93	1.79	0.46
PdCu-NC	1.93	1.42	1.57	1.08
AgMn-NC	1.23	0.98	0.60	0.76
AgFe-NC	1.39	1.45	1.46	1.21
AgCo-NC	1.54	1.60	0.74	1.31
AgNi-NC	1.48	1.55	1.04	1.33
AgZn-NC	2.08	0.94	1.34	0.49
AgCu-NC	1.40	1.40	0.86	1.09
CdMn-NC	0.47	1.03	-0.10	0.73
CdFe-NC	0.47	1.42	0.34	1.19
CdCo-NC	0.52	1.55	-0.17	1.14
CdNi-NC	0.49	1.49	-0.03	1.15
CdZn-NC	0.89	0.99	0.11	0.30
CdCu-NC	0.30	1.20	-0.06	0.96

Table S38 The dissolution potential of M_1 and M_2 atoms in eV for 3d-5d M_1M_2-NC in pH = 14.

	M_1M_2-NC-2		**M_1M_2-NC-4**	
	$U_{dis(M1)}$	$U_{dis(M2)}$	$U_{dis(M1)}$	$U_{dis(M2)}$
ReMn-NC	0.13	0.28	0.43	0.47
ReFe-NC	0.18	0.86	0.56	0.95
ReCo-NC	0.22	1.05	0.48	1.12
ReNi-NC	0.22	1.02	0.46	0.92
ReZn-NC	0.32	0.47	0.50	0.07
ReCu-NC	0.24	0.98	0.41	0.61
OsMn-NC	0.46	0.43	0.96	0.34

OsFe-NC	0.65	1.10	1.20	0.85
OsCo-NC	0.66	1.34	1.03	0.96
OsNi-NC	0.68	1.36	0.98	0.74
OsZn-NC	0.62	0.61	1.03	-0.16
OsCu-NC	0.67	1.19	0.89	0.40
IrMn-NC	1.16	0.85	1.31	0.57
IrFe-NC	1.27	1.47	1.53	1.04
IrCo-NC	1.31	1.62	1.32	1.08
IrNi-NC	1.32	1.62	1.25	0.80
IrZn-NC	1.41	0.90	1.26	-0.16
IrCu-NC	1.27	1.41	1.15	0.46
PtMn-NC	1.97	1.04	1.75	0.73
PtFe-NC	1.94	1.40	2.18	1.22
PtCo-NC	2.18	1.71	1.71	1.22
PtNi-NC	2.19	1.70	1.85	1.22
PtZn-NC	2.40	1.01	1.92	0.30
PtCu-NC	2.08	1.49	1.69	0.90

Table S39 The dissolution potential of M_1 and M_2 atoms in eV for 4d-4d M_1M_2-NC in pH = 14.

	M_1M_2-NC-2		**M_1M_2-NC-4**	
	$U_{dis(M1)}$	$U_{dis(M2)}$	$U_{dis(M1)}$	$U_{dis(M2)}$
TcRu-NC	0.41	0.86	0.62	1.09
TcRh-NC	0.44	1.37	0.70	1.28
TcPd-NC	0.40	1.48	0.69	1.07
TcCd-NC	0.35	0.16	0.84	-0.16
TcAg-NC	0.43	0.86	0.74	0.02
RhRu-NC	1.67	0.99	1.46	1.22
PdRu-NC	1.82	0.95	1.09	1.20

CdRu-NC	0.38	0.82	-0.24	1.32
AgRu-NC	1.32	0.93	-0.08	1.20
RhPd-NC	1.70	2.12	1.44	1.11
RhAg-NC	1.54	1.71	1.15	-0.64
RhCd-NC	1.41	0.61	1.46	-0.39
AgPd-NC	1.69	1.74	0.36	1.33
CdPd-NC	0.54	1.55	-0.26	1.26
CdAg-NC	0.46	1.15	-0.19	0.36
2Tc-NC	0.14	0.09	0.57	0.57
2Ru-NC	1.03	0.90	1.10	1.10
2Rh-NC	1.86	1.64	1.63	1.63
2Pd-NC	2.04	1.83	1.35	1.35
2Ag-NC	1.20	1.00	0.56	0.56
2Cd-NC	0.55	0.37	0.10	0.10

Table S40 The dissolution potential of M_1 and M_2 atoms in eV for 4d-5d M_1M_2-NC in pH = 14.

	M_1M_2-NC-2		**M_1M_2-NC-4**	
	$U_{dis(M1)}$	$U_{dis(M2)}$	$U_{dis(M1)}$	$U_{dis(M2)}$
TcIr-NC	0.40	1.05	0.59	1.12
RhIr-NC	1.88	1.23	1.40	1.21
RuIr-NC	1.09	1.11	1.08	1.14
PdIr-NC	2.10	1.24	0.82	1.09
CdIr-NC	0.58	1.18	-0.54	1.17
AgIr-NC	1.71	1.16	-0.32	1.17
RhPt-NC	1.97	2.00	1.24	1.21
TcPt-NC	0.42	1.61	0.60	1.18
RuPt-NC	1.15	1.76	1.07	1.21
PdPt-NC	2.13	1.96	1.15	1.45
AgPt-NC	1.89	1.88	-0.10	1.40

CdPt-NC	0.67	1.91	-0.41	1.40
TcOs-NC	0.38	0.58	0.51	0.80
RhOs-NC	1.56	0.65	1.25	0.91
RuOs-NC	0.97	0.60	0.98	0.83
PdOs-NC	1.75	0.65	0.84	0.87
CdOs-NC	0.33	0.64	-0.37	1.02
AgOs-NC	1.38	0.67	-0.26	0.95
RhRe-NC	1.17	0.26	1.45	0.42
TcRe-NC	0.24	0.14	0.55	0.33
RuRe-NC	0.75	0.25	1.06	0.35
PdRe-NC	1.26	0.23	1.03	0.40
CdRe-NC	0.05	0.23	-0.12	0.50
AgRe-NC	0.56	0.24	0.22	0.46

Table S41 The dissolution potential of M_1 and M_2 atoms in eV for 5d-5d M_1M_2-NC in pH = 14.

	M_1M_2-NC-2		**M_1M_2-NC-4**	
	$U_{dis(M1)}$	$U_{dis(M2)}$	$U_{dis(M1)}$	$U_{dis(M2)}$
ReIr-NC	0.27	0.99	0.36	1.13
ReOs-NC	0.22	0.49	0.28	0.76
RePt-NC	0.24	1.35	0.34	1.13
OsIr-NC	0.65	1.05	0.79	1.02
OsPt-NC	0.79	1.70	0.76	0.93
PtIr-NC	2.24	1.26	0.91	0.98
2Re-NC	0.07	0.03	0.32	0.32
2Os-NC	0.67	0.58	0.72	0.72
2Ir-NC	1.32	1.20	1.09	1.09
2Pt-NC	2.28	2.02	1.22	1.22

Table S42 The stability against leaching of 3d-3d M_1M_2-NC in the operating voltages of commercial catalysts in ORR, OER and HER at pH=0.

	M_1M_2-NC-2			**M_1M_2-NC-4**		
	ORR	OER	HER	ORR	OER	HER
MnFe-NC	×	×	√	√	×	√
MnCo-NC	×	×	√	×	×	√
NiMn-NC	×	×	√	×	×	√
CuMn-NC	×	×	√	×	×	√
ZnMn-NC	×	×	√	×	×	√
FeCo-NC	√	×	√	√	×	√
NiFe-NC	√	×	√	√	×	√
FeCu-NC	√	×	√	√	×	√
ZnFe-NC	×	×	√	×	×	√
NiCo-NC	√	×	√	√	×	√
CuCo-NC	√	×	√	√	×	√
ZnCo-NC	×	×	√	×	×	√
CuNi-NC	√	×	√	√	×	√
CuZn-NC	×	×	√	×	×	√
NiZn-NC	×	×	√	×	×	√
2Mn-NC	×	×	√	×	×	√
2Fe-NC	√	×	√	√	×	√
2Co-NC	√	×	√	√	×	√
2Ni-NC	√	×	√	√	×	√

2Cu-NC	√	×	√	√	×	√
2Zn-NC	×	×	√	×	×	√

Table S43 The stability against leaching of 3d-4d M_1M_2-NC in the operating voltages of commercial catalysts in ORR, OER and HER at pH=0.

	M_1M_2-NC-2			**M_1M_2-NC-4**		
	ORR	OER	HER	ORR	OER	HER
TcMn-NC	×	×	√	×	×	√
TcFe-NC	×	×	√	×	×	√
TcCo-NC	×	×	√	×	×	√
TcNi-NC	×	×	√	×	×	√
TcZn-NC	×	×	√	×	×	×
TcCu-NC	×	×	√	×	×	√
RuMn-NC	×	×	√	×	×	√
RuFe-NC	×	×	√	×	×	√
RuCo-NC	×	×	√	×	×	√
RuNi-NC	×	×	√	×	×	√
RuZn-NC	×	×	√	×	×	×
RuCu-NC	×	×	√	×	×	√
RhMn-NC	×	×	√	×	×	√
RhFe-NC	√	×	√	×	×	√
RhCo-NC	√	×	√	√	×	√
RhNi-NC	√	×	√	×	×	√
RhZn-NC	×	×	√	×	×	×
RhCu-NC	√	×	√	×	×	√

PdMn-NC	×	×	√	×	×	√
PdFe-NC	√	×	√	√	×	√
PdCo-NC	√	×	√	√	×	√
PdNi-NC	√	×	√	√	×	√
PdZn-NC	×	×	√	×	×	√
PdCu-NC	√	×	√	√	×	√
AgMn-NC	×	×	√	×	×	√
AgFe-NC	√	×	√	√	×	√
AgCo-NC	√	×	√	×	×	√
AgNi-NC	√	×	√	×	×	√
AgZn-NC	×	×	√	×	×	√
AgCu-NC	√	×	√	×	×	√
CdMn-NC	×	×	√	×	×	×
CdFe-NC	×	×	√	×	×	√
CdCo-NC	×	×	√	×	×	×
CdNi-NC	×	×	√	×	×	×
CdZn-NC	×	×	√	×	×	×
CdCu-NC	×	×	×	×	×	×

Table S44 The stability against leaching of 3d-5d M_1M_2-NC in the operating voltages of commercial catalysts in ORR, OER and HER at pH=0.

	M_1M_2-NC-2			**M_1M_2-NC-4**		
	ORR	OER	HER	ORR	OER	HER
ReMn-NC	×	×	×	×	×	√
ReFe-NC	×	×	√	×	×	√
ReCo-NC	×	×	√	×	×	√
ReNi-NC	×	×	√	×	×	√
ReZn-NC	×	×	√	×	×	×
ReCu-NC	×	×	√	×	×	√
OsMn-NC	×	×	√	×	×	×

OsFe-NC	×	×	√	×	×	√
OsCo-NC	√	×	√	×	×	√
OsNi-NC	√	×	√	×	×	√
OsZn-NC	×	×	√	×	×	×
OsCu-NC	√	×	√	×	×	√
IrMn-NC	×	×	√	×	×	√
IrFe-NC	√	×	√	×	×	√
IrCo-NC	√	×	√	×	×	√
IrNi-NC	√	×	√	×	×	√
IrZn-NC	×	×	√	×	×	×
IrCu-NC	√	×	√	×	×	√
PtMn-NC	×	×	√	×	×	√
PtFe-NC	√	×	√	×	×	√
PtCo-NC	√	×	√	√	×	√
PtNi-NC	√	×	√	√	×	√
PtZn-NC	×	×	√	×	×	√
PtCu-NC	√	×	√	×	×	√

Table S45 The stability against leaching of 4d-4d M_1M_2-NC in the operating voltages of commercial catalysts in ORR, OER and HER at pH=0.

	M_1M_2-NC-2			**M_1M_2-NC-4**		
	ORR	OER	HER	ORR	OER	HER
TcRu-NC	×	×	√	√	×	√
TcRh-NC	×	×	√	√	×	√
TcPd-NC	×	×	√	√	×	√
TcCd-NC	×	×	×	×	×	×
TcAg-NC	×	×	√	×	×	×
RhRu-NC	√	×	√	√	×	√
PdRu-NC	×	×	√	√	×	√

CdRu-NC	×	×	√	×	×	×
AgRu-NC	×	×	√	×	×	×
RhPd-NC	√	×	√	√	×	√
RhAg-NC	√	×	√	×	×	×
RhCd-NC	×	×	√	×	×	×
AgPd-NC	√	×	√	×	×	√
CdPd-NC	×	×	√	×	×	×
CdAg-NC	×	×	√	×	×	×
2Tc-NC	×	×	√	√	×	√
2Ru-NC	×	×	√	√	×	√
2Rh-NC	√	×	√	√	×	√
2Pd-NC	√	×	√	√	×	√
2Ag-NC	×	×	√	×	×	√
2Cd-NC	×	×	√	×	×	×

Table S46 The stability against leaching of 4d-5d M_1M_2-NC in the operating voltages of commercial catalysts in ORR, OER and HER at pH=0.

	M_1M_2-NC-2			**M_1M_2-NC-4**		
	ORR	OER	HER	ORR	OER	HER
TcIr-NC	×	×	√	√	×	√
RhIr-NC	√	×	√	√	×	√
RuIr-NC	√	×	√	√	×	√
PdIr-NC	√	×	√	√	×	√
CdIr-NC	×	×	√	×	×	×
AgIr-NC	√	×	√	×	×	×
RhPt-NC	√	×	√	√	×	√
TcPt-NC	×	×	√	√	×	√
RuPt-NC	√	×	√	√	×	√
PdPt-NC	√	√	√	√	×	√

AgPt-NC	√	×	√	×	×	×
CdPt-NC	×	×	√	×	×	×
TcOs-NC	×	×	√	√	×	√
RhOs-NC	√	×	√	√	×	√
RuOs-NC	×	×	√	√	×	√
PdOs-NC	×	×	√	√	×	√
CdOs-NC	×	×	√	×	×	×
AgOs-NC	√	×	√	×	×	×
RhRe-NC	×	×	√	×	×	√
TcRe-NC	×	×	√	×	×	√
RuRe-NC	×	×	√	×	×	√
PdRe-NC	×	×	√	×	×	√
CdRe-NC	×	×	×	×	×	×
AgRe-NC	×	×	√	×	×	×

Table S47 The stability against leaching of 5d-5d M_1M_2-NC in the operating voltages of commercial catalysts in ORR, OER and HER at pH=0.

	M_1M_2-NC-2			**M_1M_2-NC-4**		
	ORR	OER	HER	ORR	OER	HER
ReIr-NC	×	×	√	×	×	√
ReOs-NC	×	×	√	×	×	√
RePt-NC	×	×	√	×	×	√
OsIr-NC	√	×	√	√	×	√
OsPt-NC	√	×	√	√	×	√
PtIr-NC	√	×	√	√	×	√
2Re-NC	×	×	×	×	×	√
2Os-NC	×	×	√	√	×	√
2Ir-NC	√	×	√	√	×	√
2Pt-NC	√	√	√	√	×	√

Table S48 The stability against leaching of 3d-3d M_1M_2-NC in the operating voltages of commercial catalysts in ORR, OER and HER at pH=14.

	M_1M_2-NC-2			**M_1M_2-NC-4**		
	ORR	OER	HER	ORR	OER	HER
MnFe-NC	√	×	√	√	×	√
MnCo-NC	√	×	√	×	×	√
NiMn-NC	√	×	√	√	×	√
CuMn-NC	√	×	√	√	×	√
ZnMn-NC	√	×	√	×	×	√
FeCo-NC	√	×	√	√	×	√
NiFe-NC	√	×	√	√	×	√
FeCu-NC	√	×	√	√	×	√
ZnFe-NC	√	×	√	√	×	√
NiCo-NC	√	×	√	√	×	√
CuCo-NC	√	×	√	√	×	√
ZnCo-NC	√	×	√	×	×	√
CuNi-NC	√	×	√	√	×	√
CuZn-NC	√	×	√	×	×	√
NiZn-NC	√	×	√	×	×	√
2Mn-NC	×	×	√	×	×	√
2Fe-NC	√	×	√	√	×	√
2Co-NC	√	×	√	√	×	√
2Ni-NC	√	×	√	√	×	√
2Cu-NC	√	×	√	√	×	√

2Zn-NC	√	×	√	×	×	√

Table S49 The stability against leaching of 3d-4d M_1M_2-NC in the operating voltages of commercial catalysts in ORR, OER and HER at pH=14.

	M_1M_2-NC-2			**M_1M_2-NC-4**		
	ORR	OER	HER	ORR	OER	HER
TcMn-NC	×	×	√	×	×	√
TcFe-NC	×	×	√	√	×	√
TcCo-NC	×	×	√	√	×	√
TcNi-NC	×	×	√	√	×	√
TcZn-NC	×	×	√	×	×	√
TcCu-NC	×	×	√	×	×	√
RuMn-NC	√	×	√	×	×	√
RuFe-NC	√	×	√	√	×	√
RuCo-NC	√	×	√	√	×	√
RuNi-NC	√	×	√	√	×	√
RuZn-NC	√	×	√	×	×	√
RuCu-NC	√	×	√	×	×	√
RhMn-NC	√	×	√	×	×	√
RhFe-NC	√	×	√	√	×	√
RhCo-NC	√	×	√	√	×	√
RhNi-NC	√	×	√	√	×	√
RhZn-NC	√	×	√	×	×	√
RhCu-NC	√	×	√	×	×	√
PdMn-NC	√	×	√	√	×	√
PdFe-NC	√	×	√	√	×	√

PdCo-NC	√	×	√	√	×	√
PdNi-NC	√	×	√	√	×	√
PdZn-NC	√	×	√	×	×	√
PdCu-NC	√	×	√	√	×	√
AgMn-NC	√	×	√	×	×	√
AgFe-NC	√	×	√	√	×	√
AgCo-NC	√	×	√	×	×	√
AgNi-NC	√	×	√	√	×	√
AgZn-NC	√	×	√	×	×	√
AgCu-NC	√	×	√	√	×	√
CdMn-NC	×	×	√	×	×	×
CdFe-NC	×	×	√	×	×	√
CdCo-NC	×	×	√	×	×	×
CdNi-NC	×	×	√	×	×	√
CdZn-NC	√	×	√	×	×	√
CdCu-NC	×	×	√	×	×	√

Table S50 The stability against leaching of 3d-5d M_1M_2-NC in the operating voltages of commercial catalysts in ORR, OER and HER at pH=14.

	M_1M_2-NC-2			**M_1M_2-NC-4**		
	ORR	OER	HER	ORR	OER	HER
ReMn-NC	×	×	√	×	×	√
ReFe-NC	×	×	√	×	×	√
ReCo-NC	×	×	√	×	×	√
ReNi-NC	×	×	√	×	×	√
ReZn-NC	×	×	√	×	×	√
ReCu-NC	×	×	√	×	×	√
OsMn-NC	×	×	√	×	×	√
OsFe-NC	×	×	√	√	×	√
OsCo-NC	×	×	√	√	×	√

OsNi-NC	×	×	√	×	×	√
OsZn-NC	×	×	√	×	×	×
OsCu-NC	×	×	√	×	×	√
IrMn-NC	√	×	√	×	×	√
IrFe-NC	√	×	√	√	×	√
IrCo-NC	√	×	√	√	×	√
IrNi-NC	√	×	√	√	×	√
IrZn-NC	√	×	√	×	×	×
IrCu-NC	√	×	√	×	×	√
PtMn-NC	√	×	√	×	×	√
PtFe-NC	√	×	√	√	×	√
PtCo-NC	√	×	√	√	×	√
PtNi-NC	√	×	√	√	×	√
PtZn-NC	√	×	√	×	×	√
PtCu-NC	√	×	√	√	×	√

Table S51 The stability against leaching of 4d-4d M_1M_2-NC in the operating voltages of commercial catalysts in ORR, OER and HER at pH=14.

	M_1M_2-NC-2			**M_1M_2-NC-4**		
	ORR	OER	HER	ORR	OER	HER
TcRu-NC	×	×	√	√	×	√
TcRh-NC	×	×	√	√	×	√
TcPd-NC	×	×	√	×	×	√
TcCd-NC	×	×	√	×	×	×
TcAg-NC	×	×	√	×	×	√
RhRu-NC	√	×	√	√	×	√
PdRu-NC	√	×	√	√	×	√
CdRu-NC	×	×	√	×	×	×
AgRu-NC	√	×	√	×	×	√

RhPd-NC	√	×	√	√	×	√
RhAg-NC	√	×	√	×	×	×
RhCd-NC	×	×	√	×	×	×
AgPd-NC	√	×	√	×	×	√
CdPd-NC	×	×	√	×	×	×
CdAg-NC	×	×	√	×	×	×
2Tc-NC	×	×	√	×	×	√
2Ru-NC	√	×	√	√	×	√
2Rh-NC	√	×	√	√	×	√
2Pd-NC	√	×	√	√	×	√
2Ag-NC	√	×	√	×	×	√
2Cd-NC	×	×	√	×	×	√

Table S52 The stability against leaching of 4d-5d M_1M_2-NC in the operating voltages of commercial catalysts in ORR, OER and HER at pH=14.

	M_1M_2-NC-2			**M_1M_2-NC-4**		
	ORR	OER	HER	ORR	OER	HER
TcIr-NC	×	×	√	×	×	√
RhIr-NC	√	×	√	√	×	√
RuIr-NC	√	×	√	√	×	√
PdIr-NC	√	×	√	√	×	√
CdIr-NC	×	×	√	×	×	×
AgIr-NC	√	×	√	×	×	×
RhPt-NC	√	×	√	√	×	√
TcPt-NC	×	×	√	×	×	√
RuPt-NC	√	×	√	√	×	√
PdPt-NC	√	√	√	√	×	√
AgPt-NC	√	√	√	×	×	×
CdPt-NC	×	×	√	×	×	×

TcOs-NC	×	×	√	×	×	√
RhOs-NC	×	×	√	√	×	√
RuOs-NC	×	×	√	√	×	√
PdOs-NC	×	×	√	√	×	√
CdOs-NC	×	×	√	×	×	×
AgOs-NC	×	×	√	×	×	×
RhRe-NC	×	×	√	×	×	√
TcRe-NC	×	×	√	×	×	√
RuRe-NC	×	×	√	×	×	√
PdRe-NC	×	×	√	×	×	√
CdRe-NC	×	×	√	×	×	×
AgRe-NC	×	×	√	×	×	√

Table S53 The stability against leaching of 5d-5d M_1M_2-NC in the operating voltages of commercial catalysts in ORR, OER and HER at pH = 14.

	M_1M_2-NC-2			**M_1M_2-NC-4**		
	ORR	OER	HER	ORR	OER	HER
ReIr-NC	×	×	√	×	×	√
ReOs-NC	×	×	√	×	×	√
RePt-NC	×	×	√	×	×	√
OsIr-NC	×	×	√	×	×	√
OsPt-NC	×	×	√	×	×	√
PtIr-NC	√	×	√	√	×	√
2Re-NC	×	×	√	×	×	√
2Os-NC	×	×	√	×	×	√
2Ir-NC	√	×	√	√	×	√
2Pt-NC	√	√	√	√	×	√

Table S54 The data of Z_0, A, B, C, D and F for BACs.

		Z_0	a	b	c	d	f
3d metal	3d-3d	12.73	0.63	-7.99	0.20	1.03	0.032
dissolution	3d-4d/5d	-8.62	4.14	0.64	-0.62	-0.09	0.13
4d metal	4d-3d	-9.79	19.63	-10.43	-3.32	1.23	0.34
dissolution	4d-4d/5d	-5.75	2.94	-0.20	-0.27	-0.03	0.14
5d metal	5d-3d	-461.00	331.71	-9.21	-57.64	1.00	0.54
dissolution	5d-4d/5d	-376.83	260.44	0.48	-44.86	-0.03	-0.08

Table S55 The operating voltage of BACs obtained from experiments. The calculated value and predicted value by structure descriptor of dissolution potential in this work.

	Catalytic reaction	**Operating voltage**	**U_{dis} (calculated value)**	**U_{dis} (predictive value)**
2Fe-NC	ORR	0.78 V[13]	1.43 V	1.48 V
2Co-NC	ORR	0.79 V[14]	1.24 V	1.36 V
2Cu-NC	CO_2RR	-0.70 V[17]	1.03 V	0.91V
2Ni-NC	CO_2RR	-0.60 V[18]	1.42 V	1.23 V
FeCu-NC	ORR	0.85 V[19]	1.03 V	1.10 V
FeNi-NC	ORR	0.79 V[20]	1.26 V	1.25 V
	CO_2RR	-0.70 V[21]		
FeCo-NC	ORR	0.86 V[22]	1.14 V	1.35 V
NiCo-NC	ORR	0.76 V[15]	1.23 V	1.26 V
ZnCo-NC	ORR	0.80 V[23]	0.75 V	0.42 V
PdCu-NC	NRR	-0.45 V[24]	0.82 V	0.67 V
PtCo-NC	ORR	0.96 V[25]	1.33 V	0.62 V
PtRu-NC	HER	-0.05 V[16]	0.90 V	1.16 V

Supplementary Figures

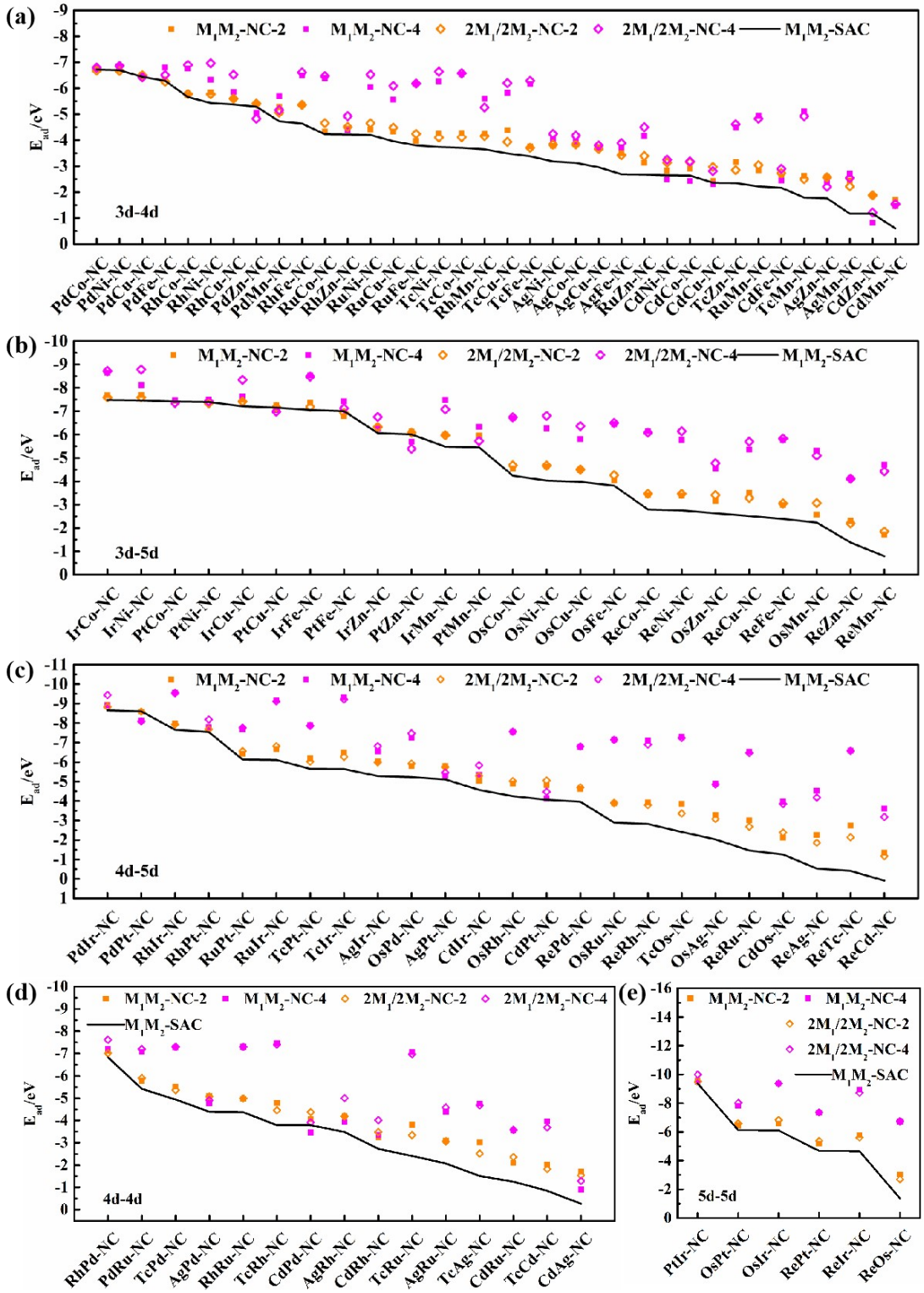

Figure S1. Adsorption energy of M_1M_2-NC, $2M_1$-NC/$2M_2$-NC and M_1M_2-SAC, which are denoted as square, rhombus and line respectively. (a~e) represent for 3d-4d, 3d-5d, 4d-5d, 4d-4d and 5d-5d atoms supported on graphene, respectively. Orange and purple represent configurations 2 and 4. The average adsorption energy of $2M_1$-NC/$2M_2$-NC is the average of the average adsorption energy

of $2M_1$-NC and $2M_2$-NC.

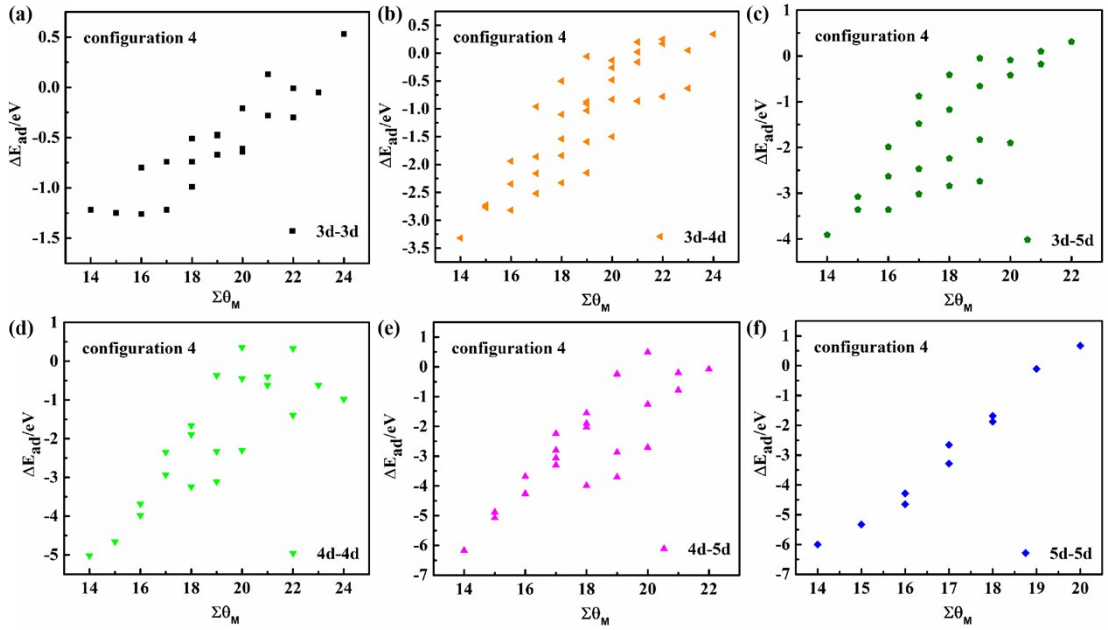

Figure S2. Correlation between $\Delta E_{ad(SAC)}$ with the sum of the number of valence electrons of transition metal atoms.

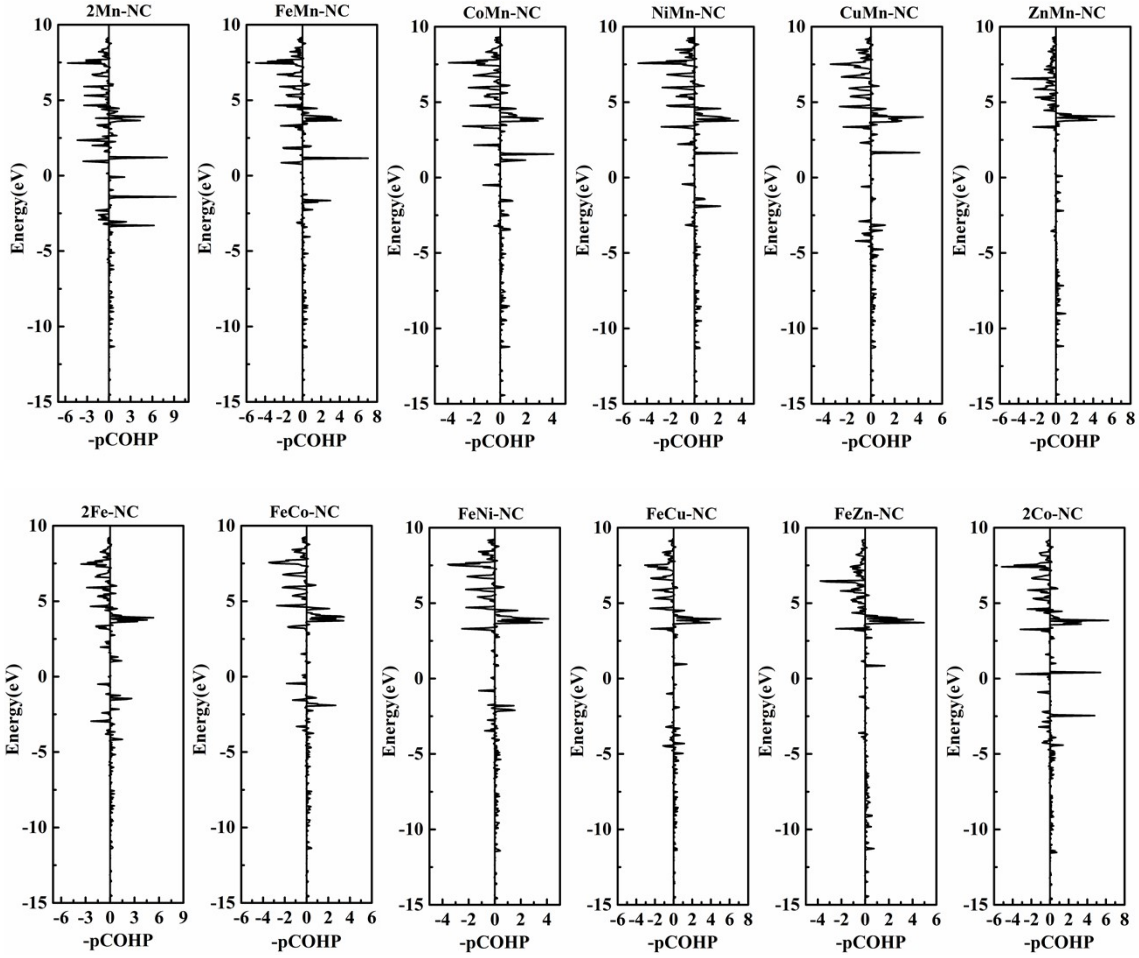

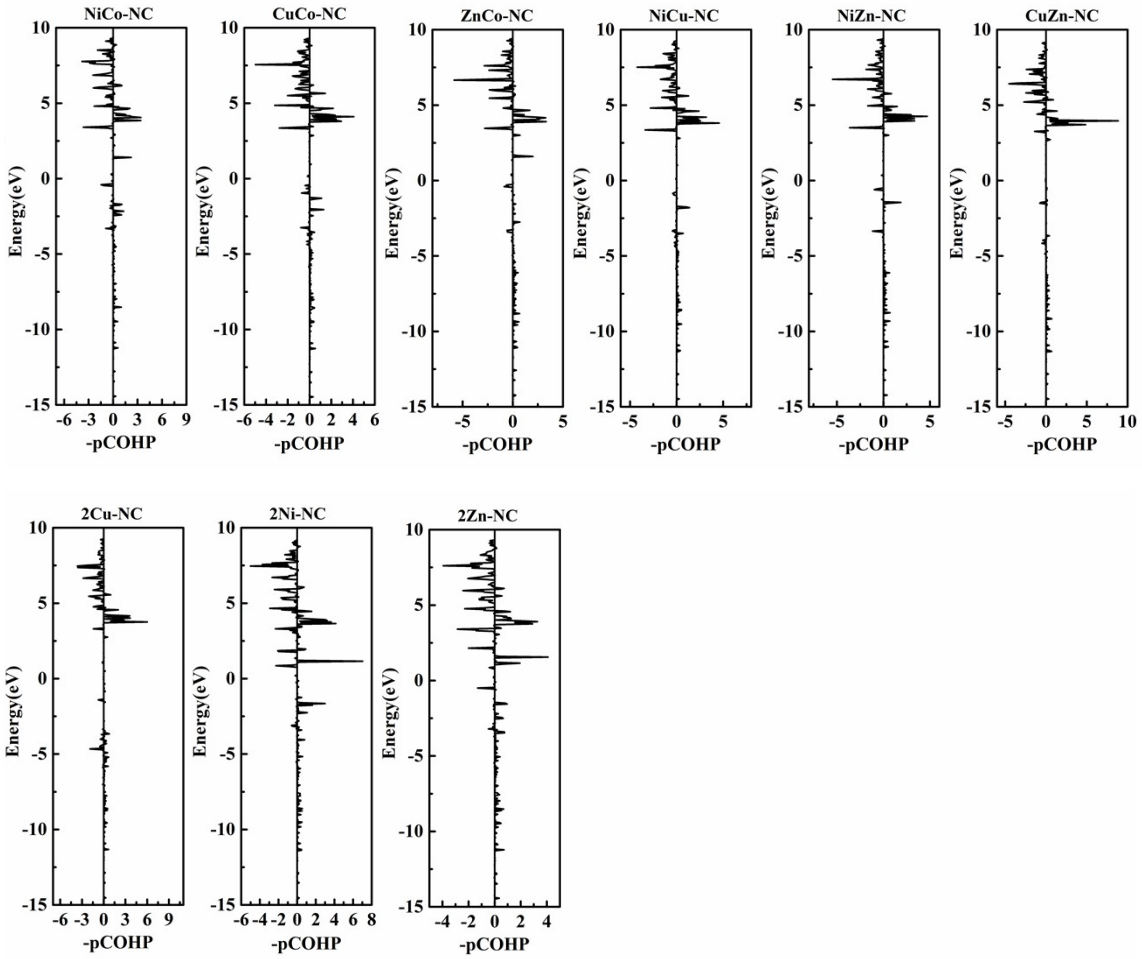

Figure S3. Crystal orbital Hamilton population (COHP) between M_1-M_2 on 3d-3d M_1M_2-NC.

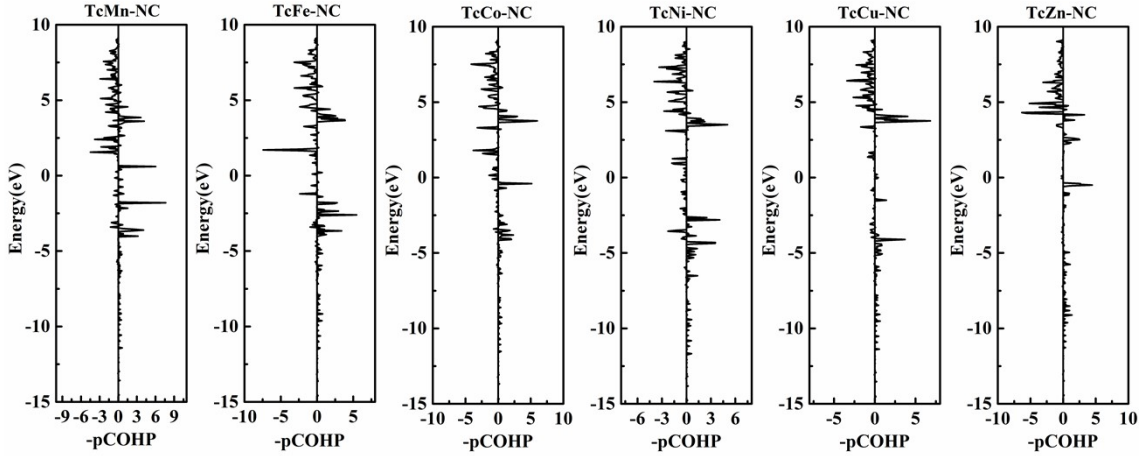

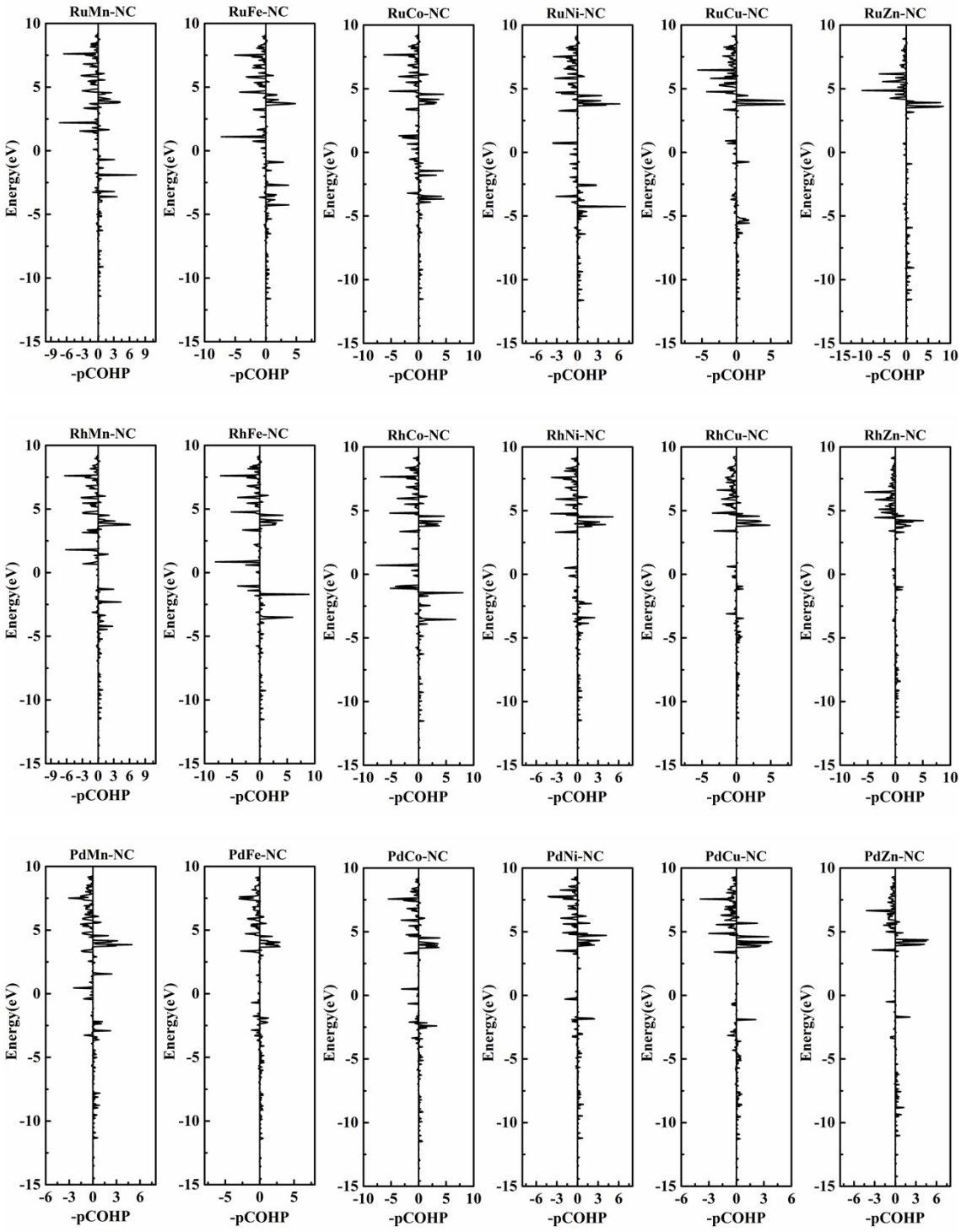
RuMn-NC
RuFe-NC
RuCo-NC
RuNi-NC
RuCu-NC
RuZn-NC
RhMn-NC
RhFe-NC
RhCo-NC
RhNi-NC
RhCu-NC
RhZn-NC
PdMn-NC
PdFe-NC
PdCo-NC
PdNi-NC
PdCu-NC
PdZn-NC
Energy(eV)
-pCOHP

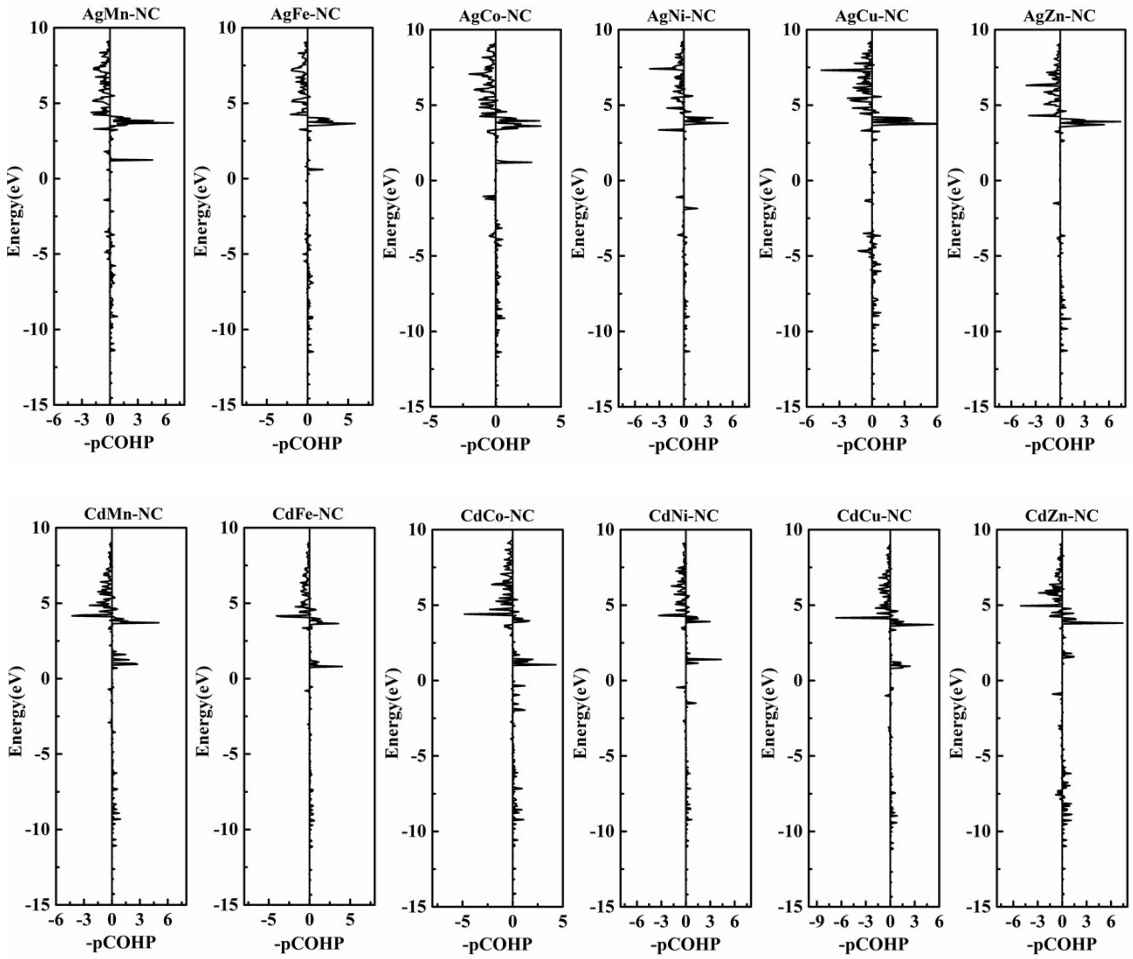

Figure S4. Crystal orbital Hamilton population (COHP) between M_1-M_2 on 3d-4d M_1M_2-NC.

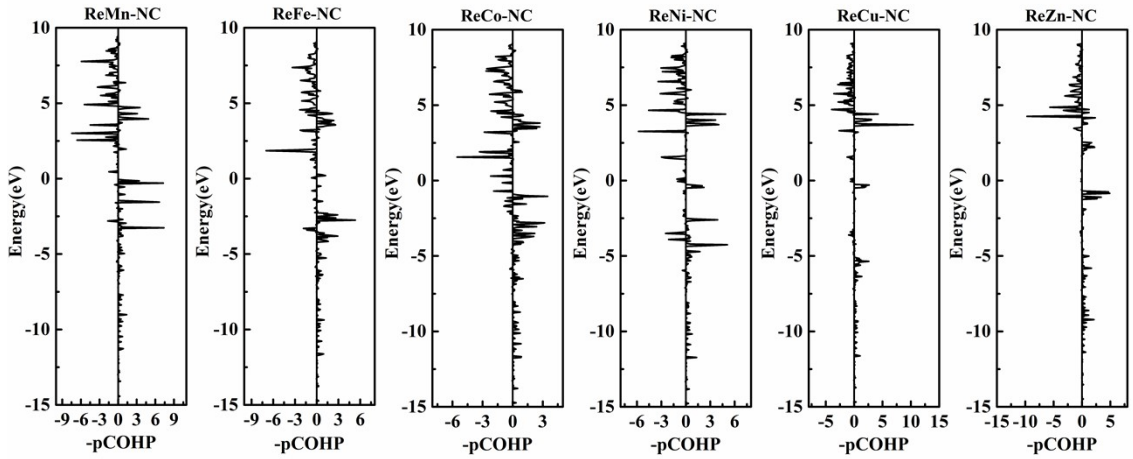

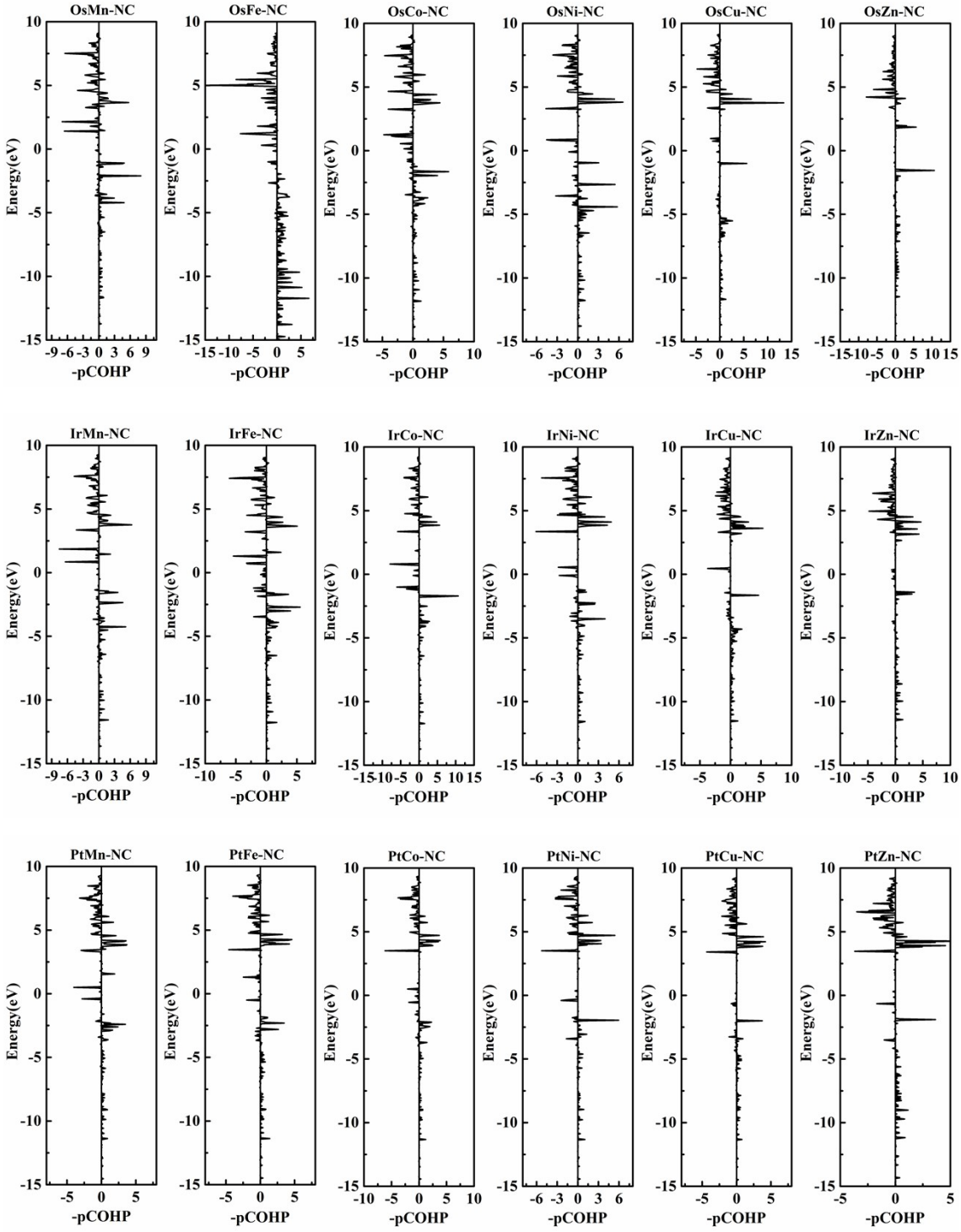

Figure S5. Crystal orbital Hamilton population (COHP) between M_1-M_2 on 3d-5d M_1M_2-NC.

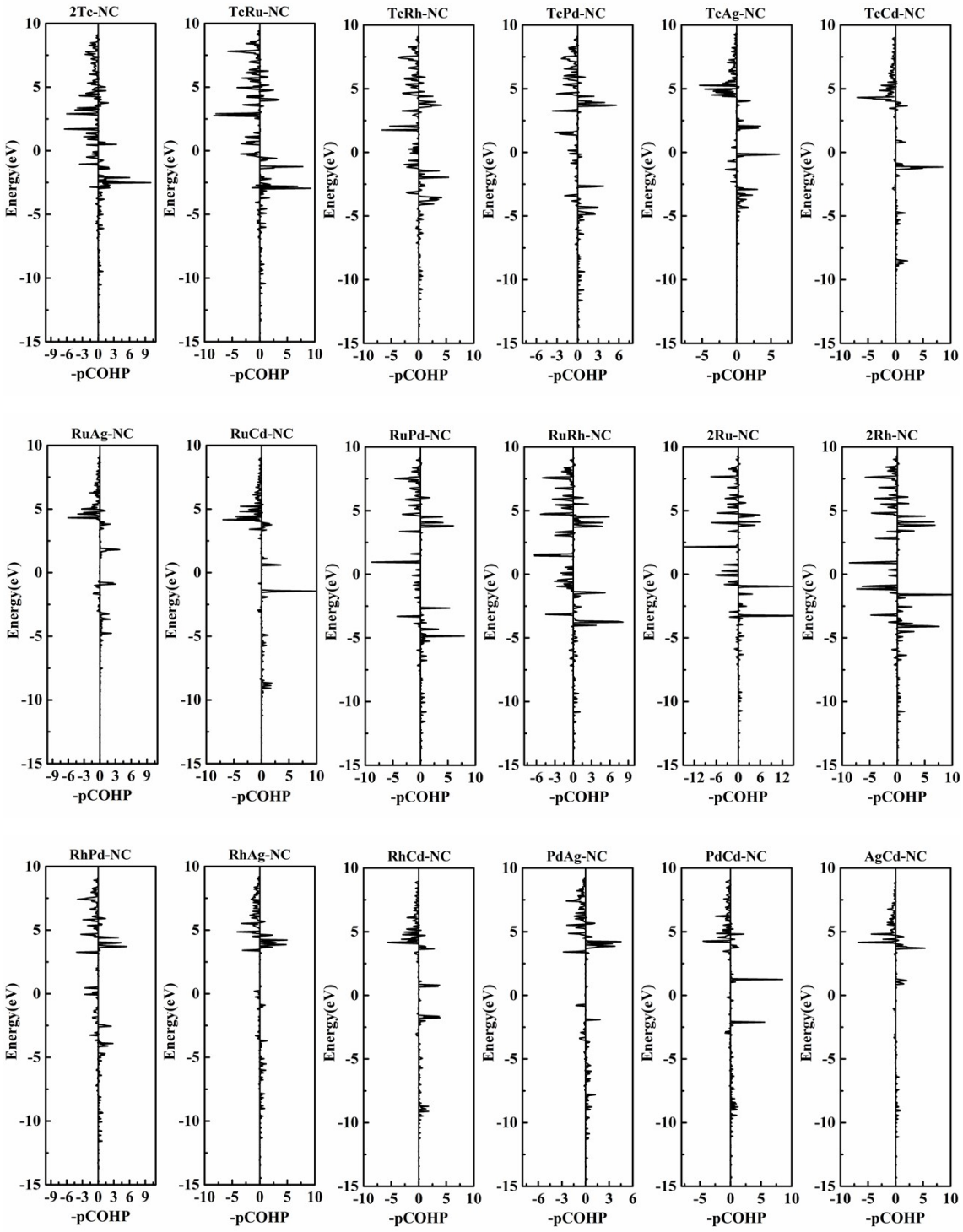
2Tc-NC
TcRu-NC
TcRh-NC
TcPd-NC
TcAg-NC
TcCd-NC
RuAg-NC
RuCd-NC
RuPd-NC
RuRh-NC
2Ru-NC
2Rh-NC
RhPd-NC
RhAg-NC
RhCd-NC
PdAg-NC
PdCd-NC
AgCd-NC
Energy(eV)
-pCOHP

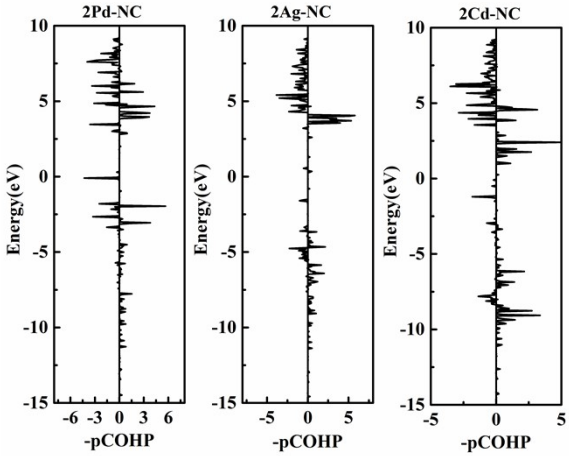

Figure S6. Crystal orbital Hamilton population (COHP) between M_1-M_2 on 4d-4d M_1M_2-NC.

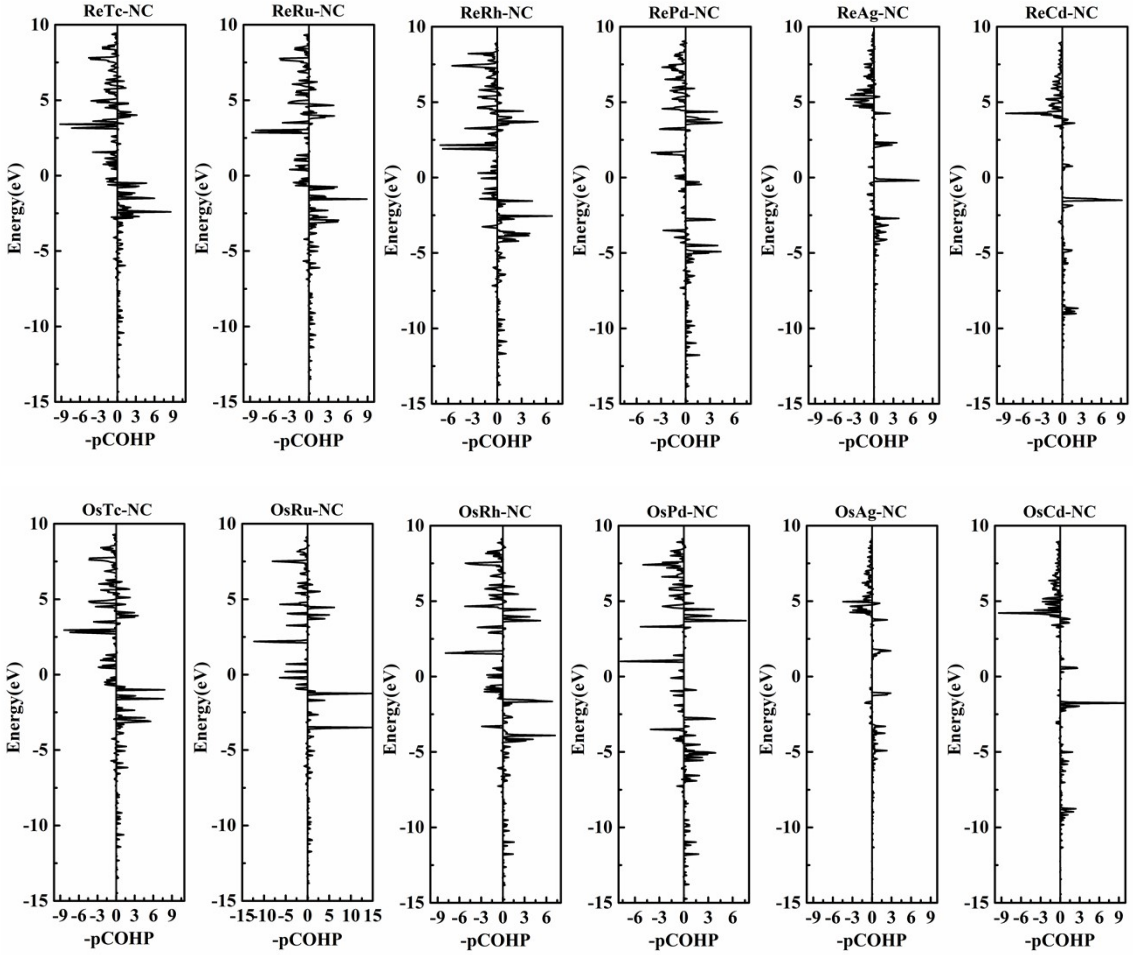

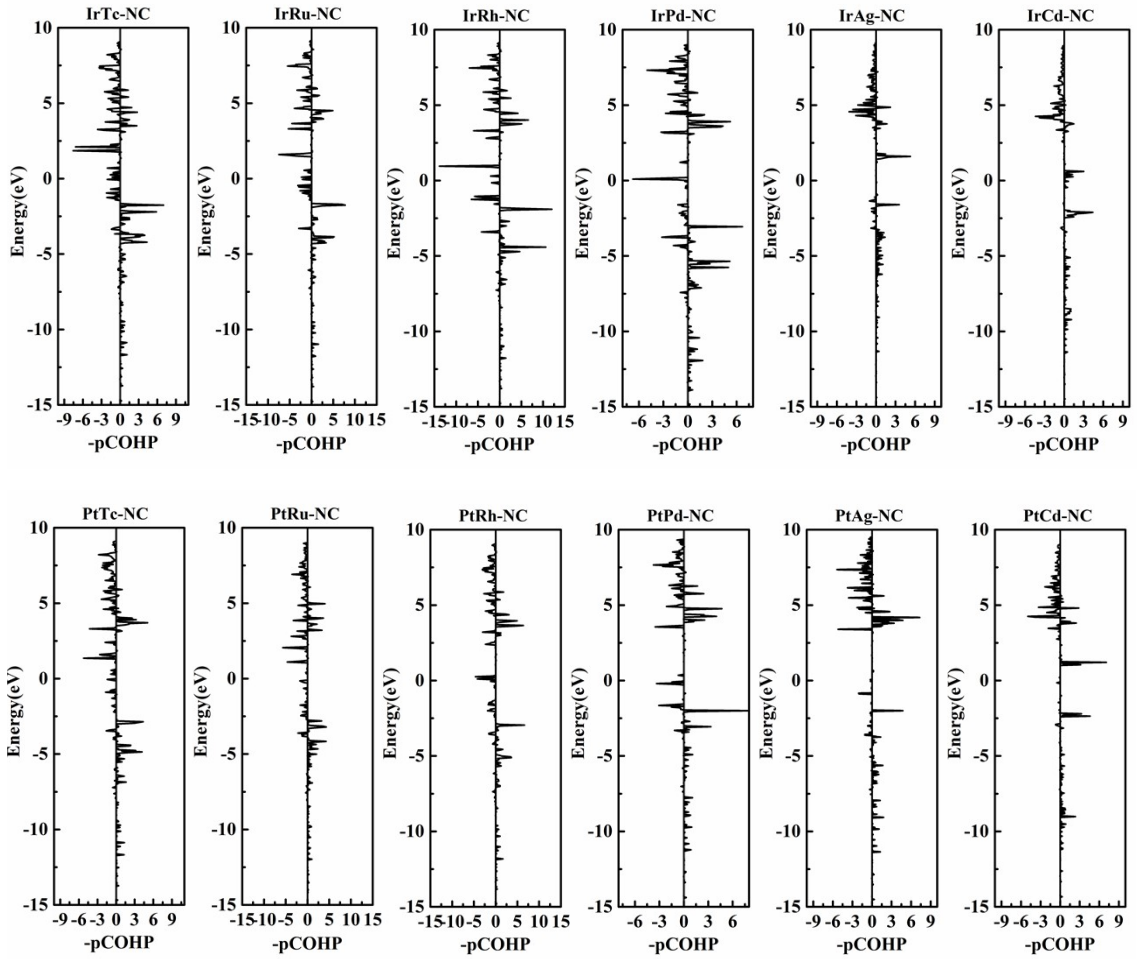

Figure S7. Crystal orbital Hamilton population (COHP) between M_1-M_2 on 4d-5d M_1M_2-NC.

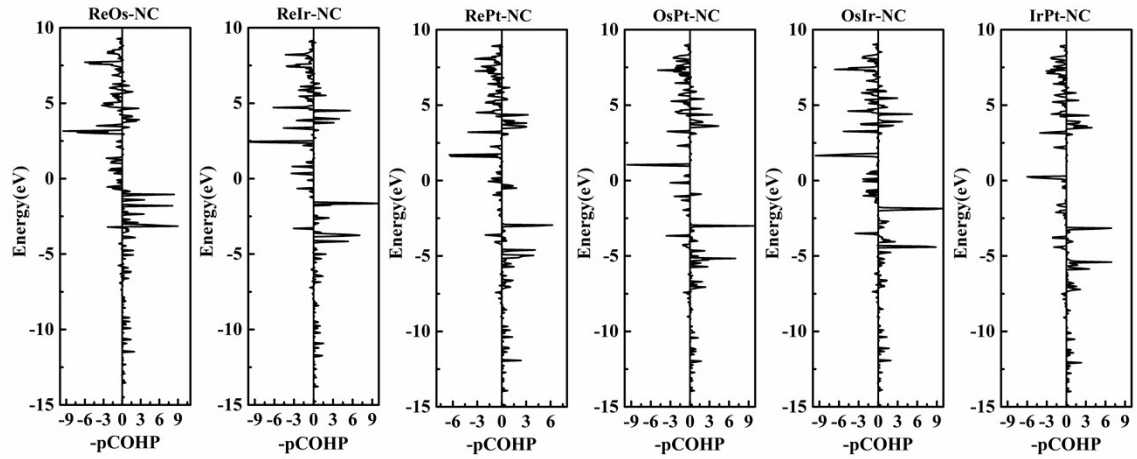

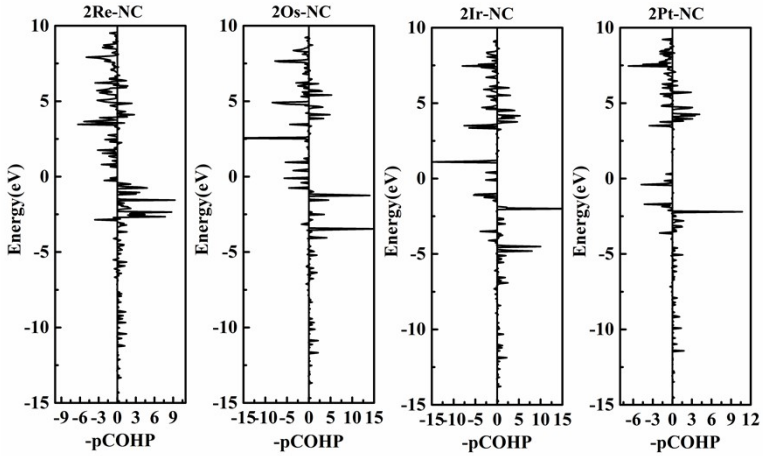

Figure S8.Crystal orbital Hamilton population (COHP) between M_1-M_2 on 5d-5d M_1M_2-NC.

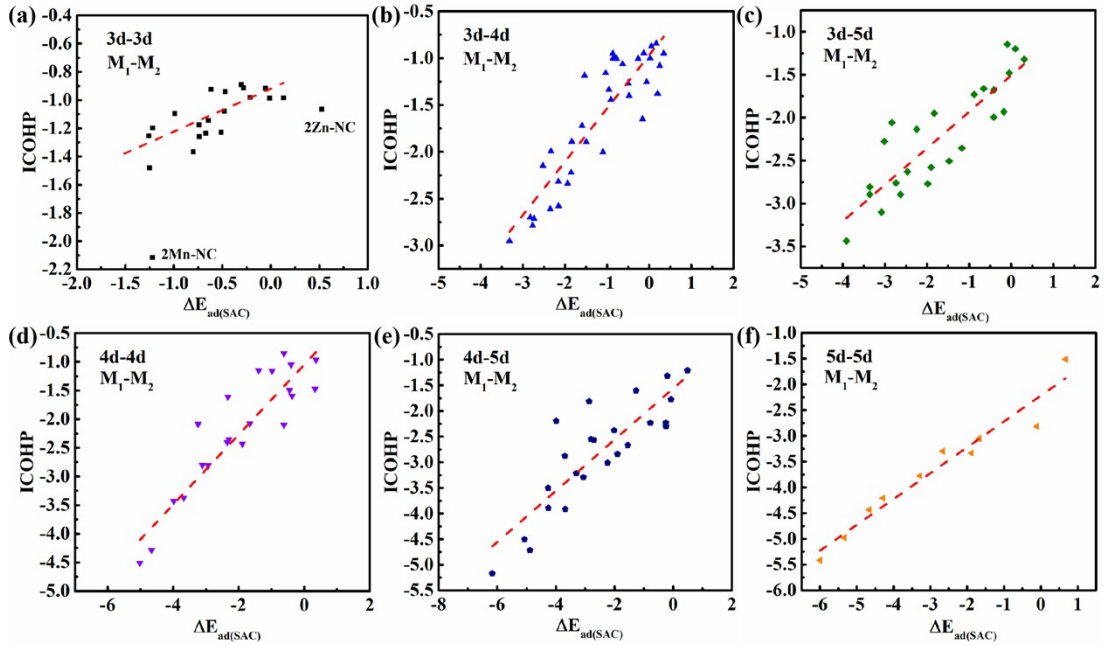

Figure S9. Correlation between $\Delta E_{ad(SAC)}$ with integrated crystal orbital Hamilton population (ICOHP) of M_1-M_2.

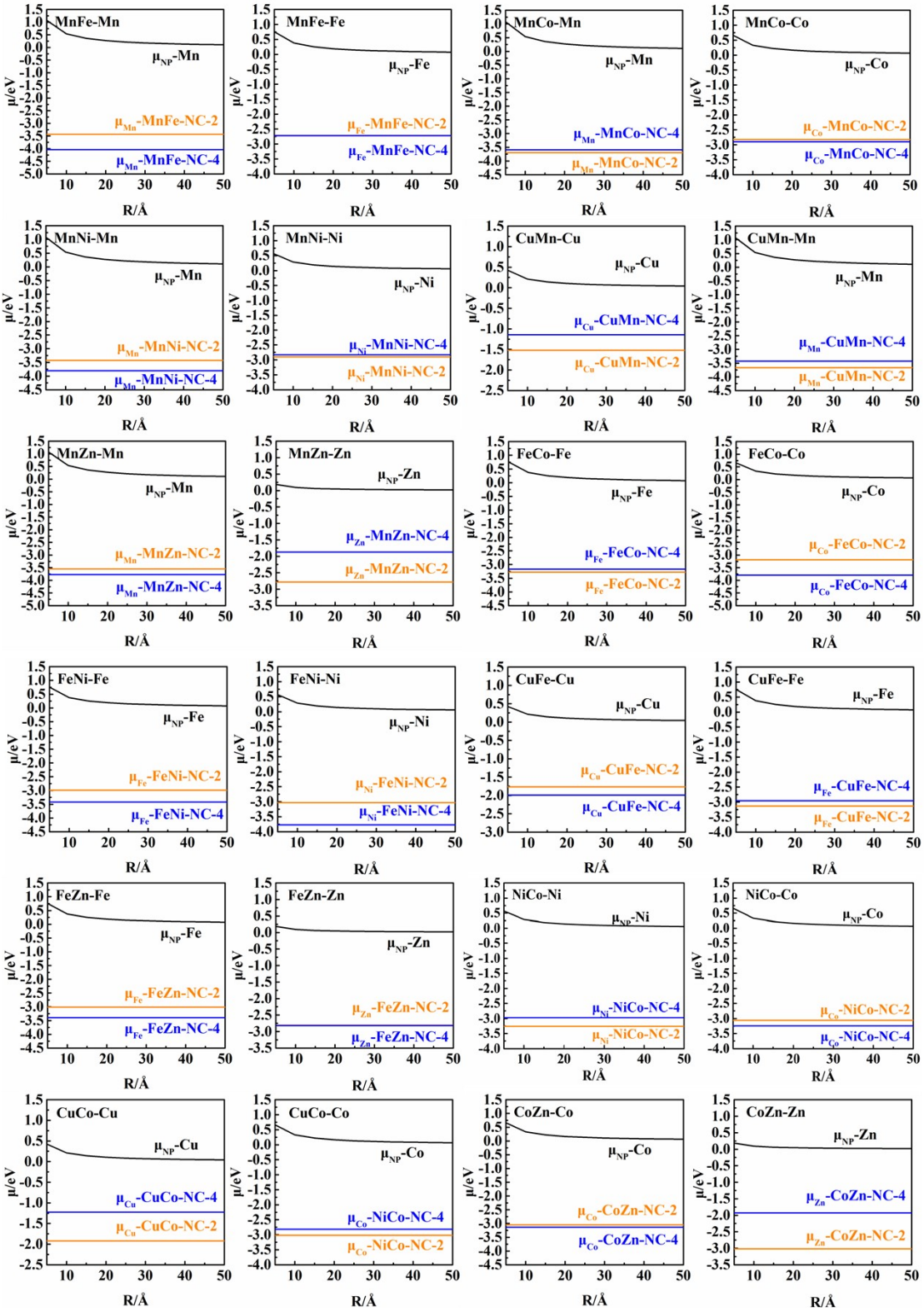
MnFe-Mn
μNP-Mn
μMn-MnFe-NC-2
μMn-MnFe-NC-4
MnFe-Fe
μNP-Fe
μFe-MnFe-NC-2
μFe-MnFe-NC-4
MnCo-Mn
μNP-Mn
μMn-MnCo-NC-4
μMn-MnCo-NC-2
MnCo-Co
μNP-Co
μCo-MnCo-NC-2
μCo-MnCo-NC-4
MnNi-Mn
μNP-Mn
μMn-MnNi-NC-2
μMn-MnNi-NC-4
MnNi-Ni
μNP-Ni
μNi-MnNi-NC-4
μNi-MnNi-NC-2
CuMn-Cu
μNP-Cu
μCu-CuMn-NC-4
μCu-CuMn-NC-2
CuMn-Mn
μNP-Mn
μMn-CuMn-NC-4
μMn-CuMn-NC-2
MnZn-Mn
μNP-Mn
μMn-MnZn-NC-2
μMn-MnZn-NC-4
MnZn-Zn
μNP-Zn
μZn-MnZn-NC-4
μZn-MnZn-NC-2
FeCo-Fe
μNP-Fe
μFe-FeCo-NC-4
μFe-FeCo-NC-2
FeCo-Co
μNP-Co
μCo-FeCo-NC-2
μCo-FeCo-NC-4
FeNi-Fe
μNP-Fe
μFe-FeNi-NC-2
μFe-FeNi-NC-4
FeNi-Ni
μNP-Ni
μNi-FeNi-NC-2
μNi-FeNi-NC-4
CuFe-Cu
μNP-Cu
μCu-CuFe-NC-2
μCu-CuFe-NC-4
CuFe-Fe
μNP-Fe
μFe-CuFe-NC-4
μFe-CuFe-NC-2
FeZn-Fe
μNP-Fe
μFe-FeZn-NC-2
μFe-FeZn-NC-4
FeZn-Zn
μNP-Zn
μZn-FeZn-NC-2
μZn-FeZn-NC-4
NiCo-Ni
μNP-Ni
μNi-NiCo-NC-4
μNi-NiCo-NC-2
NiCo-Co
μNP-Co
μCo-NiCo-NC-2
μCo-NiCo-NC-4
CuCo-Cu
μNP-Cu
μCu-CuCo-NC-4
μCu-CuCo-NC-2
CuCo-Co
μNP-Co
μCo-NiCo-NC-4
μCo-NiCo-NC-2
CoZn-Co
μNP-Co
μCo-CoZn-NC-2
μCo-CoZn-NC-4
CoZn-Zn
μNP-Zn
μZn-CoZn-NC-4
μZn-CoZn-NC-2
μ/eV
R/Å

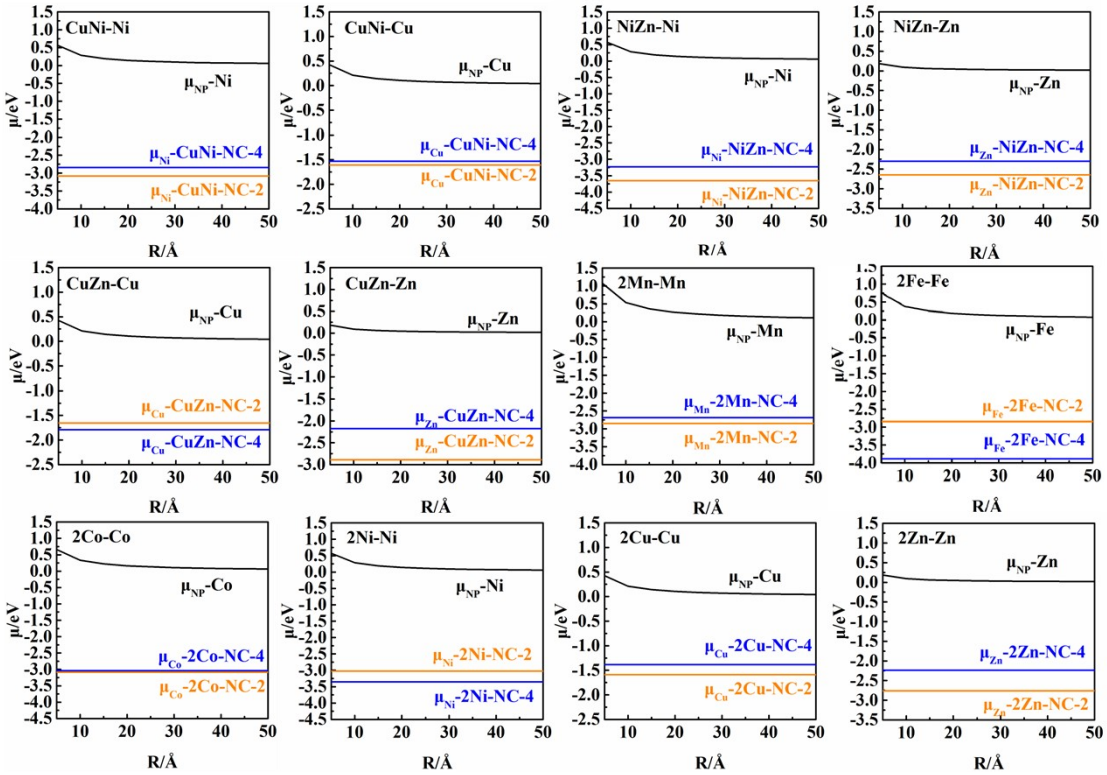

Figure S10. Chemical potential of NPs and single atom of 3d-3d BACs in vacuum.

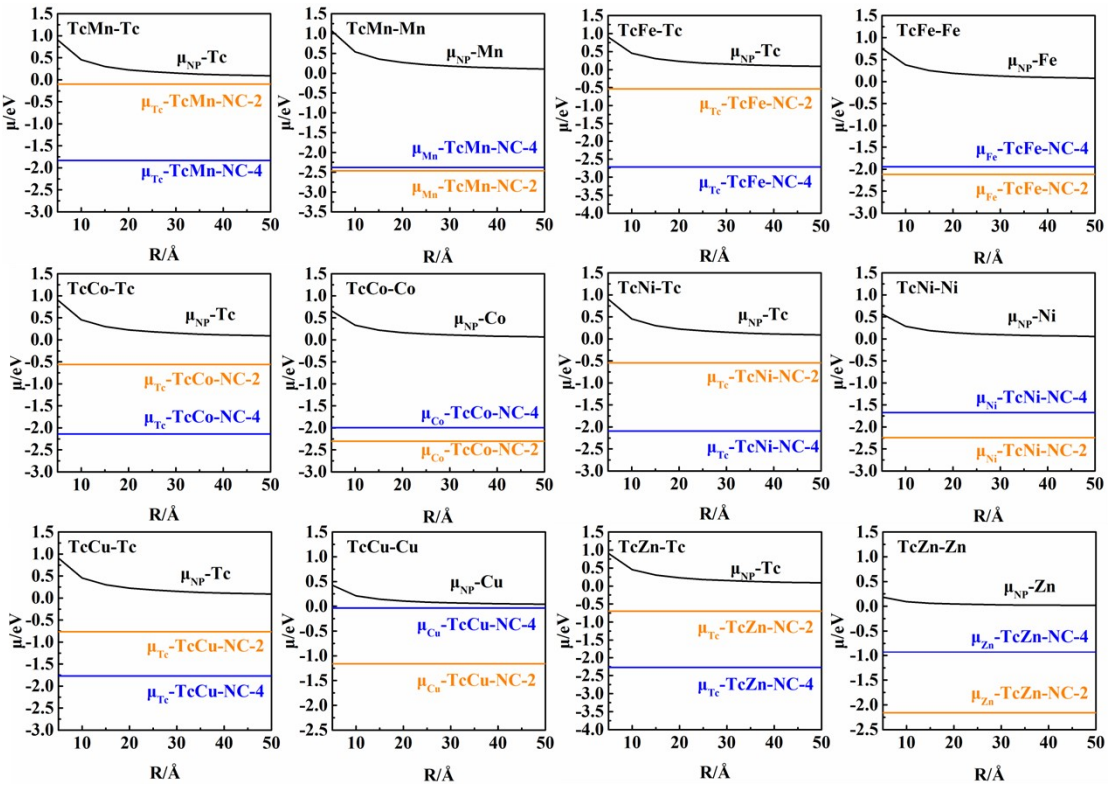

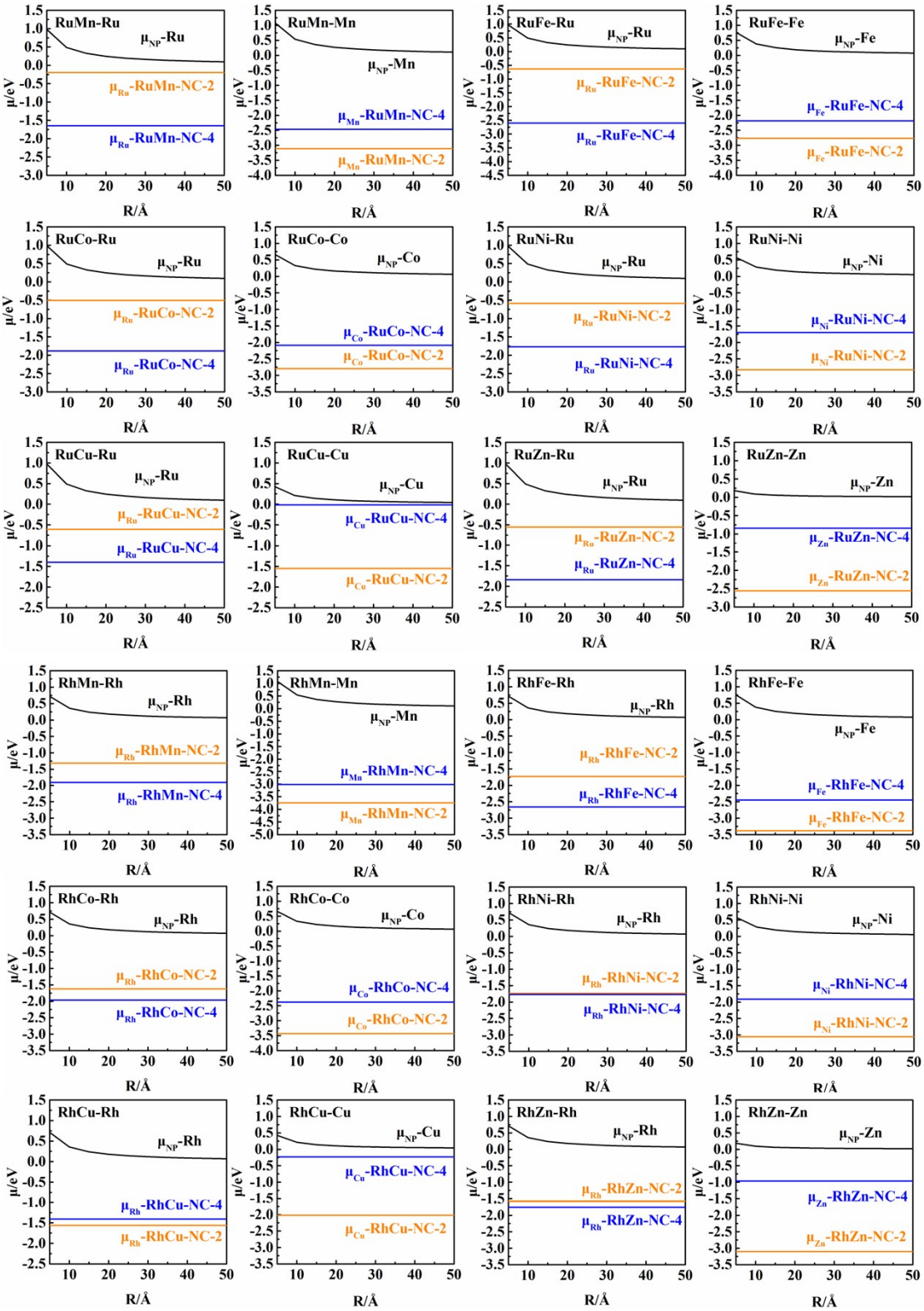
RuMn-Ru
μNP-Ru
μRu-RuMn-NC-2
μRu-RuMn-NC-4
RuMn-Mn
μNP-Mn
μMn-RuMn-NC-4
μMn-RuMn-NC-2
RuFe-Ru
μNP-Ru
μRu-RuFe-NC-2
μRu-RuFe-NC-4
RuFe-Fe
μNP-Fe
μFe-RuFe-NC-4
μFe-RuFe-NC-2
RuCo-Ru
μNP-Ru
μRu-RuCo-NC-2
μRu-RuCo-NC-4
RuCo-Co
μNP-Co
μCo-RuCo-NC-4
μCo-RuCo-NC-2
RuNi-Ru
μNP-Ru
μRu-RuNi-NC-2
μRu-RuNi-NC-4
RuNi-Ni
μNP-Ni
μNi-RuNi-NC-4
μNi-RuNi-NC-2
RuCu-Ru
μNP-Ru
μRu-RuCu-NC-2
μRu-RuCu-NC-4
RuCu-Cu
μNP-Cu
μCu-RuCu-NC-4
μCu-RuCu-NC-2
RuZn-Ru
μNP-Ru
μRu-RuZn-NC-2
μRu-RuZn-NC-4
RuZn-Zn
μNP-Zn
μZn-RuZn-NC-4
μZn-RuZn-NC-2
RhMn-Rh
μNP-Rh
μRh-RhMn-NC-2
μRh-RhMn-NC-4
RhMn-Mn
μNP-Mn
μMn-RhMn-NC-4
μMn-RhMn-NC-2
RhFe-Rh
μNP-Rh
μRh-RhFe-NC-2
μRh-RhFe-NC-4
RhFe-Fe
μNP-Fe
μFe-RhFe-NC-4
μFe-RhFe-NC-2
RhCo-Rh
μNP-Rh
μRh-RhCo-NC-2
μRh-RhCo-NC-4
RhCo-Co
μNP-Co
μCo-RhCo-NC-4
μCo-RhCo-NC-2
RhNi-Rh
μNP-Rh
μRh-RhNi-NC-2
μRh-RhNi-NC-4
RhNi-Ni
μNP-Ni
μNi-RhNi-NC-4
μNi-RhNi-NC-2
RhCu-Rh
μNP-Rh
μRh-RhCu-NC-4
μRh-RhCu-NC-2
RhCu-Cu
μNP-Cu
μCu-RhCu-NC-4
μCu-RhCu-NC-2
RhZn-Rh
μNP-Rh
μRh-RhZn-NC-2
μRh-RhZn-NC-4
RhZn-Zn
μNP-Zn
μZn-RhZn-NC-4
μZn-RhZn-NC-2
μ/eV
R/Å

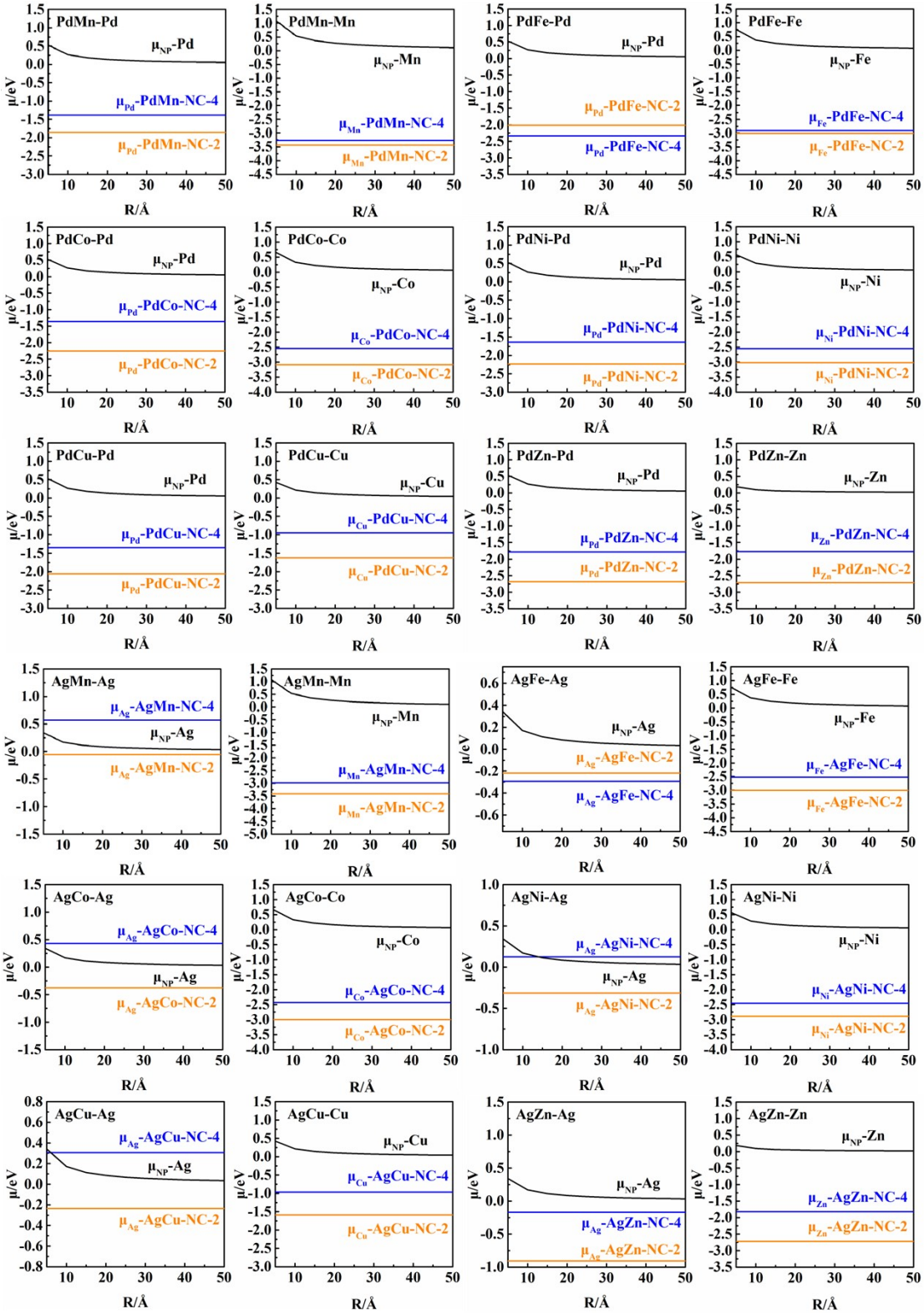
PdMn-Pd
μNP-Pd
μPd-PdMn-NC-4
μPd-PdMn-NC-2
PdMn-Mn
μNP-Mn
μMn-PdMn-NC-4
μMn-PdMn-NC-2
PdFe-Pd
μNP-Pd
μPd-PdFe-NC-2
μPd-PdFe-NC-4
PdFe-Fe
μNP-Fe
μFe-PdFe-NC-4
μFe-PdFe-NC-2
PdCo-Pd
μNP-Pd
μPd-PdCo-NC-4
μPd-PdCo-NC-2
PdCo-Co
μNP-Co
μCo-PdCo-NC-4
μCo-PdCo-NC-2
PdNi-Pd
μNP-Pd
μPd-PdNi-NC-4
μPd-PdNi-NC-2
PdNi-Ni
μNP-Ni
μNi-PdNi-NC-4
μNi-PdNi-NC-2
PdCu-Pd
μNP-Pd
μPd-PdCu-NC-4
μPd-PdCu-NC-2
PdCu-Cu
μNP-Cu
μCu-PdCu-NC-4
μCu-PdCu-NC-2
PdZn-Pd
μNP-Pd
μPd-PdZn-NC-4
μPd-PdZn-NC-2
PdZn-Zn
μNP-Zn
μZn-PdZn-NC-4
μZn-PdZn-NC-2
AgMn-Ag
μAg-AgMn-NC-4
μNP-Ag
μAg-AgMn-NC-2
AgMn-Mn
μNP-Mn
μMn-AgMn-NC-4
μMn-AgMn-NC-2
AgFe-Ag
μNP-Ag
μAg-AgFe-NC-2
μAg-AgFe-NC-4
AgFe-Fe
μNP-Fe
μFe-AgFe-NC-4
μFe-AgFe-NC-2
AgCo-Ag
μAg-AgCo-NC-4
μNP-Ag
μAg-AgCo-NC-2
AgCo-Co
μNP-Co
μCo-AgCo-NC-4
μCo-AgCo-NC-2
AgNi-Ag
μAg-AgNi-NC-4
μNP-Ag
μAg-AgNi-NC-2
AgNi-Ni
μNP-Ni
μNi-AgNi-NC-4
μNi-AgNi-NC-2
AgCu-Ag
μAg-AgCu-NC-4
μNP-Ag
μAg-AgCu-NC-2
AgCu-Cu
μNP-Cu
μCu-AgCu-NC-4
μCu-AgCu-NC-2
AgZn-Ag
μNP-Ag
μAg-AgZn-NC-4
μAg-AgZn-NC-2
AgZn-Zn
μNP-Zn
μZn-AgZn-NC-4
μZn-AgZn-NC-2
μ/eV
R/Å

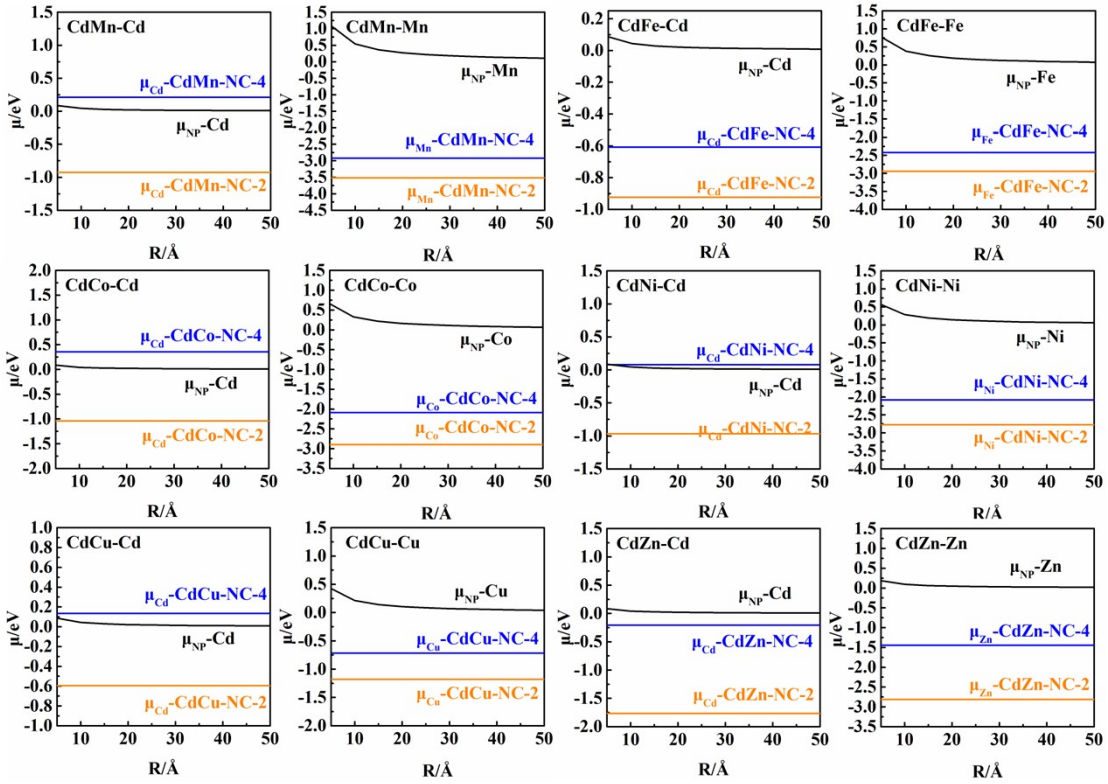

Figure S11. Chemical potential of NPs and single atom of 3d-4d BACs in vacuum.

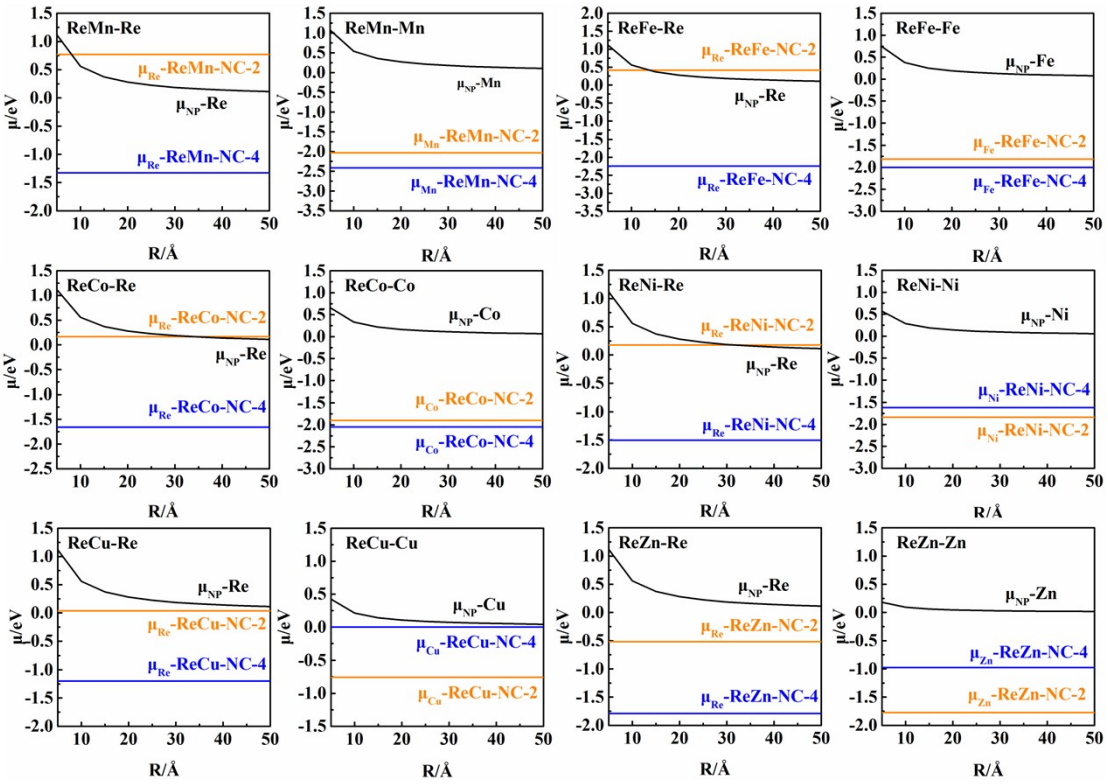

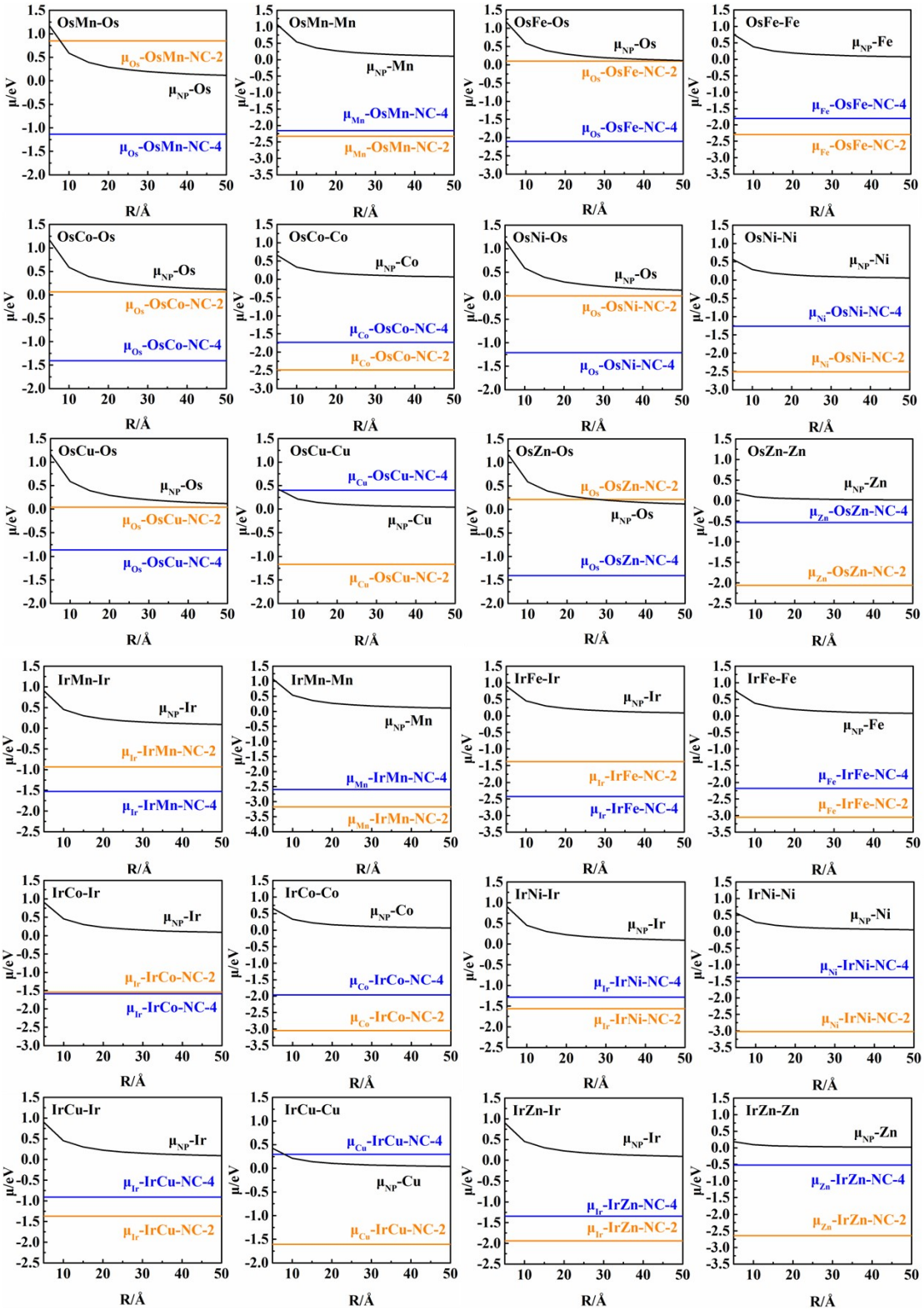
OsMn-Os
μOs-OsMn-NC-2
μNP-Os
μOs-OsMn-NC-4
OsMn-Mn
μNP-Mn
μMn-OsMn-NC-4
μMn-OsMn-NC-2
OsFe-Os
μNP-Os
μOs-OsFe-NC-2
μOs-OsFe-NC-4
OsFe-Fe
μNP-Fe
μFe-OsFe-NC-4
μFe-OsFe-NC-2
OsCo-Os
μNP-Os
μOs-OsCo-NC-2
μOs-OsCo-NC-4
OsCo-Co
μNP-Co
μCo-OsCo-NC-4
μCo-OsCo-NC-2
OsNi-Os
μNP-Os
μOs-OsNi-NC-2
μOs-OsNi-NC-4
OsNi-Ni
μNP-Ni
μNi-OsNi-NC-4
μNi-OsNi-NC-2
OsCu-Os
μNP-Os
μOs-OsCu-NC-2
μOs-OsCu-NC-4
OsCu-Cu
μCu-OsCu-NC-4
μNP-Cu
μCu-OsCu-NC-2
OsZn-Os
μOs-OsZn-NC-2
μNP-Os
μOs-OsZn-NC-4
OsZn-Zn
μNP-Zn
μZn-OsZn-NC-4
μZn-OsZn-NC-2
IrMn-Ir
μNP-Ir
μIr-IrMn-NC-2
μIr-IrMn-NC-4
IrMn-Mn
μNP-Mn
μMn-IrMn-NC-4
μMn-IrMn-NC-2
IrFe-Ir
μNP-Ir
μIr-IrFe-NC-2
μIr-IrFe-NC-4
IrFe-Fe
μNP-Fe
μFe-IrFe-NC-4
μFe-IrFe-NC-2
IrCo-Ir
μNP-Ir
μIr-IrCo-NC-2
μIr-IrCo-NC-4
IrCo-Co
μNP-Co
μCo-IrCo-NC-4
μCo-IrCo-NC-2
IrNi-Ir
μNP-Ir
μIr-IrNi-NC-4
μIr-IrNi-NC-2
IrNi-Ni
μNP-Ni
μNi-IrNi-NC-4
μNi-IrNi-NC-2
IrCu-Ir
μNP-Ir
μIr-IrCu-NC-4
μIr-IrCu-NC-2
IrCu-Cu
μCu-IrCu-NC-4
μNP-Cu
μCu-IrCu-NC-2
IrZn-Ir
μNP-Ir
μIr-IrZn-NC-4
μIr-IrZn-NC-2
IrZn-Zn
μNP-Zn
μZn-IrZn-NC-4
μZn-IrZn-NC-2
μ/eV
R/Å

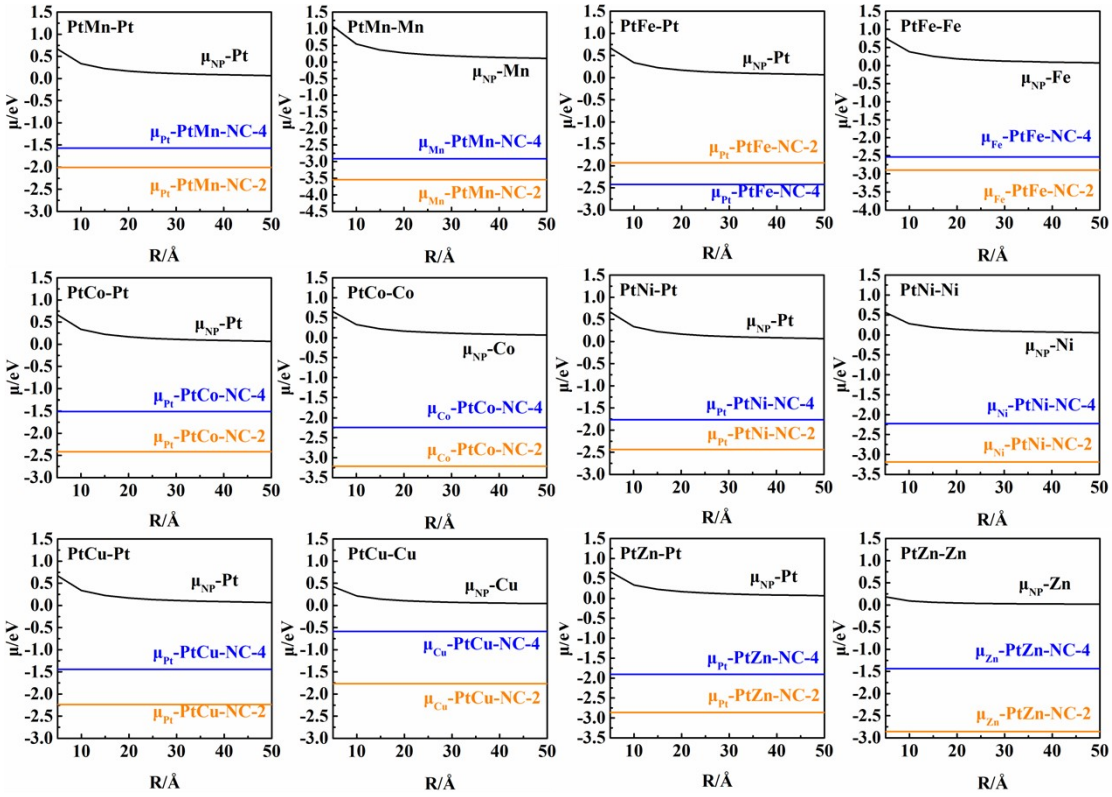

Figure S12. Chemical potential of NPs and single atom of 3d-5d BACs in vacuum.

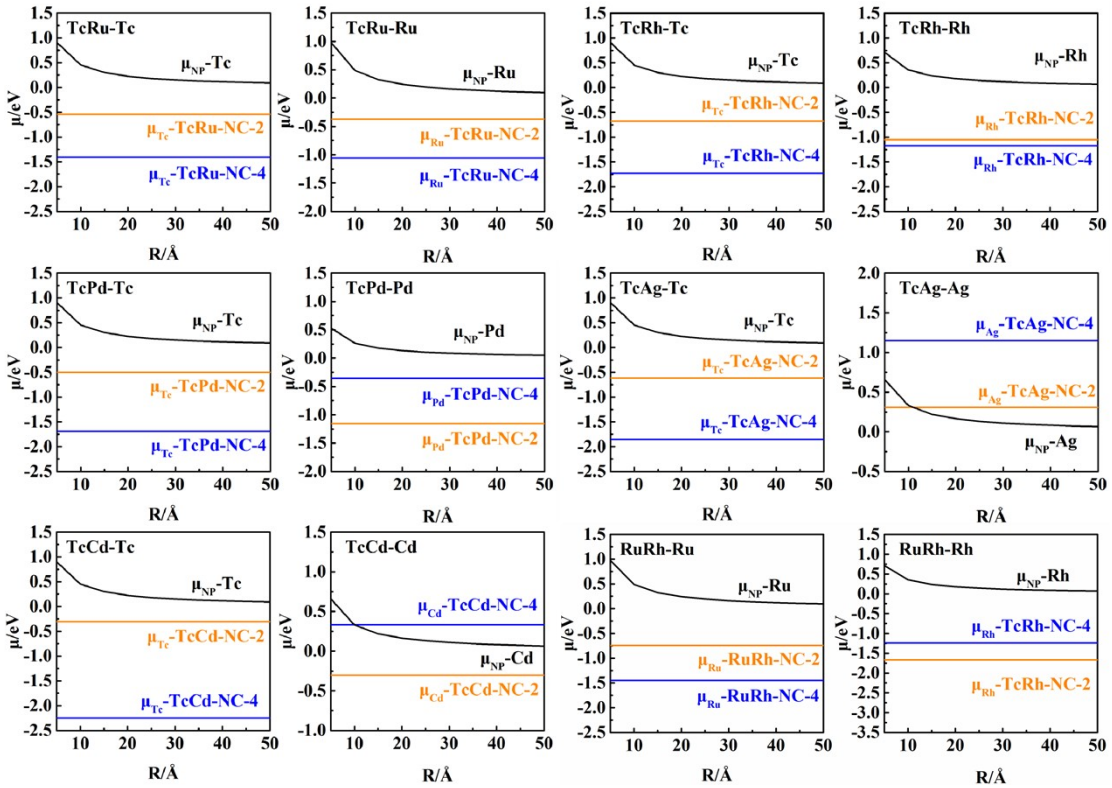

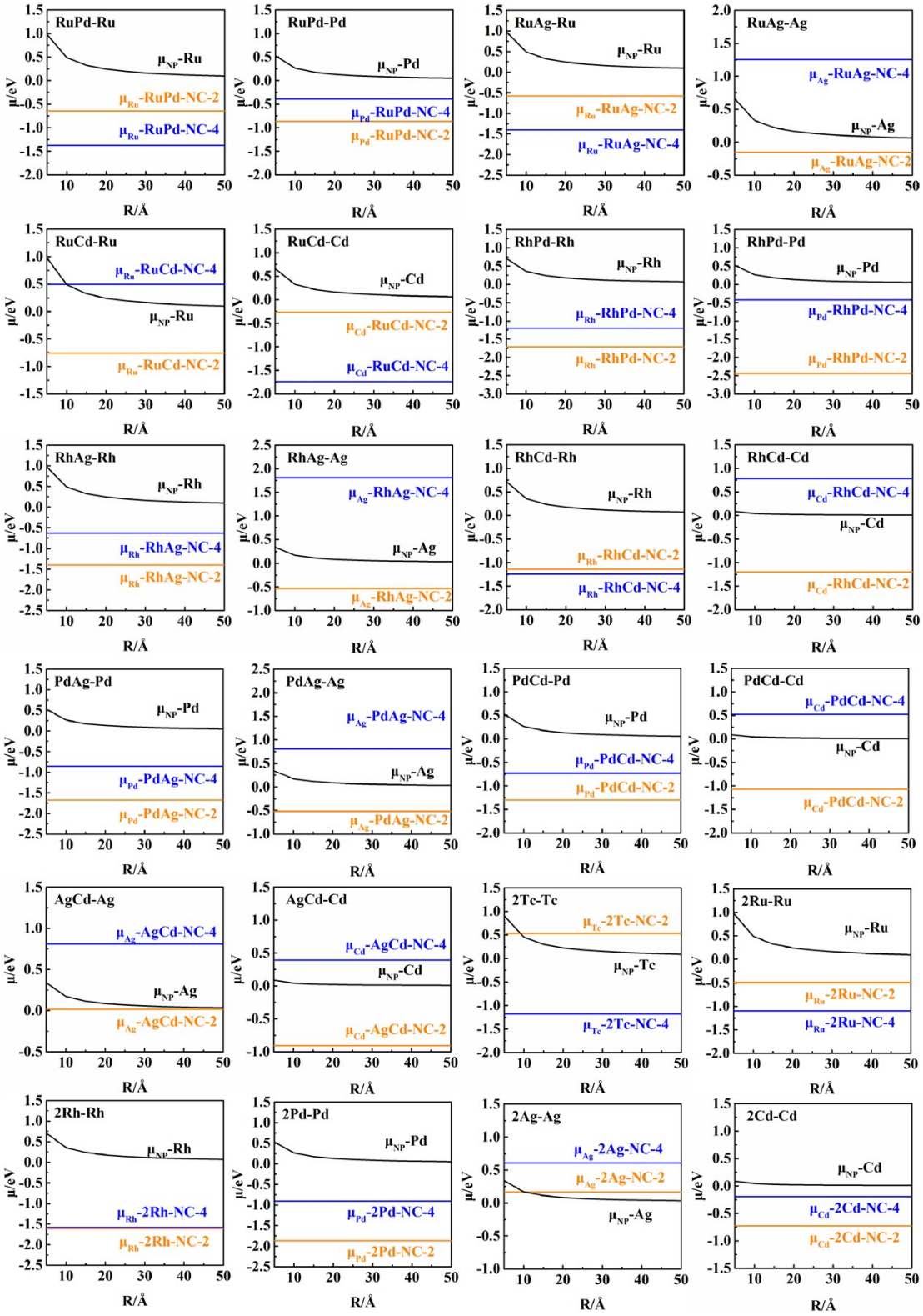

Figure S13. Chemical potential of NPs and single atom of 4d-4d BACs in vacuum.

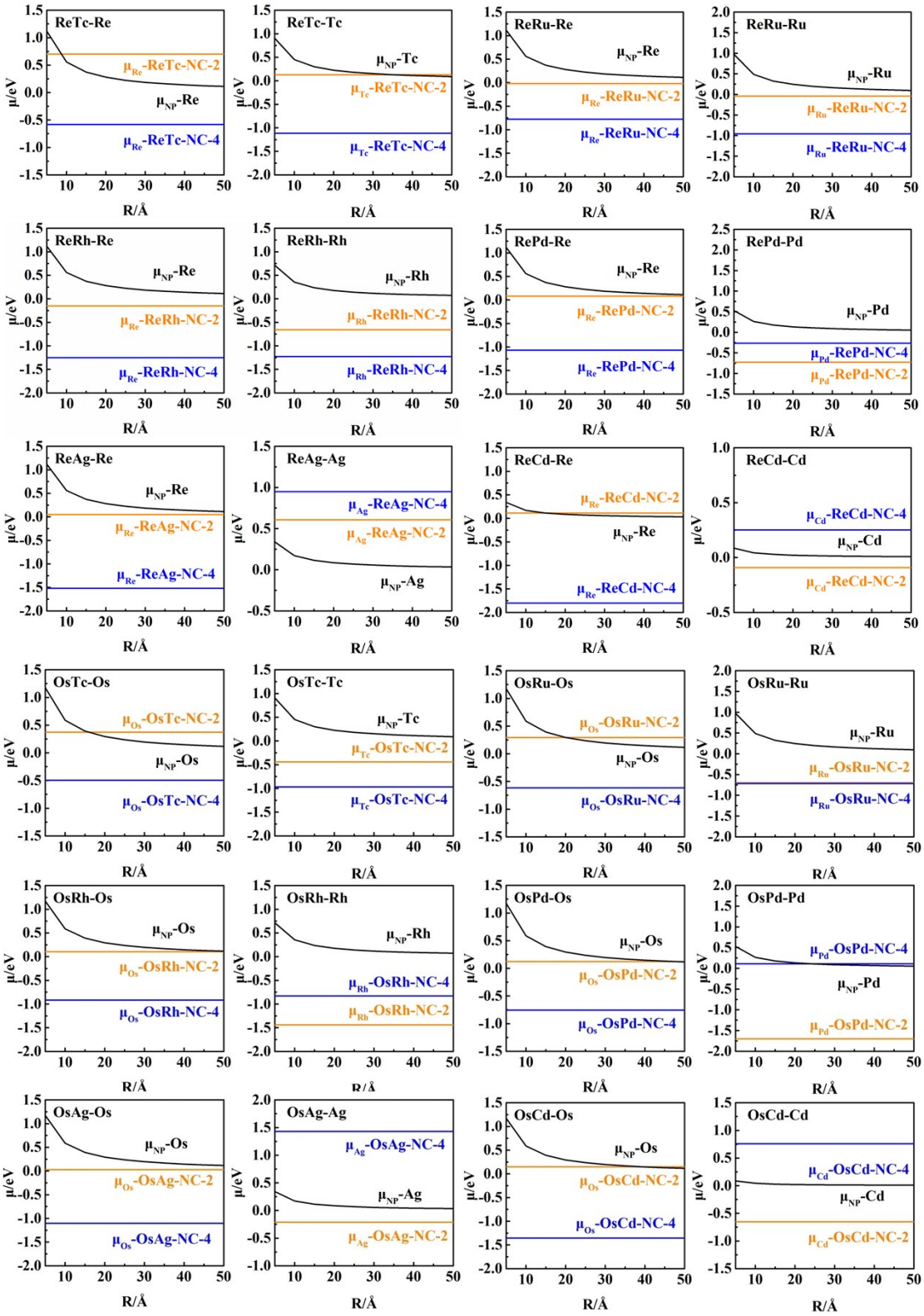
ReTc-Re
μRe-ReTc-NC-2
μNP-Re
μRe-ReTc-NC-4
ReTc-Tc
μNP-Tc
μTc-ReTc-NC-2
μTc-ReTc-NC-4
ReRu-Re
μNP-Re
μRe-ReRu-NC-2
μRe-ReRu-NC-4
ReRu-Ru
μNP-Ru
μRu-ReRu-NC-2
μRu-ReRu-NC-4
ReRh-Re
μNP-Re
μRe-ReRh-NC-2
μRe-ReRh-NC-4
ReRh-Rh
μNP-Rh
μRh-ReRh-NC-2
μRh-ReRh-NC-4
RePd-Re
μNP-Re
μRe-RePd-NC-2
μRe-RePd-NC-4
RePd-Pd
μNP-Pd
μPd-RePd-NC-4
μPd-RePd-NC-2
ReAg-Re
μNP-Re
μRe-ReAg-NC-2
μRe-ReAg-NC-4
ReAg-Ag
μAg-ReAg-NC-4
μAg-ReAg-NC-2
μNP-Ag
ReCd-Re
μRe-ReCd-NC-2
μNP-Re
μRe-ReCd-NC-4
ReCd-Cd
μCd-ReCd-NC-4
μNP-Cd
μCd-ReCd-NC-2
OsTc-Os
μOs-OsTc-NC-2
μNP-Os
μOs-OsTc-NC-4
OsTc-Tc
μNP-Tc
μTc-OsTc-NC-2
μTc-OsTc-NC-4
OsRu-Os
μOs-OsRu-NC-2
μNP-Os
μOs-OsRu-NC-4
OsRu-Ru
μNP-Ru
μRu-OsRu-NC-2
μRu-OsRu-NC-4
OsRh-Os
μNP-Os
μOs-OsRh-NC-2
μOs-OsRh-NC-4
OsRh-Rh
μNP-Rh
μRh-OsRh-NC-4
μRh-OsRh-NC-2
OsPd-Os
μNP-Os
μOs-OsPd-NC-2
μOs-OsPd-NC-4
OsPd-Pd
μPd-OsPd-NC-4
μNP-Pd
μPd-OsPd-NC-2
OsAg-Os
μNP-Os
μOs-OsAg-NC-2
μOs-OsAg-NC-4
OsAg-Ag
μAg-OsAg-NC-4
μNP-Ag
μAg-OsAg-NC-2
OsCd-Os
μNP-Os
μOs-OsCd-NC-2
μOs-OsCd-NC-4
OsCd-Cd
μCd-OsCd-NC-4
μNP-Cd
μCd-OsCd-NC-2
μ/eV
R/Å

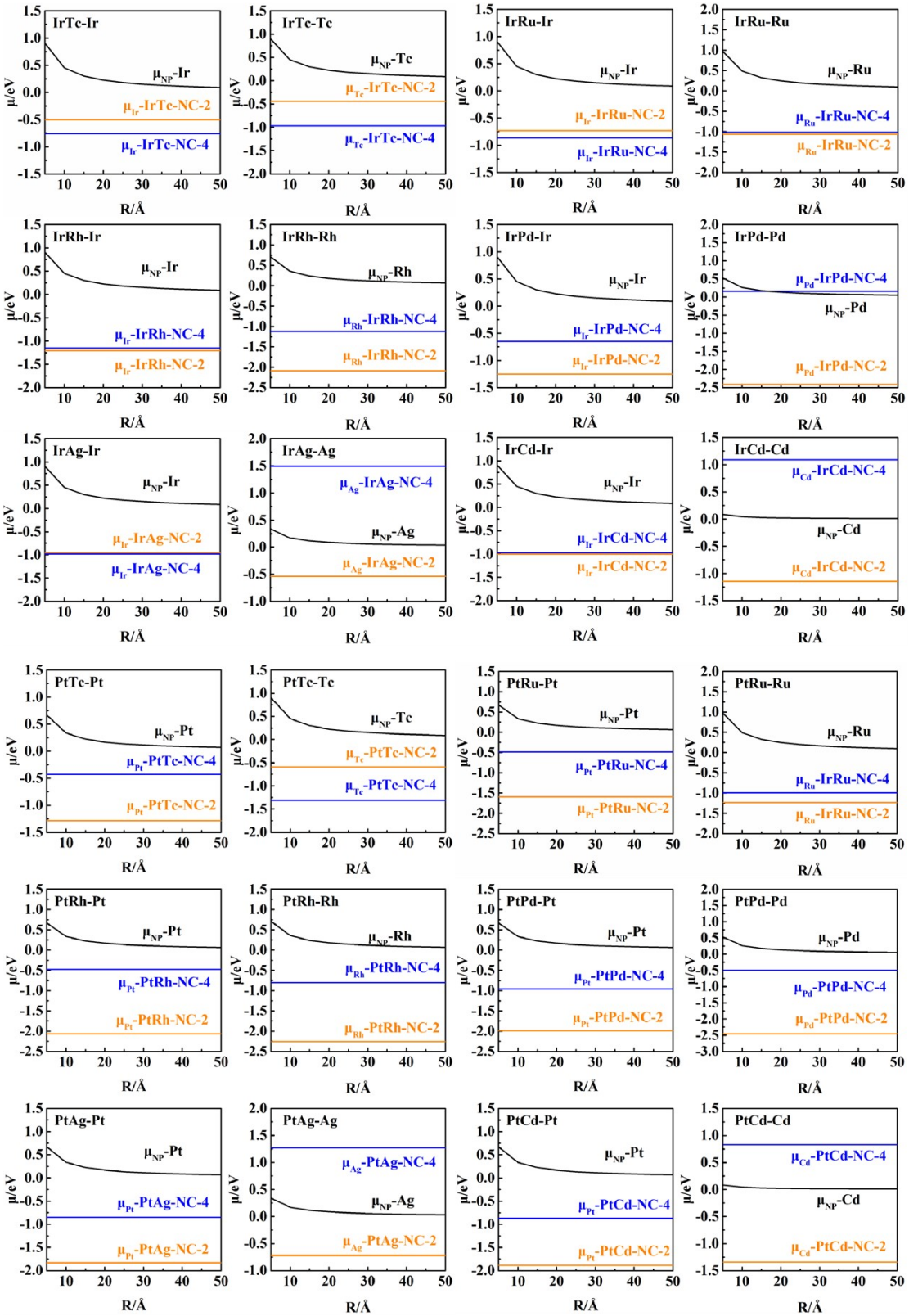

Figure S14. Chemical potential of NPs and single atom of 4d-5d BACs in vacuum.

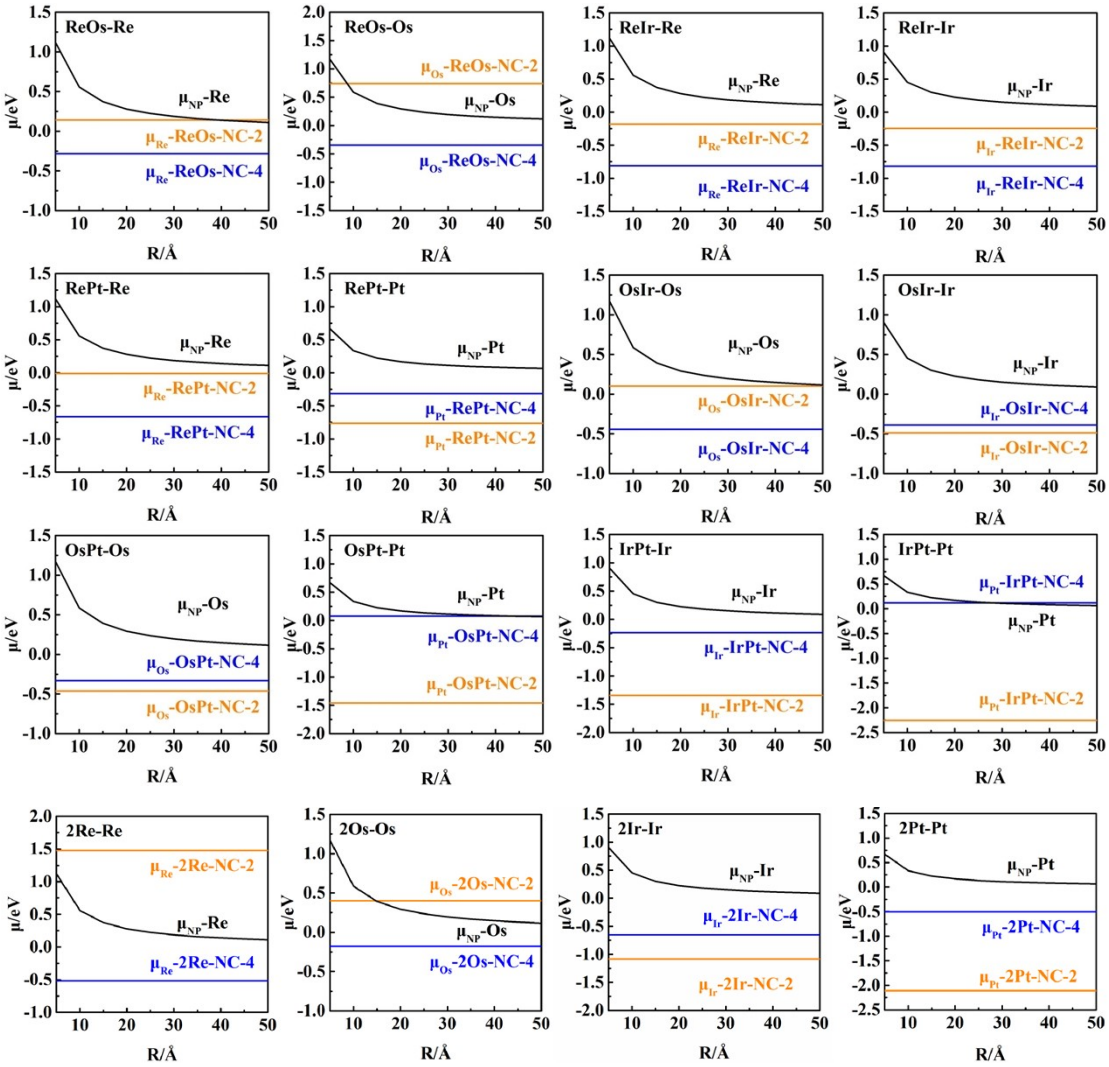

Figure S15. Chemical potential of NPs and single atom of 5d-5d BACs in vacuum.

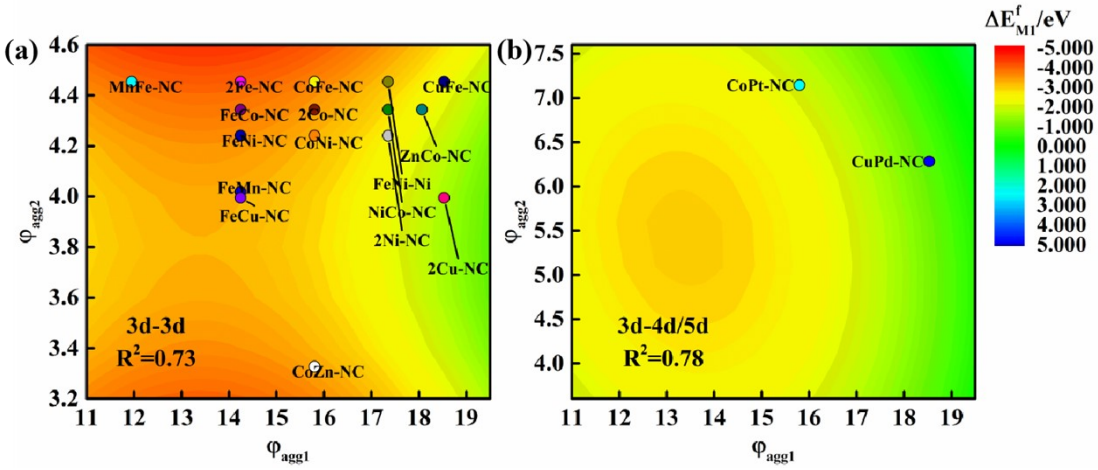

Figure S16. Computed the ΔE_{SA}^{f} versus φ_{agg1} and φ_{agg2} for 3d-3d(a) and 3d-4d/5d(b) M_1M_2-NC-4. The aggregated metal atoms are M_1 atom. The experimentally stable BACs were marked in this figure.

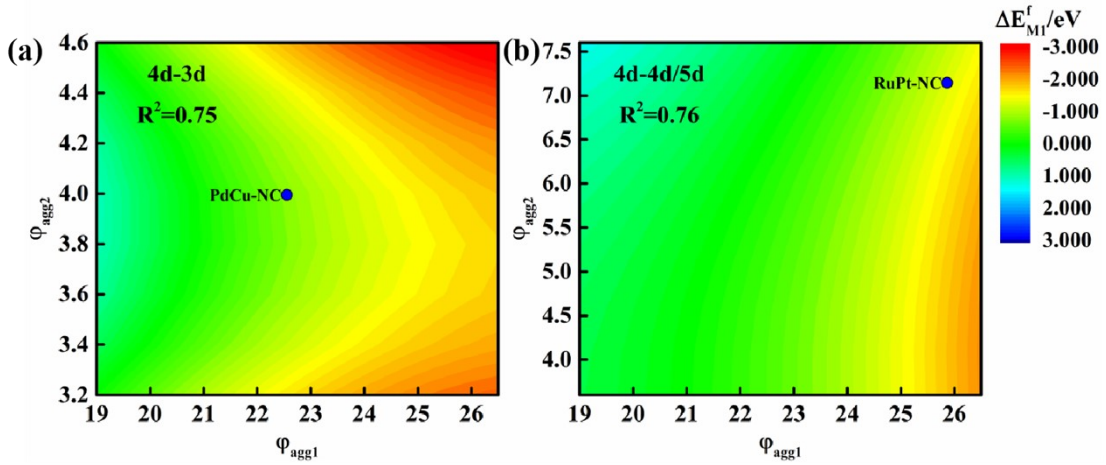

Figure S17. Computed the ΔE_{SA}^{f} versus φ_{agg1} and φ_{agg2} for 4d-3d (a) and 4d-4d/5d (b) M_1M_2-NC-4. The aggregated metal atoms are M_1 atom, and the experimentally stable BACs were marked in this figure.

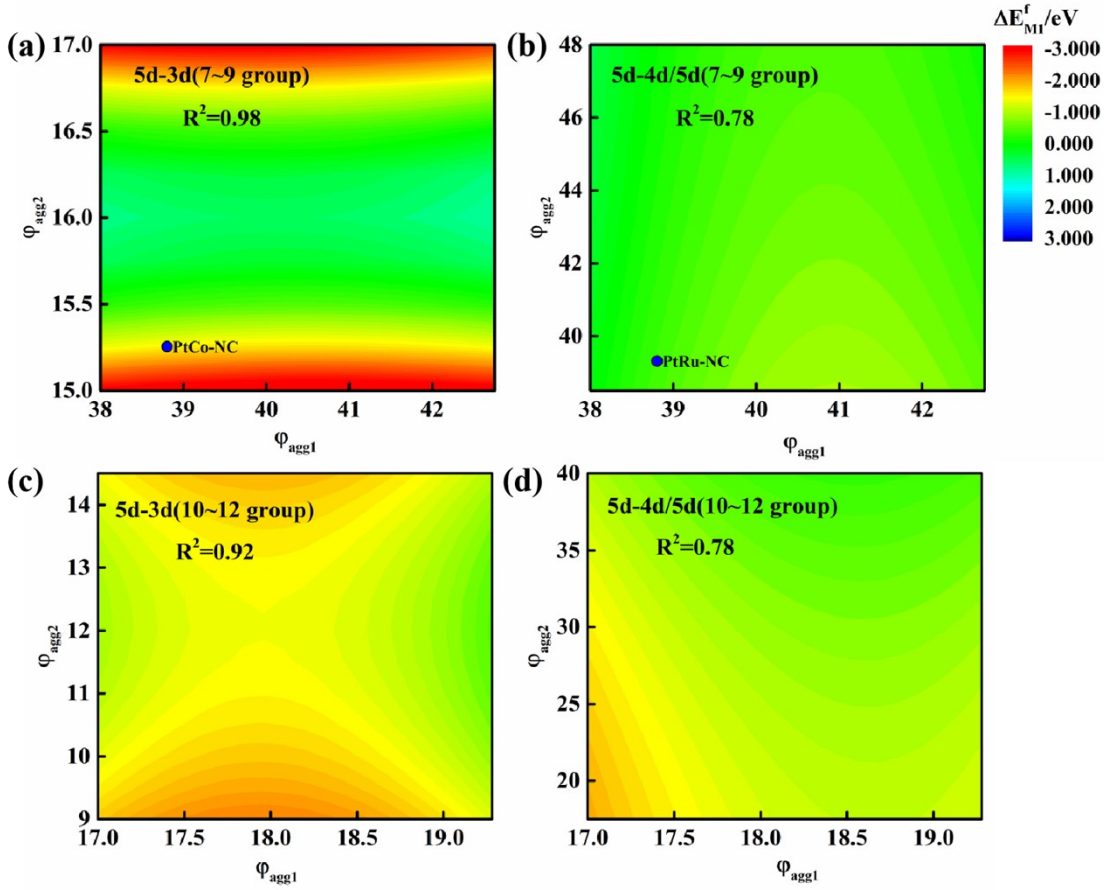

Figure S18. Computed the ΔE_{SA}^{f} versus φ_{agg1} and φ_{agg2} for 5d M_1M_2-NC. (a~b) the transition metal atoms of the 7~9 group serve as M_2 metal atoms for 5d-3d(a) and 5d-4d/5d(b). (c~d) the transition

metal atoms of the 10~12 group serve as M_2 metal atoms for 5d-3d(c) and 5d-4d/5d(d). The aggregated metal atoms are M_1 atom, and the experimentally stable BACs were marked in this figure.

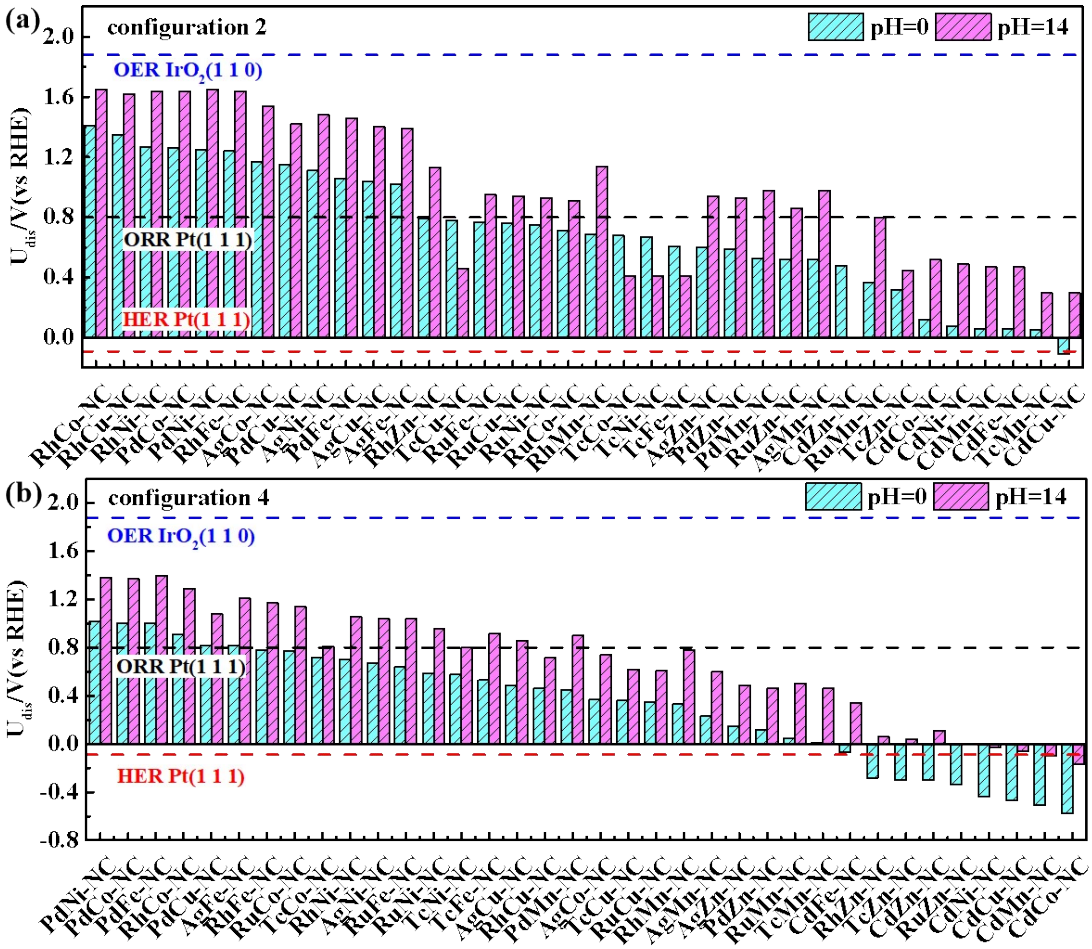

Figure S19. The dissociation potentials U_{dis} (vs RHE) for 3d-4d M_1M_2-NC of configuration 2 (a) and 4 (b) at pH = 0 and pH = 14. The dash line represents the theoretical working voltage of commercial catalysts for various electrocatalytic reactions, including OER, ORR and HER[7].

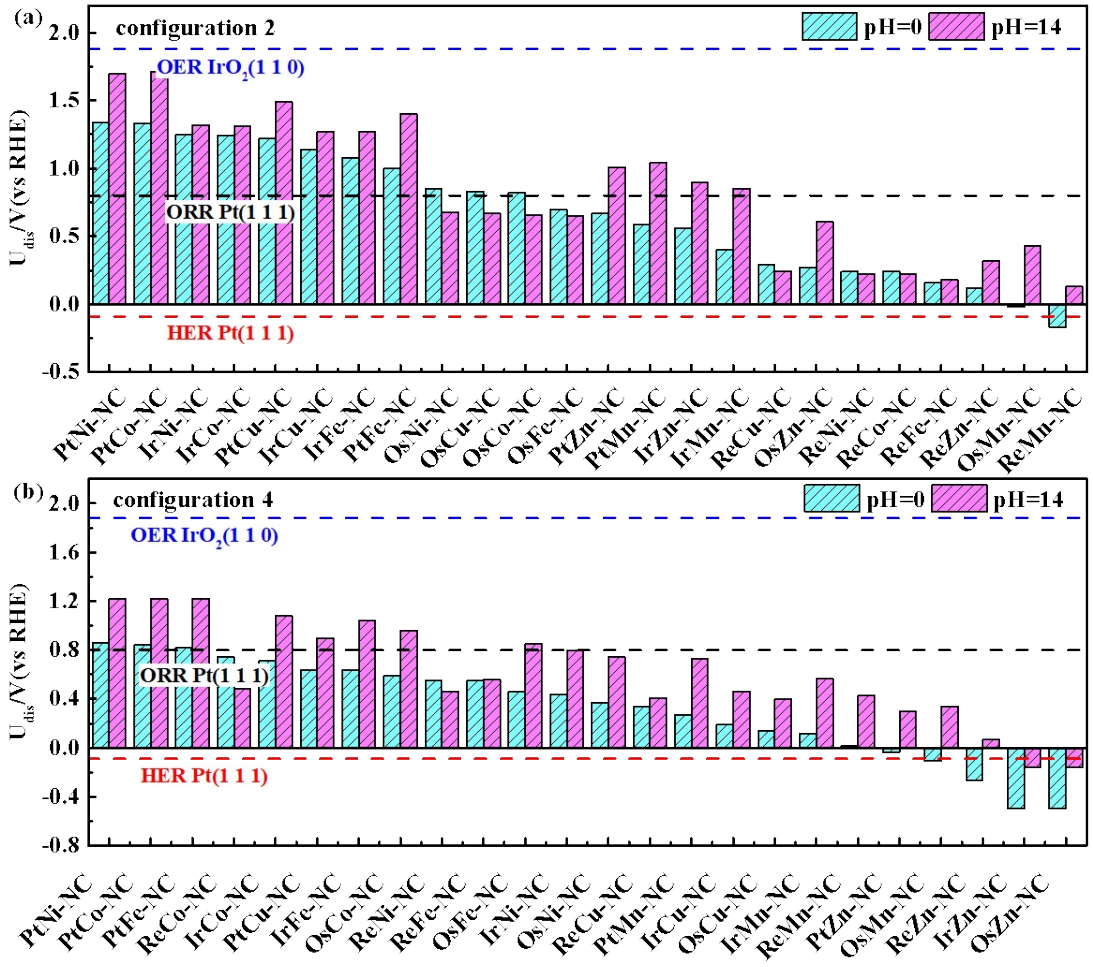

Figure S20. The dissociation potentials U_{dis} (vs RHE) for 3d-5d M_1M_2-NC of configuration 2 (a) and 4 (b) at pH = 0 and pH = 14. The dash line represents the theoretical working voltage of commercial catalysts for various electrocatalytic reactions, including OER, ORR and HER[7].

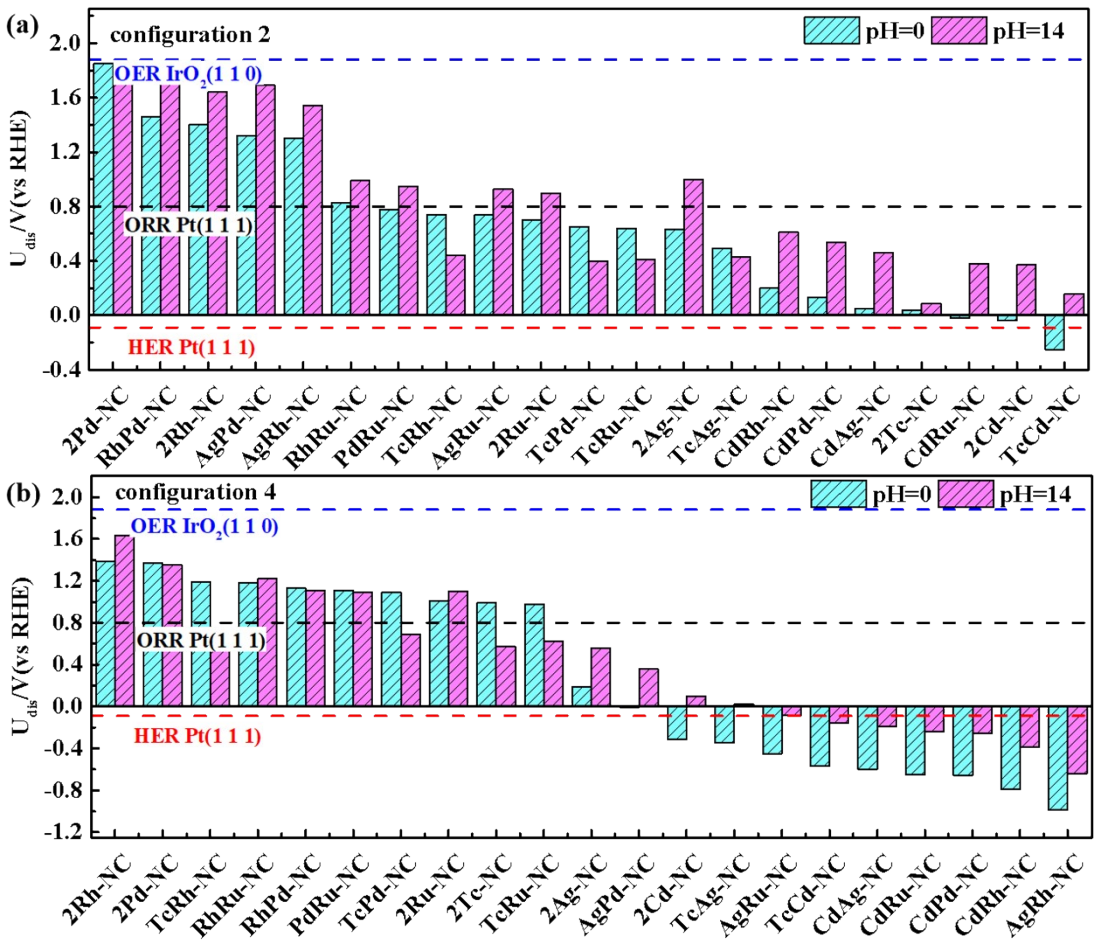

Figure S21. The dissociation potentials U_{dis} (vs RHE) for 4d-4d M_1M_2-NC of configuration 2 (a) and 4 (b) at pH = 0 and pH = 14. The dash line represents the theoretical working voltage of commercial catalysts for various electrocatalytic reactions, including OER, ORR and HER[7].

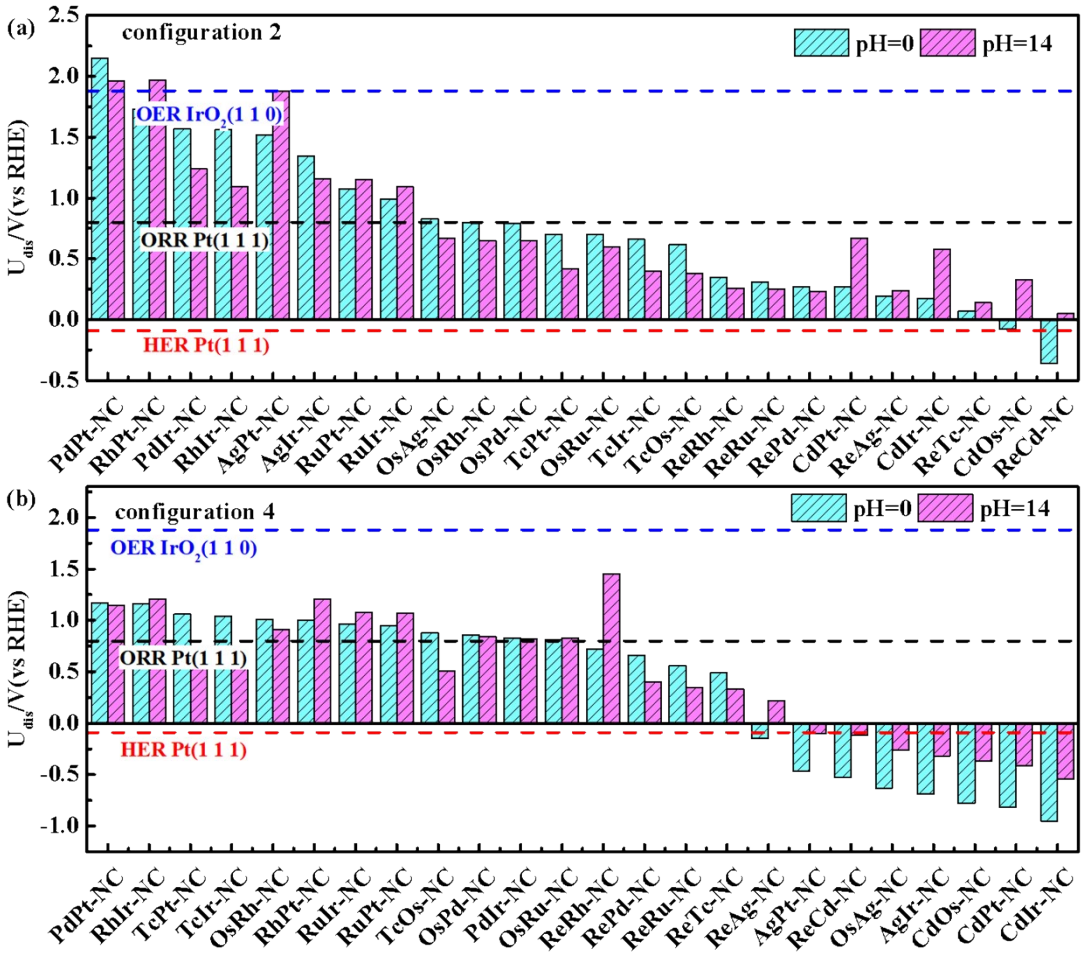

Figure S22. The dissociation potentials U_{dis} (vs RHE) for 4d-5d M_1M_2-NC of configuration 2 (a) and 4 (b) at pH = 0 and pH = 14. The dash line represents the theoretical working voltage of commercial catalysts for various electrocatalytic reactions, including OER, ORR and HER[7].

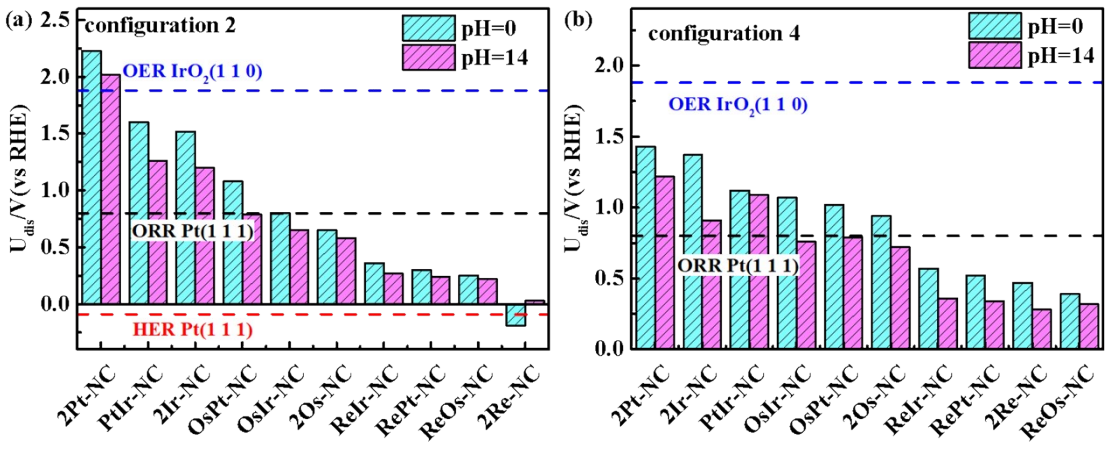

Figure S23. The dissociation potentials U_{dis} (vs RHE) for 5d-5d M_1M_2-NC of configuration 2 (a) and 4 (b) at pH = 0 and pH = 14. The dash line represents the theoretical working voltage of commercial catalysts for various electrocatalytic reactions, including OER, ORR and HER[7].

Supplementary References

1. G. Kresse and J. Furthmüller, *Phys. Rev. B*, 1996, **54**, 11169-11186.
2. G. Kresse and J. Furthmüller, *Comp. Mater. Sci.*, 1996, **6**, 0-50.
3. C. Rostgaard, *Physics*, 2009, **62**, 11556-11570.
4. P. E. Blöchl, *Phys. Rev. B*, 1994, **50**, 17953-17979.
5. S. Grimme, J. Antony, S. Ehrlich and H. Krieg, *J. Chem. Phys.*, 2010, **132**, 154104.
6. S. L. Dudarev, G. A. Botton, S. Y. Savrasov, C. J. Humphreys and A. P. Sutton, *Phys. Rev. B*, 1998, **57**, 1505-1509.
7. H. X. Xu, D. J. Cheng, D. P. Cao and X. C. Zeng, *Nat. Catal.*, 2018, **1**, 339-348.
8. J. C. Liu, Y. G. Wang and J. Li, *J. Am. Chem. Soc.*, 2017, **139**, 6190-6199.
9. S. C. Parker and C. T. Campbell, *Phys. Rev. B*, 2007, **75**, 035430.
10. R. Tran, Z. H. Xu, B. Radhakrishnan, D. Winston, W. H. Sun, K. A. Persson and S. P. Ong, *Sci. Data*, 2016, **3**, 160080.
11. J. C. Liu, H. Xiao and J. Li, *J. Am. Chem. Soc.*, 2020, **142**, 3375-3383.
12. M. Pourbaix, *Atlas of Electrochemical Equilibria in Aqueous Solution*, National Association of Corrosion Engineers, Houston, Texas, 1974.
13. W. Ye, S. M. Chen, Y. Lin, L. Yang, S. J. Chen, X. S. Zheng, Z. M. Qi, C. M. Wang, R. Long, M. Chen, J. F. Zhu, P. Gao, L. Song, J. Jiang and Y. J. Xiong, *Chem*, 2019, **5**, 2865-2878.
14. M. L. Xiao, H. Zhang, Y. T. Chen, J. B. Zhu, L. Q. Gao, Z. Jin, J. J. Ge, Z. Jiang, S. L. Chen, C. P. Liu and W. Xing, *Nano Energy*, 2018, **46**, 396-403.
15. X. P. Han, X. F. Ling, D. S. Yu, D. Y. Xie, L. L. Li, S. J. Peng, C. Zhong, N. Q. Zhao, Y. D. Deng and W. B. Hu, *Adv. Mater.*, 2019, **31**, 1905622.
16. L. Zhang, R. T. Si, H. S. Liu, N. Chen, Q. Wang, K. Adair, Z. Q. Wang, J. T. Chen, Z. X. Song, J. J. Li, M. N. Banis, R. Y. Li, T. K. Sham, M. Gu, L. M. Liu, G. A. Botton and X. L. Sun, *Nat. Commun.*, 2019, **10**, 4936.
17. A. X. Guan, Z. Chen, Y. L. Quan, C. Peng, Z. Q. Wang, T.-K. Sham, C. Yang, Y. L. Ji, L. P. Qian, X. Xu and G. F. Zheng, *ACS Energy Lett.*, 2020, **5**, 1044-1053.
18. T. Ding, X. K. Liu, Z. N. Tao, T. Y. Liu, T. Chen, W. Zhang, X. Y. Shen, D. Liu, S. C. Wang, B. B. Pang, D. Wu, L. L. Cao, L. Wang, T. Liu, Y. F. Li, H. T. Sheng, M. Z. Zhu and T. Yao, *J. Am. Chem. Soc.*, 2021, **143**, 11317-11324.
19. C. Du, Y. J. Gao, H. Q. Chen, P. Li, S. Y. Zhu, J. G. Wang, Q. G. He and W. Chen, *J. Mater. Chem. A*, 2020, **8**, 16994-17001.
20. Y. D. Zhou, W. Yang, W. Utetiwabo, Y. M. Lian, X. Yin, L. Zhou, P. W. Yu, R. J. Chen and S. R. Sun, *J. Phys. Chem. Lett.*, 2020, **11**, 1404-1410.
21. W. H. Ren, X. Tan, W. F. Yang, C. Jia, S. M. Xu, K. X. Wang, S. C. Smith and C. Zhao, *Angew. Chem. Int. Ed.*, 2019, **58**, 6972-6976.
22. J. Wang, Z. Q. Huang, W. Liu, C. R. Chang, H. L. Tang, Z. J. Li, W. X. Chen, C. J. Jia, T. Yao, S. Q. Wei, Y. Wu and Y. D. Li, *J. Am. Chem. Soc.*, 2017, **139**, 17281-17284.
23. Z. Y. Lu, B. Wang, Y. F. Hu, W. Liu, Y. F. Zhao, R. O. Yang, Z. P. Li, J. Luo, B. Chi, Z. Jiang, M. S. Li, S. C. Mu, S. J. Liao, J. J. Zhang and X. L. Sun, *Angew. Chem. Int. Ed.*, 2019, **58**, 2622-2626.
24. L. L. Han, Z. H. Ren, P. F. Ou, H. Cheng, N. Rui, L. L. Lin, X. J. Liu, L. C. Zhuo,

J. Song, J. Q. Sun, J. Luo and H. L. L. Xin, *Angew. Chem. Int. Ed.*, 2021, **60**, 345-350.
25. L. Z. Zhang, J. Fischer, Y. Jia, X. C. Yan, W. Xu, X. Y. Wang, J. Chen, D. J. Yang, H. W. Liu, L. Z. Zhuang, M. Hankel, D. J. Searles, K. K. Huang, S. H. Feng, C. L. Brown and X. D. Yao, *J. Am. Chem. Soc.*, 2018, **140**, 10757-10763.
26. J. Wang, W. Liu, G. Luo, Z. J. Li, C. Zhao, H. R. Zhang, M. Z. Zhu, Q. Xu, X. Q. Wang, C. M. Zhao, Y. T. Qu, Z. K. Yang, T. Yao, Y. F. Li, Y. Lin, Y. Wu and Y. D. Li, *Energy Environ. Sci.*, 2018, **11**, 3375-3379.
27. Z. Chen, X. B. Liao, C. L. Sun, K. N. Zhao, D. X. Ye, J. T. Li, G. Wu, J. H. Fang, H. B. Zhao and J. J. Zhang, *Appl. Catal. B Environ.*, 2021, **288**, 120021.